Pergamon

Prog. Energy Combust. Sci. Vol. 24, pp. 259–296, 1998

0360–1285/98 $19.00

PII: S0360–1285(98)00002–1

FUNDAMENTALS OF TURBULENT GAS–SOLID FLOWS APPLIED TO CIRCULATING FLUIDIZED BED COMBUSTION

Eric Peirano and Bo Leckner*

Department of Energy Conversion, Chalmers University of Technology, S-41296 Göteborg, Sweden

Abstract—A summary is made of the present state of knowledge of turbulent gas–solid flow modeling and in particular its application to circulating fluidized bed combustion chambers. Models are presented to close the set of equations describing isothermal non-reacting turbulent gas–particle flows applied to fluidization, and it is shown under which assumptions the models can be derived. With the kinetic theory of granular flow, transport equations for the velocity moments and closure laws for the stress tensor and the energy flux are derived for the particle phase. Closure equations for the drift velocity and for the fluid–particle velocity correlation tensor are presented, first based on algebraic models and, second, based on transport equations with the fluid–particle joint probability density function. An alternative derivation of the fluid–particle velocity covariance transport equation is compared to the formulation based on the fluid–particle joint probability density function. Two-way coupling is discussed, and a transport equation for the second-order velocity moments is used to derive a two-equation model accounting for the modulation of gas phase turbulence by particles. Boundary conditions for the set of equations describing a turbulent gas–solid flow are discussed. Provided that the domain of applicability of the models is known, a discussion on the usefulness of the models is given, as well as an application to fluidization and especially to circulating fluidized bed combustors. Prospects for improvement of the existing models are presented.

Keywords: turbulent gas–solid flows, circulating fluidized bed.

CONTENTS

*Corresponding author.

NOMENCLATURE

List of symbols

a, a', a_1–a_5	coefficients for wall boundary conditions	g_u	parameter function
b_1–b_8	coefficients for wall boundary conditions	g_0	radial distribution function
B_1–B_5	coefficients for wall boundary conditions	G_{1ij}	one-point statistics function (sec^{-1})
a_{ij}	second-order coefficient ($m^2\,sec^{-2}$)	G_{12ij}	one-point statistics function (sec^{-1})
a_{ijm}	third-order coefficient ($m^3\,sec^{-3}$)	$H^{(n)}(\mathbf{x},t)$	Hermite polynomial of order n
$a^{(n)}(\mathbf{x},t)$	coefficient of order n	I_{ki}	interfacial momentum transfer ($N\,m^{-3}$)
C_D	drag coefficient for a sphere in a suspension	J_i	collision impulse force (N)
$C(\psi)$	collisional rate of change for ψ	k_i, $\mathbf{k}$	particle collision unit vector
C_β	constant in equation for τ'_{12}	k_k	fluctuation kinetic energy in phase k ($m^2\,sec^{-2}$)
C_{ϵ_2}	constant in ϵ_1 equation	k_{12}	fluid–particle fluctuation kinetic energy ($m^2\,sec^{-2}$)
C_{ϵ_3}	constant in ϵ_1 equation	K_2^t	particle turbulent diffusion coefficient ($m^2\,sec^{-1}$)
C_μ	constant in k_1–ϵ_1 model	K_2^c	collisional diffusion coefficient ($m^2\,sec^{-1}$)
C_{ϵ_1}	constant in ϵ_1 equation	L_1^t	fluid Eulerian integral scale (m)
c_i, $\mathbf{c}$	local instantaneous velocity of a particle before collision ($m\,sec^{-1}$)	m	mass of a single particle (kg)
c_i'	local instantaneous velocity of a particle after collision ($m\,sec^{-1}$)	M_i	momentum supply per unit area of the wall ($N\,m^{-2}$)
C_i, $\mathbf{C}$	fluctuation velocity of a particle ($m\,sec^{-1}$)	$M_{kij\ldots p}$	moment of order p for phase k ($m^p\,sec^{-p}$)
d_p	particle diameter (m)	$M_{12ij\ldots p}$	fluid–particle fluctuation tensor of order p ($m^p\,sec^{-p}$)
d_1–d_3	coefficients for wall boundary conditions	n	number of particles per unit volume (m^{-3})
dW_{1i}	random vector ($sec^{1/2}$)	n_{1j}	normal unit vector associated with gas phase
dW_{12i}	random vector ($sec^{1/2}$)	N	normal component of M_i ($N\,m^{-2}$)
D_{kij}^t	dispersion or diffusion tensor ($m^2\,sec^{-1}$)	$\tilde{p}_1$	local instantaneous pressure of undisturbed flow (Pa)
D_{k_1}	diffusion coefficient for k_1 equation ($m^2\,sec^{-1}$)	P_1	mean pressure in the gas phase (Pa)
D_{ϵ_1}	diffusion coefficient for ϵ_1 equation ($m^2\,sec^{-1}$)	P_2	mean pressure in the particle phase (Pa)
D_{12ij}^t	binary dispersion tensor ($m^2\,sec^{-1}$)	Q	energy rate supply per unit area of the wall ($J\,m^{-2}\,sec^{-1}$)
e, e_w	particle–particle and wall–particle restitution coefficient	R_{kij}	Lagrangian correlation tensor
f_u	parameter function	$\Re_{1ij}$	fluid Lagrangian tensor along particle trajectories
f^0	normal distribution function ($m^{-6}\,sec^3$)	S	tangential component of M_i ($N\,m^{-2}$)
f^1	single particle distribution function ($m^{-6}\,sec^3$)	S_{kij}	strain rate tensor of phase k (sec^{-1})
f^2	pair distribution function ($m^{-12}\,sec^6$)	$\hat{S}_{kij}$	deviatoric part of the strain rate tensor of phase k (sec^{-1})
f_{12}	fluid–particle joint probability density function ($m^{-9}\,sec^6$)	S_{12ij}	fluid–particle strain rate tensor (sec^{-1})
F_i	external force acting on a particle per mass unit ($N\,kg^{-1}$)	$\hat{S}_{12ij}$	deviatoric part of the fluid–particle strain rate tensor (sec^{-1})
g_i	gravitational acceleration or relative velocity before collision ($m\,sec^{-2}$ or $m\,sec^{-1}$)	t	time (sec)
g_i'	relative velocity after collision ($m\,sec^{-1}$)		

T_2	granular temperature ($m^2\ sec^{-2}$)
u_{ki}	local instantaneous velocity of phase k ($m\ sec^{-1}$)
u_{ki}'	fluctuation velocity of phase k ($m\ sec^{-1}$)
$\tilde{u}_{1i}$	local instantaneous velocity of undisturbed flow ($m\ sec^{-1}$)
u_{1i}'	fluctuating velocity of gas phase ($m\ sec^{-1}$)
u''_{1i}	fluctuating velocity of gas phase seen by the particles ($m\ sec^{-1}$)
u_{ri}'	fluctuating relative velocity ($m\ sec^{-1}$)
u^*	friction velocity ($m\ sec^{-1}$)
U_{di}	fluid particle drift velocity ($m\ sec^{-1}$)
U_{mi}	mean mixture velocity ($m\ sec^{-1}$)
U_{ri}	mean fluid particle relative velocity ($m\ sec^{-1}$)
U_{ki}	mean velocity of phase k ($m\ sec^{-1}$)
$\mathbf{x}$	spatial coordinate (m)
$\mathbf{x}_1(t)$	trajectory of a fluid particle (m)
$\mathbf{x}_2(t)$	trajectory of a particle (m)
X_k	phase indicator function
X_{12}	loading
Y_2	mass fraction of particle phase

Greek letters

α_k	mean volume concentration of phase k
α_m	maximum volume concentration of particle phase
β_0	wall–particle tangential coefficient of restitution
δ_1	Dirac function associated with gas phase
δ_{ij}	Kronecker's symbol
ϵ_1	dissipation of gas phase turbulent kinetic energy ($m^2\ sec^{-3}$)
η	turbulence efficiency to entrain particles
θ_{kij}	stress tensor of phase k ($N\ m^{-2}$)
$\theta_i(\psi)$	flux term for collisional rate of change for ψ
μ_1	laminar viscosity of gas phase (Pa sec)
μ_2	dynamic viscosity of particulate phase (Pa sec)
μ_w	wall–particle friction coefficient
ν_1	kinematic viscosity of gas phase ($m^2\ sec^{-1}$)
ν_2^c	collisional viscosity of particle phase ($m^2\ sec^{-1}$)
ν_k'	turbulent viscosity of phase k ($m^2\ sec^{-1}$)
ν_{12}'	fluid–particle turbulent viscosity ($m^2\ sec^{-1}$)
ξ_2	bulk viscosity in particle phase (Pa sec)
ρ_k	density of phase k ($kg\ m^{-3}$)
ρ_m	mixture density ($kg\ m^{-3}$)
Π_1	interaction term in k_1 transport equation ($m^2\ sec^{-3}$)
Π_{11}	interaction term in ϵ_1 transport equation ($m^2\ sec^{-4}$)
Π_{12}	interaction term in k_{12} transport equation ($kg\ m^{-1}\ sec^{-3}$)
σ_{k_1}	effective Prandtl number in k_1 transport equation
σ_{ϵ_1}	effective Prandtl number in ϵ_1 transport equation
σ_{1ij}	local instantaneous stress tensor in gas phase ($N\ m^{-2}$)
Σ_{kij}	effective stress tensor in phase k ($N\ m^{-2}$)
τ	time (sec)
τ_{1ij}	local instantaneous shear stress tensor in gas phase ($N\ m^{-2}$)
τ_{kij}'	Lagrangian integral time scale for phase k (sec)
τ_{12ij}'	fluid integral time scale along particle trajectories (sec)
τ_1'	time scale of large scales in gas phase (sec)
τ_{12}^c	particle relaxation time (sec)
τ_{12}'	eddy life time seen by a particle (sec)
τ_2^c	characteristic collision time (sec)
$\chi(\psi)$	source term for collisional rate of change for ψ
ψ, ψ'	transported property before and after collision, respectively

Subscripts

1	related to the gas phase or particle 1
2	related to the particulate phase or particle 2
k	related to phase k
$kij...p$	tensor indices $ij...p$ related to phase k
$(ij...p)$	sum of all possible permutations on indices $ij...p$

Superscripts

$'$	fluctuation component related to present phase
$''$	fluctuation component in gas phase seen by particle phase
$\sim$	non-disturbed flow

Special notation

$< >$	general averaging operator
$< >_k$	averaging operator associated with phase k
$\|\|$	norm of vector
∂	partial derivative
d/dt	ordinary time derivative
D_k/Dt	$\partial/\partial t + U_{ki}\partial/\partial x_i$
$U_{i,j}$	$\partial U_i/\partial x_j$
det	determinant

Dimensionless groups

$Re = \|\mathbf{u}_r\| d_p/\nu_1$	particle Reynolds number
$St = \tau_{12}^c/\tau_1'$	Stokes number
$U_{1i}^+ = U_{1i}/u^*$	velocity in wall layer
$y^+ = yu^*/\nu_1$	distance from the wall

1. INTRODUCTION

With the development of the performance of computers during the last few years and in anticipation of further increases in computing power, new possibilities are emerging of treating complex computational tasks like, for example, numerical computations of turbulent gas–solid flows. The present work aims at establishing the fundamentals for numerical calculations of turbulent gas–solid flows. A survey is made of available information for the formulation of the two-phase flow transport equations. The formulation is general and therefore applicable to any turbulent gas–solid suspension, but it is focussed on the requirements posed by the computation of the flow in a circulating fluidized bed (CFB) combustor. The application to CFB combustors specifically is treated in the final section.

There are two main applications of CFB technology, circulating fluidized beds for catalytic cracking (FCCs) and circulating fluidized bed combustors (CFBCs),

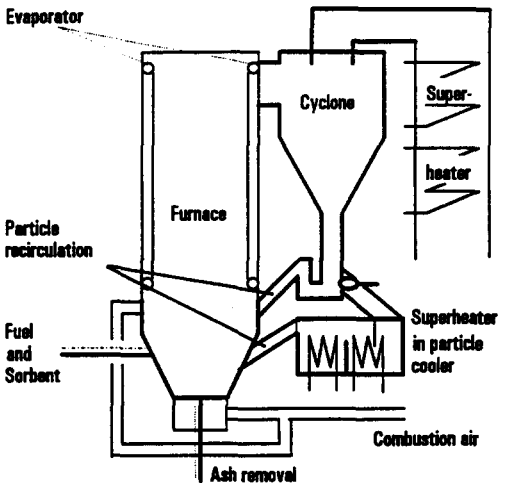

Fig. 1. A CFB combustor (Lurgi type with an external heat exchanger).

which both consist of vertical risers in which air is introduced at the bottom to elevate (fluidize) particles. Despite the similarities of the two CFB applications, there are significant differences in their design and in their gas–solid flow patterns.[1] An FCC is characterized by a circular cross-section, a high height-to-diameter ratio (over 20), a small mean particle diameter (about 60 μm), high fluidization velocities (up to 20 m sec^{-1} at the top) and high recirculation rates (over 300 kg m^{-2} sec^{-1}). On the contrary, a CFBC is most commonly built with a rectangular cross-section, and has a low height-to-diameter ratio (under 10), a large mean particle diameter (about 100–300 μm), low fluidization velocities (less than 6 m sec^{-1}) and low recirculation rates (less than 30 kg m^{-2} sec^{-1}). More precisely, a CFBC is a device where solids, Geldart Group B (with a particle size distribution from 100 μm to 1 mm and an average particle density of 2000–2600 kg m^{-3}),[2] are transported vertically by a gas through a combustion chamber. The solids are captured at the exit by a separator (usually a cyclone) and reintroduced near the bottom of the combustion chamber, whereas the gas leaves the cyclone through an outlet duct and the convective pass, as shown in Fig. 1. The recirculation part of the boiler, also called the return loop, is composed of the cyclone, a return leg, a particle seal and sometimes a heat exchanger. The fluidizing gas is introduced at the bottom of the combustion chamber through nozzles (or a gas distributor plate) and secondary air can be injected at different heights. Fuel is fed to the bottom part of the combustion chamber through a fuel chute. The flow pattern of the bed material (fuel, ash, sand and possibly limestone) is characterized by a vertical distribution of the particle concentration. This vertical distribution consists of three interacting zones: (1) a bottom bed with constant time-averaged solid concentration, (2) a splash zone with an exponential decay of particle concentration in height, and (3) a transport zone, also with an exponential decay, but with a lower decay value than in the splash zone. The set of equations presented in this work is valid for isothermal flows; the small temperature gradient observed in the combustion chamber of a CFBC (850 ± 20°C under normal operating conditions), except near the walls, makes this approach a suitable one, and useful results can be obtained from simulations.[3,4]

In the derivation of the differential equations describing the particle phase (the discrete phase), two formulations are possible: the Lagrangian formulation or the Eulerian formulation. The Lagrangian formulation gives an accurate description of the motion of a single particle (rotation of the particle, collision with another particle and so on), but the major difficulty is to describe how the particle sees the gas turbulent field along its trajectory and to accurately predict the forces applied to a particle in a suspension. In addition, the number of particles which can be employed in a numerical computation is limited by the available computer capacity. Consequently, most Lagrangian simulations have been carried out in small scale, experimental units. Some recent advances in Lagrangian simulations are due to, for example, Kawaguchi *et al.*[5] and Hoomans *et al.*,[6] who simulated a single rising bubble in a two-dimensional fluidized bed, and Yonemura *et al.*,[7] who studied numerically the effects of the physical properties of particles on the structure of particle clusters. In the present work, the Eulerian/Eulerian formulation is chosen, which means that both phases are described by a Eulerian formulation. In the Eulerian formulation, the statistical treatment necessary to produce two interpenetrating continua introduces interfacial terms, stress tensors and turbulent correlations that must be modeled. Models for the stress tensors and the turbulent correlations are given in this paper, whose aim is to review these models and discuss their application to the field of fluidization.

1.1. *Fundamental Equations and Scope of This Study*

A detailed derivation of the Eulerian/Eulerian formulation can be found, for example, in Enwald *et al.*[8] The main points of this derivation are repeated here as a reminder. A general averaging operator, $< >$, satisfying the Reynolds axioms, is applied to the local instantaneous continuity and momentum equations. These equations are treated beforehand with the phase indicator function, $X_k(\mathbf{x},t)$ (equal to 1 if phase k is present and 0 otherwise). In order to separate the average of products into products of averaged values, weighted averaged values are introduced: the phasic average, $<f>_{X_k} = <X_k f> / <X_k>$, and the Favre average, $<f>_{X_k\rho_k} = <X_k\rho_k f> / <X_k\rho_k>$. The average of the phase indicator function is denoted $\alpha_k = <X_k>$. A Reynolds decomposition on the velocity and pressure fields yields $u_{ki} = <u_{ki}>_{X_k\rho_k} + u_{ki}' = U_{ki} + u_{ki}'$ and $p_k = <p_k>_{X_k} + p_k' = P_k + p_k'$, where $<u_{ki}'>_k = 0$ and $<p_k'>_k = 0$. From now on, the same index $<>_k$ is used for all averaged quantities, where index $k = 1$ denotes the continuous phase and index $k = 2$ the

discrete phase. The choice of the averaging operator has been discussed extensively in the literature.[9] It can be stated that, if the flow is homogeneous, the volume average is a suitable operator that satisfies the Reynolds axioms and, if the flow is stationary, the time average is a suitable operator that satisfies the Reynolds axioms. If the flow is homogeneous and stationary, all three operators are equivalent (ergodicity hypothesis).

Applying the Reynolds decomposition to the local instantaneous equations, the averaged continuity equation can be expressed as

$$\frac{\partial}{\partial t}(\alpha_k \rho_k) + \frac{\partial}{\partial x_j}(\alpha_k \rho_k U_{kj}) = 0 \tag{1}$$

and the averaged momentum equation as

$$\alpha_k \rho_k \frac{D_k}{Dt} U_{ki} = -\alpha_k \frac{\partial P_1}{\partial x_i} - \frac{\partial}{\partial x_j}(\Theta_{kij} + \alpha_k \rho_k M_{kij}) + I_{ki} + \alpha_k \rho_k g_i, \tag{2}$$

where the interfacial momentum transfer, I_{ki}, is given by $I_{1i} = -I_{2i} = \alpha_2 \rho_2 U_{ri}/\tau_{12}^x$, with U_{ri} and τ_{12}^x being the mean relative velocity and the particle relaxation time, respectively. The derivations for the interfacial terms can be found in Peirano.[10] The mean relative velocity is defined by $U_{ri} = (U_{2i} - U_{1i}) - U_{di}$, where $U_{di} = <u_{1i}'>_2$ represents the correlation between the fluctuating velocity of the continuous phase and the instantaneous spatial distribution of the discrete phase. This term, called the drift velocity, represents the dispersion of particles by the large scales of the fluctuation motion in the continuous phase, large with respect to the particle diameter.[11] To close the system, the drift velocity, the stress tensors Θ_{kij} and the second-order velocity moments $M_{kij} = <u_{ki}' u_{kj}'>_k$ in each phase have to be modeled. The stress tensor in the gas phase is modeled with the classical Newtonian strain–stress relation, and therefore this matter is not discussed further in the present work. The second-order velocity moment of the discrete phase is modeled by the kinetic theory of granular flow (Section 2). In this work, Grad's 13 moment method is used; the particle velocity probability density function is expanded in series using Hermite polynomials which are written in terms of the normal distribution function.[12] This differs from the original work of Jenkins and Savage,[13] where the particle velocity probability density function is identified as the normal distribution function, a model which has been numerically tested for bubbling fluidized beds by Ding and Gidaspow.[14] In the present review, applications of the kinetic theory for dry (without an interstitial gas) granular flow applied to gas–particle flows (e.g. Ding and Gidaspow[14]) are not considered (the reason for this is developed in Section 2). A review of such applications is given by Sinclair.[15] The drift velocity is modeled using a detailed study of particle dispersion in a turbulent flow field (Section 3). A binary dispersion coefficient is introduced.[16] The second-order moment in the continuous phase is modeled in terms of turbulent kinetic energy, with a modified k–ϵ model which takes into account the influence of the particles (Section 4).

1.2. *Characteristic Time Scales*

In the formulation of the transport equations, several characteristic time scales are defined. These time scales are fundamental in the classification and the understanding of the dominant mechanisms in suspensions. The characteristic time scale of the large eddies in the continuous phase is defined in accordance with the k–ϵ model as $\tau_1^t = C_\mu k_1/\epsilon_1$, where $C_\mu = 0.09$ and $k_1 = <u_{1i}' u_{1i}'>_1 /2$ is the turbulent kinetic energy associated with the dissipation ϵ_1. The time of interaction between particle motion and continuous phase fluctuations is defined by

$$\tau_{12}^t = \tau_1^t (1 + C_\beta \xi_r)^{-1/2}, \tag{3}$$

where $\xi_r = 3|\mathbf{U_r}|^2/2k_1$ and C_β is a constant which depends on the type of flow, but also on the direction. This time scale is the Lagrangian integral time scale seen by the particles (computed along the trajectory of the particle). It depends mainly on the loss of correlation due to the mean relative movement of the particles, or the so-called crossing trajectories effect.[17] Practically,

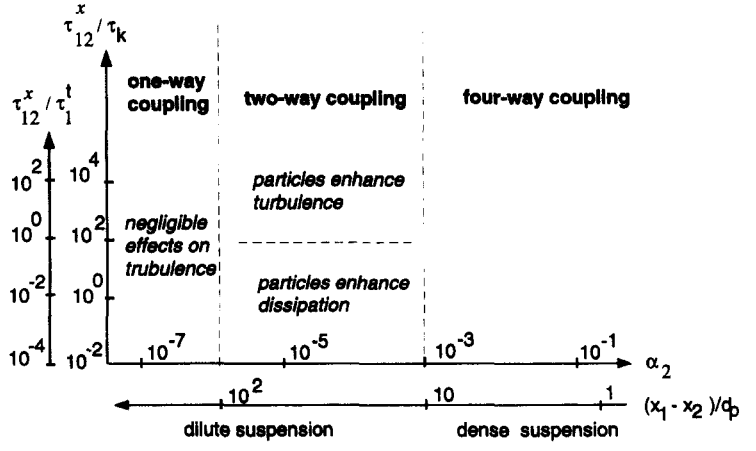

Fig. 2. Classification of flow regimes for gas–solid flows according to Elgobashi.[19]

this means that the time spent by a virtual fluid particle in an eddy is not the same as the time experienced by a solid particle, because of the mean relative velocity between the two phases. The particle relaxation time is defined by

$$\tau_{12}^{x} = \frac{4 d_p \rho_2}{3 \rho_1 < C_D >_2 < |\mathbf{u}_r| >_2}, \tag{4}$$

where $< C_D >_2$ is the averaged drag coefficient for a single particle in a suspension. It is calculated using $< C_D >_2 = f(< Re >_2)$, where the mean Reynolds number is defined by $< Re >_2 = < |\mathbf{u}_r| >_2 d_p/\nu_1$. The norm of the instantaneous relative velocity is, according to He and Simonin,[18] approximated to $< |\mathbf{u}_r| >_2^2 = U_{ri} U_{ri} + < u_{ri}' u_{ri}' >_2$. The particle relaxation time represents the entrainment of the particles by the continuous phase. Therefore, the ratio $\eta = \tau_{12}^{t}/\tau_{12}^{x}$ represents the efficiency of turbulence to entrain particles. In the frame of the kinetic theory, the particle–particle collision time is

$$\tau_2^c = \frac{d_p}{24 \alpha_2 g_0} \left(\frac{\pi}{T_2} \right)^{1/2}, \tag{5}$$

where $T_2 = < u_{2i}' u_{2i}' >_2 /3$ is the granular temperature and g_0 is a distribution function to be described later. τ_2^c represents the time experienced by a given particle between two consecutive binary collisions.

1.3. *Classification of Gas–Solid Flows*

Elgobashi[19] proposed a classification for gas–solid suspensions based on some of the previous characteristic time scales, but also on the relative distance between the particles, $(\mathbf{x_2} - \mathbf{x_1})/d_p$, and the Kolmogorov time scale, τ_K (Fig. 2). When the suspension is very dilute, say $\alpha_2 < 10^{-6}$, Fig. 2 shows that particles have no effect on the turbulent motion of the continuous phase, but their motion can be governed by the turbulent motion of the continuous phase if their inertia is sufficiently small. This is called "**one-way coupling**". When the particle volume fraction is increased, say up to $\alpha_2 = 10^{-3}$, the effects of the presence of particles on the turbulent motion of the continuous phase can be observed. This is called "**two-way coupling**". In this region, turbulence can be modified in two ways: it can be enhanced or it can be damped. For a given volumetric fraction, turbulence can be enhanced when the particle relaxation time is increased (which means that the particle diameter is increased; Eq. (4)). It is commonly accepted that when the particle Reynolds number exceeds some critical value, vortex shedding occurs and enhances (or produces) turbulent kinetic energy.[20] On the contrary, when the particle relaxation time is decreased, there is no vortex shedding and energy is dissipated due to the work done by the eddies to accelerate particles. Two-way coupling has been observed experimentally.[21] The two mechanisms, vortex shedding and work done by the eddies, are believed to be the dominant mechanisms for turbulence modulation is gas–solid flows. In general, for gas–solid flows, five mechanisms may be responsible for turbulence modulation.[22] These mechanisms are (1) dissipation of turbulent kinetic energy by the particles, (2) increase of the turbulent viscosity due to the presence of particles, (3) shedding of vortices behind the particles, (4) fluid moving with the particles as added fluid mass to the particles and (5) enhancement of the velocity gradient between two particles. These mechanisms may not be independent and, moreover, mechanisms (2) and (5) might be of minor importance in very dilute flows. When the particle volume fraction exceeds a certain value, say $\alpha_2 > 10^{-3}$, the relative distance between particles is small enough so that particles collide. This is called "**four-way coupling**". In most fluidization applications, four-way coupling is expected to occur, at least in the dense regions of the bed.

A systematic classification of gas–solid flows, which does not include the turbulence modulation aspect, can be made from the characteristic time scales. When $\tau_{12}^{x} \ll \tau_{12}^{t}$, particle motion is governed by gas phase turbulence, whereas when $\tau_{12}^{x} \gg \tau_{12}^{t}$, particle motion is only slightly affected by gas phase turbulence, in a random way. These two asymptotic behaviors are called the scalar limit case and the coarse particle case, respectively. When $\tau_2^c \ll \tau_{12}^{x}$, particle motion is governed by particle collision mechanisms, whereas when $\tau_{12}^{x} \ll \tau_2^c$ particle motion is governed by gas phase turbulence, so that the interstitial gas influences the mean free path. These two asymptotic behaviors are called dense and dilute suspensions, respectively. When the mean relative velocity is zero, it can be shown that $\tau_{12}^{t} \sim \tau_1^{t}$ (non-settling particles), whereas when there is a mean relative velocity $\tau_{12}^{t} < \tau_1^{t}$ (settling particles).

A third alternative for the classification of gas–solid flows is given by Koch.[23] This classification is limited to dilute suspensions with particles having small Reynolds numbers, $Re \ll 1$, and a large Stokes number, $St \gg 1$. If $St \gg \alpha_2^{-3/2}$, very massive particles, the collisional mechanism is dominant. If $\alpha_2^{-3/4} \ll St \ll \alpha_2^{-3/2}$, moderately massive particles, the fluid–particle interaction mechanism is dominant and is similar to the one observed in fixed beds, so that the particle velocity does not change significantly during a fluid–dynamic interaction. If $1 \ll St \ll \alpha_2^{-3/4}$, slightly massive particles, the fluid–particle interactions are dominant but are no longer similar to the fixed bed case.

Finally, it should be noted that other scales can be of importance, for example the integral Eulerian length scale, $L_1^{t} = C_\mu k_1^{3/2}/\epsilon_1$. This dependency is illustrated by Gore and Crowe,[21] who classify two-way coupling as a function of the ratio of the particle diameter to the integral Eulerian length scale. Below a certain value of d_p/L_1^{t}, 0.1 according to Gore and Crowe, turbulence is attenuated, whereas above this value turbulence is enhanced.

2. KINETIC THEORY OF GRANULAR FLOW

The kinetic theory of granular flow is based on the similarities between the flow of a granular material, a

population of particles with or without an interstitial gas, and the molecules of a gas. This treatment uses classical results from the kinetic theory of gases[24] in order to predict the form of the transport equations, mass, momentum and energy, and the corresponding specific quantities, the mean flux of momentum and energy and the mean rate of energy dissipation, for a granular material. One of the most complete works in the field of the kinetic theory of granular flow is due to Jenkins and Richman.[12] Their results are derived from the classical results of the kinetic theory of dense gases,[24] in combination with Grad's theory.[25] In this review, the method of Grad is preferred to that of Chapman–Enskog, which has been used by Lun *et al.*[26] to derive equations similar to the ones proposed by Jenkins and Richman. As a matter of fact, it will be shown in the following that the method of Grad gives direct access to the moments, whereas in the method of Chapman–Enskog integration has to be performed when the probability density function is known. The contribution of Jenkins and Richman[12] is a linear theory (perturbation analysis) which gives analytical solutions for mean flux of momentum and energy and for the mean dissipation rate, but it also gives an expression for the particle velocity probability density function. The complete derivation of the results of Jenkins and Richman[12] requires a great many intermediary results (Section 2.1–2.6) before the final formulation (Section 2.7). We begin with the Maxwell–Boltzmann equation.

2.1. *Maxwell–Boltzmann Equation*

The probability of finding a sphere at a position $\mathbf{x}$ with a velocity $\mathbf{c}$ in the volume element $\mathrm{d}\mathbf{x}$ and in the element of volume in the velocity space $\mathrm{d}\mathbf{c}$ is $f^1(\mathbf{x},\mathbf{c},t)\mathrm{d}\mathbf{x}\mathrm{d}\mathbf{c}$, where $f^1(\mathbf{x},\mathbf{c},t)$ is the particle velocity probability density function. Considering a population of identical, smooth, rigid spheres, a conservation equation for the number of spheres in a volume element can be formulated in terms of $f^1(\mathbf{x},\mathbf{c},t)$ as[24]

$$\frac{\partial f^1}{\partial t}+\frac{\partial}{\partial x_i}(c_i f^1)+\frac{\partial}{\partial c_i}(F_i f^1)=\left.\frac{\partial f^1}{\partial t}\right|_{\mathrm{c}}, \tag{6}$$

where F_i is the external force per unit of mass acting on a sphere and $\partial f^1/\partial t|_{\mathrm{c}}$ is the rate of change of the distribution function due to particle collisions. According to Simonin,[27] F_i can be written as

$$F_i=\frac{1}{\tau_{12}^{\mathrm{x}}}(\tilde{u}_{li}-c_i)-\frac{1}{\rho_2}\frac{\partial \tilde{p}_1}{\partial x_i}+g_i. \tag{7}$$

The number of particles per unit volume is defined by

$$n=\int f^1(\mathbf{x},\mathbf{c},t)\mathrm{d}\mathbf{c} \tag{8}$$

and the averaged value of a given function $\psi(c)$ by

$$<\psi(\mathbf{c})>_2=\frac{1}{n}\int\psi(\mathbf{c})f^1(\mathbf{x},\mathbf{c},t)\mathrm{d}\mathbf{c}. \tag{9}$$

The mean velocity of the discrete phase, U_{2i}, is defined by Eq. (9) with $\psi(\mathbf{c})=c_i$. The peculiar velocity or fluctuation velocity is introduced, $C_i=U_{2i}-c_i$. Multiplying Eq. (6) by $\psi(\mathbf{c})$ and integrating over the whole velocity domain gives a transport equation for $<\psi(\mathbf{c})>_2$, as proposed by Chapman and Cowling.[24] The transport equation for the mean quantity, $<\psi(\mathbf{c})>_2$, is

$$\frac{\partial}{\partial t}(n<\psi>_2)+\frac{\partial}{\partial x_i}(n<\psi c_i>_2)-n\left(\left\langle\frac{\partial\psi}{\partial t}\right\rangle_2+\left\langle c_i\frac{\partial\psi}{\partial x_i}\right\rangle_2+\left\langle F_i\frac{\partial\psi}{\partial x_i}\right\rangle_2\right)=C(\psi), \tag{10}$$

where the collisional rate of change (per unit volume) for ψ, $C(\psi)$, is given by

$$C(\psi)=\int\psi\left.\frac{\partial f^1}{\partial t}\right|_{\mathrm{c}}\mathrm{d}\mathbf{c}. \tag{11}$$

In Eq. (10), the time and space derivatives of ψ are not eliminated, because in this equation ψ can be a function of time and space, $\psi(\mathbf{x},t)$. However, it is more convenient to rewrite Eq. (10) using the fluctuating velocity as the independent variable: $f^1(\mathbf{x},\mathbf{c},t)$ is changed to $f^1(\mathbf{x},\mathbf{C},t)$. In this case, ψ is a function of the fluctuating velocity, $\psi(\mathbf{C})$. The Maxwell–Boltzmann equation, Eq. (6), can be rewritten using the chain rule on the derivative operators, $\partial/\partial t=\partial/\partial t-(\partial U_{2i}/\partial t)\partial/\partial C_i$ for the time derivative, $\partial/\partial x_i=\partial/\partial x_i-(\partial U_{2j}/\partial x_i)\partial/\partial C_j$ for the space derivative and $\partial/\partial c_i=\partial/\partial C_i$ for the velocity derivative. With the same averaging procedure as for Eq. (10), the Enskog equation can be written (Ref. 24, Section 3.12). This equation reads

$$\frac{D_2}{Dt}n<\psi>_2+<n\psi>_2\frac{\partial U_{2i}}{\partial x_i}+\frac{\partial}{\partial x_i}(n<\psi C_i>_2)+n\left(\frac{D_2U_{2i}}{Dt}\left\langle\frac{\partial\psi}{\partial C_i}\right\rangle_2-\left\langle F_i\frac{\partial\psi}{\partial C_i}\right\rangle_2+\frac{\partial U_{2j}}{\partial x_i}\left\langle C_i\frac{\partial\psi}{\partial C_j}\right\rangle_2\right)=C(\psi). \tag{12}$$

In this expression, terms involving a space or time derivative of ψ are equal to zero. We now express the collisional rate of change of ψ in a more useful form.

2.2. *Collisional Rate of Change*

The collisional rate of change of ψ per unit volume is the integral, over all possible binary collisions, of the change of ψ due to a binary collision multiplied by the probability of such a collision. In order to evaluate the probability per unit of time of a binary collision, the pair distribution function f^2 is introduced, where $f^2(\mathbf{x}_1,\mathbf{x}_2,\mathbf{c}_1,\mathbf{c}_2)\,\mathrm{d}\mathbf{x}_1\,\mathrm{d}\mathbf{x}_2\,\mathrm{d}\mathbf{c}_1\,\mathrm{d}\mathbf{c}_2$ is the probability of finding a pair of particles 1 and 2 centered at $\mathbf{x}_1$, $\mathbf{x}_2$ with a velocity $\mathbf{c}_1$, $\mathbf{c}_2$ in the volume element $\mathrm{d}\mathbf{x}_1$, $\mathrm{d}\mathbf{x}_2$ and the velocity range $\mathrm{d}\mathbf{c}_1$, $\mathrm{d}\mathbf{c}_2$, respectively. A particle 1 $(\mathbf{x}_1,\mathbf{c}_1)$ collides with a particle 2 $(\mathbf{x},\mathbf{c}_2)$ if the center of particle 1 is located in an elementary cylinder of volume $d_{\mathrm{p}}^2(\mathbf{g}\cdot\mathbf{k})\,\mathrm{d}\mathbf{k}\,\mathrm{d}t$ (at this point of the derivation, $\mathbf{x}$ is used for a reason of expediency in order not to repeat indices with

derivatives). The relative velocity is $\mathbf{g} = \mathbf{c}_1 - \mathbf{c}_2$, the unit vector $\mathbf{k}$ is defined by $d_p\mathbf{k} = \mathbf{x} - \mathbf{x}_1$ with $\mathbf{g}\cdot\mathbf{k} > 0$ (this condition means that collision is possible). The number of probable binary collisions per unit of time between two such particles is given by Chapman and Cowling[24] (Sections 3.4, 3.5 and 16.2) as

$$f^2(\mathbf{x} - d_p\mathbf{k}, \mathbf{x}, \mathbf{c}_1, \mathbf{c}_2, t) d_p^2(\mathbf{g}\cdot\mathbf{k})\, \mathrm{d}\mathbf{k}\, \mathrm{d}\mathbf{x}\, \mathrm{d}\mathbf{c}_1\, \mathrm{d}\mathbf{c}_2. \quad (13)$$

Therefore, the collisional rate of change for a property ψ_2, of particle 2, which is changed into ψ_2' after collision, can be written

$$C(\psi) = \int_{\mathbf{g}\cdot\mathbf{k}>0} (\psi_2' - \psi_2) f^2(\mathbf{x} - d_p\mathbf{k}, \mathbf{x}, \mathbf{c}_1, \mathbf{c}_2, t) d_p^2(\mathbf{g}\cdot\mathbf{k}) \times \mathrm{d}\mathbf{k}\, \mathrm{d}\mathbf{c}_1\, \mathrm{d}\mathbf{c}_2. \quad (14)$$

Due to the symmetry of a collision, the problem can be reformulated for a particle 2 ($\mathbf{x}_2$,$\mathbf{c}_2$), which will collide with a particle 1 ($\mathbf{x}$,$\mathbf{c}_1$). Changing $\mathbf{k}$ in $-\mathbf{k}$, the collisional rate of change for a property ψ_1, of particle 1, which is changed into ψ_1' after collision can be written as

$$C(\psi) = \int_{\mathbf{g}\cdot\mathbf{k}>0} (\psi_1' - \psi_1) f^2(\mathbf{x}, \mathbf{x} + d_p\mathbf{k}, \mathbf{c}_1, \mathbf{c}_2, t) d_p^2(\mathbf{g}\cdot\mathbf{k}) \times \mathrm{d}\mathbf{k}\, \mathrm{d}\mathbf{c}_1\, \mathrm{d}\mathbf{c}_2. \quad (15)$$

According to Jenkins and Richman,[12] a more symmetric expression of $C(\psi)$ is written as half the sum of Eqs (14) and (15). In order to express this half sum in a more useful way, the following Taylor series expansion is used, where the velocity and time dependence are dropped for the sake of simplicity:

$$f^2(\mathbf{x} - d_p\mathbf{k}, \mathbf{x}) = f^2(\mathbf{x}, \mathbf{x} + d_p\mathbf{k}) - d_p k_i \frac{\partial}{\partial x_i}\left(1 - \frac{d_p}{2!} k_j \frac{\partial}{\partial x_j} + \ldots\right) \times f^2(\mathbf{x}, \mathbf{x} + d_p\mathbf{k}). \quad (16)$$

Inserting Eq. (16) in Eq. (15), Jenkins and Richman[12] rewrite the collisional rate of change as

$$C(\psi) = \chi(\psi) - \frac{\partial}{\partial x_i}\theta_i(\psi) - \frac{\partial U_{2j}}{\partial x_i}\theta_i\left(\frac{\partial \psi}{\partial C_j}\right). \quad (17)$$

In the derivation of this expression, several transformations are made. The chain rule is applied and the integral operator and the derivative operator in Eq. (16) are commuted. The latter manipulation is valid because the Taylor series expansion is written for a fixed point in space, which allows the commutation of both operators. The fluctuating velocity is then introduced to obtain the third term in Eq. (17). The source term, $\chi(\psi)$, is defined by

$$\chi(\psi) = \frac{1}{2}\int_{\mathbf{g}\cdot\mathbf{k}>0} \Delta\psi f^2(\mathbf{x}_1, \mathbf{x}_2, \mathbf{c}_1, \mathbf{c}_2, t) d_p^2(\mathbf{g}\cdot\mathbf{k})\, \mathrm{d}\mathbf{k}\, \mathrm{d}\mathbf{c}_1\, \mathrm{d}\mathbf{c}_2, \quad (18)$$

where $\mathbf{x}_2 - \mathbf{x}_1 = d_p\mathbf{k}$ and $\Delta\psi = (\psi_2' + \psi_1') - (\psi_2 + \psi_1)$.

The flux term, $\theta_i(\psi)$, is defined by

$$\theta_i(\psi) = -\frac{d_p}{2}\int_{\mathbf{g}\cdot\mathbf{k}>0} (\psi_1' - \psi_1) k_i \left(1 - \frac{d_p}{2!} k_j \frac{\partial}{\partial x_j} + \ldots\right) \times f^2(\mathbf{x}_1, \mathbf{x}_2, \mathbf{c}_1, \mathbf{c}_2, t) d_p^2(\mathbf{g}\cdot\mathbf{k})\, \mathrm{d}\mathbf{k}\, \mathrm{d}\mathbf{c}_1\, \mathrm{d}\mathbf{c}_2. \quad (19)$$

The flux term, $\theta_i(\psi)$, represents the transfer of ψ during collision, whereas the source term, $\chi(\psi)$, represents the loss of ψ caused by inelastic collisions. To calculate the integrals defining the source term and the flux term, appropriate expressions for the pair distribution functions, $\Delta\psi$ and $\psi_1' - \psi_1$, have to be found. We begin with $\Delta\psi$ and $\psi_1' - \psi_1$.

2.3. *Binary Collisions*

Let us consider an inelastic collision between two smooth identical spherical particles 1 and 2, of mass m and diameter d_p. If $\mathbf{J}$ is the impulse of the force exerted by particle 1 on particle 2, the momentum conservation over a collision gives

$$m\mathbf{c}_1 = m\mathbf{c}_1' - \mathbf{J}, \quad m\mathbf{c}_2 = m\mathbf{c}_2' + \mathbf{J}, \quad (20)$$

where $\mathbf{c}_1'$, $\mathbf{c}_2'$ are the velocities of the particles after collision and $\mathbf{c}_1$, $\mathbf{c}_2$ those before collision. It is stated that the relative velocity component normal to the plane of contact, $\mathbf{g}\cdot\mathbf{k}$ (before collision) and $\mathbf{g}'\cdot\mathbf{k}$ (after collision), satisfies

$$\mathbf{g}'\cdot\mathbf{k} = -e(\mathbf{g}\cdot\mathbf{k}), \quad (21)$$

where the relative velocity after collision is defined by $\mathbf{g}' = \mathbf{c}_1' - \mathbf{c}_2'$ and e is the restitution coefficient. The restitution coefficient varies form zero to one: if it is equal to one, the collision is elastic, which means that there is no energy loss during collision, otherwise the collision is inelastic, which means that there is energy dissipation during collision. With Eqs (20) and (21), the impulse of the force exerted by particle 1 on particle 2 is given by

$$J_i = \frac{1}{2}m(1+e)(g_j k_j)k_i. \quad (22)$$

Expressions for the change in the velocity moments can now be derived from Eqs (20)–(22). The change in the first, second and third velocity moments of particle 1 are defined by $\delta(c_{1i}) = c_{1i}' - c_{1i}$, $\delta(c_{1i}c_{1j}) = c_{1i}'c_{1j}' - c_{1i}c_{1j}$ and $\delta(c_{1i}c_{1j}c_{1m}) = c_{1i}'c_{1j}'c_{1m}' - c_{1i}c_{1j}c_{1m}$, respectively. The change in the first moment is of course $\delta(c_{1i}) = -J_i$ (Eq. (20)) and the change in the second and third moments is, where the index 1 is dropped for the sake of simplicity,

$$\delta(c_i c_j) = \frac{1}{2}(1+e)(g_m k_m) \times \left(\frac{1}{2}(1+e)(g_m k_m)k_i k_j - (c_j k_i + c_i k_j)\right),$$

$$\delta(c_i c_j c_m) = -\frac{1}{2}(1+e)(g_n k_n) \times [k_{(i}c_j c_{m)} - \frac{1}{2}(1+e)(g_n k_n)k_{(i}k_j c_{m)} - \frac{1}{2}(1+e)^2(g_n k_n)^2 k_i k_j k_m]. \quad (23)$$

The notation with parentheses as an index stands for the sum of all possible permutations, $k_{(i}c_jc_{m)} = k_ic_jc_m + k_jc_mc_i + k_mc_ic_j$. Similar expressions can be derived for the change in the velocity moments of particle 2. The total change in the first, second and third moments are defined by $\Delta(c_i) = \delta(c_{1i}) + \delta(c_{2i})$, $\Delta(c_ic_j) = \delta(c_{1i}c_{1j}) + \delta(c_{2i}c_{2j})$ and $\Delta(c_{1i}c_{1j}c_{1p}) = \delta(c_{1i}c_{1j}c_{1p}) + \delta(c_{2i}c_{2j}c_{2p})$, respectively. The total change in the first, second and third moments is expressed by

$$\Delta(c_i) = 0,$$

$$\Delta(c_jc_j) = \frac{1}{2}(1+e)(g_mk_m)((1+e)(g_mk_m)k_ik_j - (g_ik_i + g_ik_j)),$$

$$\Delta(c_ic_jc_p) = Q_{(i}\Delta(c_jc_{p)}), \tag{24}$$

where $Q_i = \frac{1}{2}(c_{1i} + c_{2i})$. These expressions are also valid for the fluctuating velocities. $\Delta\psi$ and $\delta\psi$ have been expressed in terms of the velocity parameters before collision and the restitution coefficient.

2.4. *Pair Distribution Function*

In the kinetic theory of dilute gases, molecular chaos can be assumed and the velocities of two colliding particles are uncorrelated. The pair distribution function $f^2(\mathbf{x}_1,\mathbf{x}_2,\mathbf{c}_1,\mathbf{c}_2,t)$ can then be expressed simply as the product of the two particle velocity probability density functions $f^1(\mathbf{x}_1,\mathbf{c}_1,t)$ and $f^1(\mathbf{x}_2,\mathbf{c}_2,t)$. In the case of a very dilute suspension, this hypothesis can be applied if the particle inertia is high enough so that the particle is not transported by the velocity fluctuations of the continuous phase. In dense suspensions, the velocities of two colliding particles are correlated and the pair distribution function can be expressed, according to Chapman and Cowling[24] (Chap. 16), by

$$f^2(\mathbf{x}_1,\mathbf{x}_2,\mathbf{c}_1,\mathbf{c}_2,t) = g_0(\mathbf{x})f^1(\mathbf{x} - \frac{1}{2}d_p\mathbf{k},\mathbf{c}_1,t) \times f^1(\mathbf{x} + \frac{1}{2}d_p\mathbf{k},\mathbf{c}_2,t), \tag{25}$$

where the radial distribution function, $g_0(\mathbf{x}) \geq 1$, represents the increase of the binary collision probability when the suspension becomes denser. The position of the point of collision, $\mathbf{x}$, is now defined by $\mathbf{x}_1 + \mathbf{x}_2 = 2\mathbf{x}$. An empirical expression for $g_0(\mathbf{x})$ is discussed in Section 2.9.

2.5. *Transport Equations*

The pair distribution function has now been expressed in terms of the particle velocity probability density function. To proceed, an expression for the particle velocity probability density function has to be found. Let us leave this problem for a moment and formulate the transport equations, and show that the second- and third-order moment (velocity moment) equations can be used to find an expression for the particle velocity probability density function. The transport equation for the moment of order p, $M_{2ij\ldots p} = < C_iC_j\ldots C_p >_2$, can be obtained from Eq. (10) in combination with Eq. (17) with $\psi = C_iC_j\ldots C_p$. In this case, the time and space derivatives of ψ in (10) must be kept because the mean velocity is a function of time and space, $U_{2i}(\mathbf{x},t)$, and therefore the fluctuating velocity is a function of $\mathbf{x},\mathbf{c},t$. Noticing that $\alpha_2\rho_2 = nm$, the general transport equation has the final form

$$\frac{\partial}{\partial t}(\alpha_2\rho_2 < \psi >_2) + \frac{\partial}{\partial x_i}(\alpha_2\rho_2 < \psi c_i >_2) = -\frac{\partial}{\partial x_i}\theta_i(m\psi) - \frac{\partial U_{2j}}{\partial x_i}\theta_i\left(m\frac{\partial\psi}{\partial C_j}\right) + \alpha_2\rho_2\left(\left\langle\frac{\partial\psi}{\partial t}\right\rangle_2 + \left\langle c_i\frac{\partial\psi}{\partial x_i}\right\rangle_2 + \left\langle F_i\frac{\partial\psi}{\partial c_i}\right\rangle_2\right) + \chi(m\psi). \tag{26}$$

The transport equations for the different moments can also be obtained from Eq. (12) in combination with Eq. (17). In this case, the independent variable is the fluctuating velocity, and therefore all time and space derivatives of ψ are equal to zero. This form is more convenient than Eq. (26), especially for the moments of order 2 and higher, because all terms appear naturally. This general transport equation has the final form

$$\frac{D_2}{Dt}\alpha_2\rho_2 < \psi >_2 + \alpha_2\rho_2 < \psi >_2 \frac{\partial U_{2i}}{\partial x_i} + \frac{\partial}{\partial x_i}(\alpha_2\rho_2 < \psi C_i >_2) = -\frac{\partial}{\partial x_i}\theta_i(m\psi) - \alpha_2\rho_2\left(\frac{D_2U_{2i}}{Dt}\left\langle\frac{\partial\psi}{\partial C_i}\right\rangle_2 - \left\langle F_i\frac{\partial\psi}{\partial C_i}\right\rangle_2\right) - \frac{\partial U_{2j}}{\partial x_i}\left(\alpha_2\rho_2\left\langle C_i\frac{\partial\psi}{\partial C_j}\right\rangle_2 + \theta_i\left(m\frac{\partial\psi}{\partial C_j}\right)\right) + \chi(m\psi). \tag{27}$$

In the following sections, the source term of the collisional rate of change is written, $\chi(mC_iC_j\ldots C_n) = \chi_{ij\ldots n}$, and the flux term of the collisional rate of change is denoted, $\theta_p(mC_iC_j\ldots C_n) = \theta_{ij\ldots np}$.

2.5.1. *Continuity equation*

The continuity equation is obtained from Eq. (26) with $\psi = 1$,

$$\frac{\partial}{\partial t}(\alpha_2\rho_2) + \frac{\partial}{\partial x_j}(\alpha_2\rho_2U_{2j}) = 0. \tag{28}$$

2.5.2. *Momentum equation*

The momentum equation is obtained from Eq. (27) with $\psi = C_i$,

$$\alpha_2\rho_2\frac{D_2}{Dt}U_{2i} = -\alpha_2\frac{\partial P_1}{\partial x_i} - \frac{\partial}{\partial x_j}\Sigma_{2ij} - \frac{\alpha_2\rho_2}{\tau_{12}^r}U_{ri} + \alpha_2\rho_2g_i, \tag{29}$$

where $\sum_{2ij} = \theta_{ij} + \alpha_2\rho_2 M_{2ij}$ is the effective stress tensor and $\chi_i = 0$ (see Eqs (18) and (24)). The second term on the right-hand-side (RHS) represents the transport of momentum by velocity fluctuations and by collisions, whereas the remaining terms on the RHS represent the influence of the forces acting on the particles. Pressure fluctuations have been neglected, which is a correct assumption for gas–solid flows according to Bel Fdhila and Simonin.[28]

2.5.3. *Second-order moment equation*

The transport equation for the moment of order 2 is obtained from Eq. (27) using $\psi = C_iC_j$ and neglecting the pressure fluctuations as done for the momentum equation. The equation for the second-order moment is

$$\alpha_2\rho_2 \frac{D_2}{Dt} M_{2ij} = -\frac{\partial}{\partial x_m} E_{ijm} - \Sigma_{2im}\frac{\partial U_{2j}}{\partial x_m} - \Sigma_{2jm}\frac{\partial U_{2i}}{\partial x_m} - \frac{2\alpha_2\rho_2}{\tau_{12}^x}(M_{2ij} - M_{12ij}) + \chi_{ij}, \tag{30}$$

where $E_{ijm} = \theta_{ijm} + \alpha_2\rho_2 M_{2ijm}$. The third-order moment is defined by $M_{2ijm} = < C_iC_jC_m >_2$ and the fluid–particle velocity correlation tensor is given by $2M_{12ij} = < u''_{1(i}C_{j)} >_2$, where $u''_{1i} = \tilde{u}_{1i} - < \tilde{u}_{1i} >_2$ represents the fluctuating velocity of the continuous phase seen by the particle phase. The first term on the RHS represents the transport of stress by velocity fluctuations and collisions. The second and third terms represent the production of stress by the mean velocity gradient. The fourth term represents the interaction with the continuous phase (a production or a destruction term). The last term represents the interactions due to collisions. The fourth term, $\prod_{2ij}$, can be split into two terms, $\prod_{2ij} = \prod_{2ij}^{D} + \prod_{2ij}^{P}$. The first term, $\prod_{2ij}^{D} = -2\alpha_2\rho_2 M_{2ij}/\tau_{12}^x$, represents the dissipation due to the drag force, and the second term, $\prod_{2ij}^{P} = 2\alpha_2\rho_2 M_{12ij}/\tau_{12}^x$, production due to the interaction with turbulence.

2.5.4. *Energy equation*

The transport equation for the granular temperature T_2 is obtained from Eq. (30) by summing up the diagonal terms, $i = j$, and changing indices, or from Eq. (27) with $\psi = C_mC_m$

$$3\alpha_2\rho_2 \frac{D_2}{Dt} T_2 = -\frac{\partial}{\partial x_i} E_{mmi} - 2\Sigma_{2im}\frac{\partial U_{2m}}{\partial x_i} - \frac{2\alpha_2\rho_2}{\tau_{12}^x}(3T_2 - M_{12mm}) + \chi_{mm}. \tag{31}$$

A transport equation for the turbulent kinetic energy of the discrete phase, k_2, can also be written with $2k_2 = 3T_2$. The first term on the RHS represents the transport of energy by velocity fluctuations and collisions. The second term represents the production of energy by the mean velocity gradient. The third term represents the interaction with the continuous phase (a production or a destruction term). The last term represents the loss of energy due to collisions.

2.5.5. *Third-order moment equation*

The transport equation for the moment of order 3 is obtained from Eq. (27) using $\psi = C_iC_jC_m$ and neglecting the pressure fluctuations,

$$\alpha_2\rho_2 \frac{D_2}{Dt} M_{2ijm} = -\frac{\partial}{\partial x_n} E_{ijmn} - E_{imn}\frac{\partial U_{2j}}{\partial x_n} - E_{jmn}\frac{\partial U_{2i}}{\partial x_n} - E_{ijn}\frac{\partial U_{2m}}{\partial x_n} + M_{2ij}\frac{\partial}{\partial x_n}\Sigma_{2mn} + M_{2im}\frac{\partial}{\partial x_n}\Sigma_{2jn} + M_{2jm}\frac{\partial}{\partial x_n}\Sigma_{2in} - \frac{3\alpha_2\rho_2}{\tau_{12}^x}(M_{2ijm} - M_{12ijm}) + \chi_{ijm}, \tag{32}$$

where $E_{ijmn} = \theta_{ijmn} + \alpha_2\rho_2 M_{2ijmn}$ and where the fourth-order moment is defined by $M_{2ijmn} = < C_iC_jC_mC_n >_2$. The fluid–particle velocity correlation tensor is defined by $3M_{12ijm} = < u''_{1(i}C_jC_{m)} >_2$. The first term on the RHS represents the transport of the third-order moment by velocity fluctuations and collisions. The six following terms on the RHS represent the production by mean velocity gradients and by second-order moment gradients, respectively. The two remaining terms on the RHS represent the interactions with the continuous phase and the interactions due to collisions, respectively.

2.6. *Grad's Theory*

The transport equations have been written up to the third-order moment. We use these equations with a third-order approximation of the particle velocity probability density function to express a closed set of equations. Following the idea of Enskog, Chapman and Cowling[24] (Section 7.1), Grad[25] wrote the particle velocity probability density function as a series of Hermite polynomials, $H_i^{(n)}(\mathbf{c})$, as

$$f^1(\mathbf{x}, \mathbf{c}, t) = f^0(\mathbf{x}, \mathbf{c}, t) \sum_{n=0}^{\infty} \frac{1}{n!} a_i^n(\mathbf{x}, t) H_i^n(\mathbf{c}), \tag{33}$$

where the tensors $a_i^n(\mathbf{x}, t)$ are symmetric in all of their indices and where the Hermite polynomials can be expressed in terms of $f^0(\mathbf{x},\mathbf{c},t)$, the Maxwellian distribution function,

$$f^0(\mathbf{x}, \mathbf{c}, t) = \frac{n}{(2\pi T_2)^{3/2}} \exp(-\mathbf{C}^2/2T_2). \tag{34}$$

Here, $C_i^2 = (c_i - U_{2i})^2$ and the granular temperature, T_2, have been used in analogy with the kinetic theory of gases. In the frame of the kinetic theory of gases, the Maxwellian distribution function is the solution to the Maxwell–Boltzmann equation under the following assumptions: a gas at uniform steady state, whose spherical molecules possess only energy of translational motion and are subject to no external forces. This is called the Maxwellian state. Equation (34) simply means that for a uniform gas in which density, mean velocity and temperature are assigned, there is only one possible mode of distribution of the molecular velocities (Ref. 24, Section 4.1). Grad proposed to make a

third-order approximation in Eq. (33), which is a reasonable assumption if the flow is not varying too quickly (this assumption is not valid, for instance, in strong shock waves). The particle velocity probability density function can then be written

$$f^1 = f^0\left(H^0 + a_i H_i^1 + \frac{1}{2!}a_{ij}H_{ij}^2 + \frac{1}{3!}a_{ijm}H_{ijm}^3\right), \quad (35)$$

where the Hermite polynomials are defined in terms of the derivatives of the Maxwellian distribution function,

$$f^1 = \left(1 - a_i\frac{\partial}{\partial c_i} + \frac{1}{2!}a_{ij}\frac{\partial^2}{\partial c_i \partial c_j} - \frac{1}{3!}a_{ijm}\frac{\partial^3}{\partial c_i \partial c_j \partial c_m}\right)f^0, \quad (36)$$

and

$$H^0 = 1,$$

$$H_i^1 = \frac{1}{f^0}\frac{\partial f^0}{\partial c_i} = -C_i/T_2,$$

$$H_{ij}^2 = \frac{1}{f^0}\frac{\partial^2 f^0}{\partial c_i \partial c_j} = -\delta_{ij}/T_2 + C_iC_j/T_2^2,$$

$$H_{ijm}^3 = \frac{1}{f^0}\frac{\partial^3 f^0}{\partial c_i \partial c_j \partial c_m}$$

$$= (C_i\delta_{jm} + C_j\delta_{im} + C_m\delta_{ij})/T_2^2 - C_iC_jC_m/T_2^3. \quad (37)$$

With Eqs (9) and (36), the velocity moments and the coefficients of the series expansion, a_i, a_{ij}, a_{ijm}, can be related. For the velocity moment of order 0 (Eq. (8)), no constraint is put on Grad's approximation, whereas for the velocity moment of order 1, we find of course that $a_i = 0$. Furthermore, it can be shown[12] that the second-order velocity moment is defined by

$$M_{2ij} = \delta_{ij}T_2 + a_{ij} \Rightarrow a_{ii} = 0, \quad (38)$$

the third-order velocity moment by

$$M_{2ijm} = a_{ijm}, \quad (39)$$

and the fourth-order velocity moment by

$$M_{2ijmn} = 3T_2^2\delta_{(ij}\delta_{mn)} + 6T_2 a_{(ij}\delta_{mn)}. \quad (40)$$

In theory, with a third-order truncation, the 20 unknown variables α_2, U_{2i}, T_2, a_{ij}, a_{ijm} are determined by 20 distinct transport equations: the continuity, momentum, granular temperature equations and the second- and third-moment equations. Grad proposes to simplify this system of 20 unknown variables to 13 unknown variables by making a contraction on the third-order tensor:

$$a_{ijm} = \frac{1}{5}(a_{inn}\delta_{jm} + a_{jnn}\delta_{in} + a_{mnn}\delta_{ij}) + \beta_{ijm} \text{ with } \beta_{ijm} = 0. \quad (41)$$

This decomposition is similar to that of a second-order tensor in a deviatoric and an isotropic part. This gives a physical meaning to the coefficients a_{ij} and a_{ijm}. The first one is the deviatoric part of the fluctuation stress tensor (see Eq. (38)) and the second is the transport part of the energy flux vector (see Eqs (31) and (39)). The particle velocity probability distribution function can then be written as

$$f^1 = \left(1 + \frac{a_{ij}}{2T_2^2}C_iC_j + \frac{a_{imm}}{10T_2^2}\left(\frac{\mathbf{C}^2}{T_2} - 5\right)C_i\right)f^0. \quad (42)$$

The system of 13 unknowns can be solved with the continuity equation (Eq. (28)), the momentum equation (Eq. (29)), the energy equation (Eq. (31)) and a transport equation for a_{ij} and for a_{imm}. The transport equation for a_{ij} is written using Eqs (30), (31), (38), (39) and (41). This yields

$$\alpha_2\rho_2\frac{D_2}{Dt}a_{ij} + \frac{\partial}{\partial x_m}(\theta_{ijm} - \theta_{nnm}\delta_{ij}/3) + \left(\Xi_{im}\frac{\partial U_{2j}}{\partial x_m} - \Xi_{jm}\frac{\partial U_{2i}}{\partial x_m} - \frac{2}{3}\Xi_{nm}\frac{\partial U_{2n}}{\partial x_m}\delta_{ij}\right) + \frac{1}{5}\left(\frac{\partial}{\partial x_j}(\alpha_2\rho_2 a_{imm}) + \frac{\partial}{\partial x_i}(\alpha_2\rho_2 a_{jmm}) - \frac{2}{3}\frac{\partial}{\partial x_n}2(\alpha_{2\rho 2}a_{nmm})\delta_{ij}\right) + 2\alpha_2\rho_2 T_2\hat{S}_{2ij} - \frac{2\alpha_2\rho_2}{\tau_{12}^x}(a_{ij} - (M_{12ij} - M_{12mm}\delta_{ij}/3)) = \chi_{ij} + \chi_{mm}\delta_{ij}/3, \quad (43)$$

where $\Xi_{ij} = \theta_{ij} + \alpha_2\rho_2 a_{ij}$ and where $\hat{S}_{2ij} = S_{2ij} - S_{2mm}\delta_{ij}/3$ is the deviatoric part of the strain rate tensor S_{2ij}, which is defined by $2S_{2ij} = U_{2i,j} + U_{2j,i}$. The transport equation for a_{imm} is written using Eqs (32), (38)–(41). This yields

$$\alpha_2\rho_2\frac{D_2}{D_t}a_{imm} + 5\frac{\partial}{\partial x_i}(\alpha_2\rho_2 T_2^2) + 7\frac{\partial}{\partial x_j}(\alpha_2\rho_2 T_2 a_{ij}) + \frac{\partial}{\partial x_n}\theta_{ijjn} - (5T_2\delta_{ij} + 2a_{ij})\frac{\partial}{\partial x_m} \times (\alpha_2\rho_2 T_2\delta_{jm} + \Xi_{jm}) + \frac{1}{5}\alpha_2\rho_2 \times \left(7a_{jmm}\frac{\partial U_{2i}}{\partial x_j} + 2a_{jmm}\frac{\partial U_{2j}}{\partial x_i} + 2a_{imm}\frac{\partial U_{2j}}{\partial x_j}\right) + 2\theta_{ijm}\frac{\partial U_{2j}}{\partial x_m} + 2\theta_{jjm}\frac{\partial U_{2i}}{\partial x_m} - \frac{3\alpha_2\rho_2}{\tau_{12}^x} \times (M_{22ijj} - M_{12ijj}) = \chi_{ijj}. \quad (44)$$

These equations are identical to the ones proposed by Jenkins and Richman,[12] except for the coupling terms which represent, in both equations, the interactions between the continuous and discrete phases (see Eqs (30) and (32)). Let us find expressions for a_{ij} and a_{ijm}, and before this, expressions for the source and flux terms in the collisional rate of change.

2.7. *Linear Theory (Jenkins and Richman)*

Consider a population of spheres in the Maxwellian state, $f^1 = f^0$, with $\alpha_2 = \alpha_0$, $U_2 = U_0$ and $T_2 = T_0$. A

perturbation analysis is carried out in the vicinity of the Maxwellian state with small perturbations (linear domain), $f^1 = f^0(1+\varepsilon), \partial\alpha_2/\partial x_i \sim \varepsilon, \partial U_{2i}/\partial x_j \sim \varepsilon$ and $\partial T_2/\partial x_i \sim \varepsilon$, where ε is small. The particle velocity probability density function is expanded in Taylor series as

$$f^1\left(\mathbf{x} - \frac{d_p}{2}\mathbf{k}, \mathbf{c}, t\right) = f^1(\mathbf{x}, \mathbf{c}, t) - \frac{d_p}{2}k_i \frac{\partial}{\partial x_i} f^1(\mathbf{x}, \mathbf{c}, t) + \ldots \tag{45}$$

In the rest of the analysis, $f^1(\mathbf{x},\mathbf{c}_1,t)$ is denoted f_1^1 and $f^1(\mathbf{x},\mathbf{c}_2,t)$ is denoted f_2^1. Equations (25) and (45) can be combined using a first-order approximation to yield

$$f^2(\mathbf{x}_1, \mathbf{x}_2, \mathbf{c}_1, \mathbf{c}_2, t) = g_0(\mathbf{x}) f_1^1 f_2^1 \left(1 + \frac{1}{2} d_p k_i \frac{\partial}{\partial x_i} \ln(f_2^1/f_1^1)\right). \tag{46}$$

As mentioned by Jenkins and Richman,[12] this order of approximation (first-order truncation) is justified in the frame of the perturbation analysis, when the spatial gradients of the mean fields are small. This approximation should be remembered as it is a limiting one. Using Eq. (18), $\chi(\psi)$ can now be written, with the differential part $d_p^2(\mathbf{g}\cdot\boldsymbol{k})\mathrm{d}\boldsymbol{k}\mathrm{d}\mathbf{c}_1\mathrm{d}\mathbf{c}_2$ denoted as $\mathrm{d}\mathbf{X}$ for reasons of expediency,

$$\chi(\psi) = \frac{1}{2} g_0(\mathbf{x}) \int_{\mathbf{g}\cdot\mathbf{k}>0} \Delta\psi f_1^1 f_2^1 \left(1 + \frac{d_p}{2} k_i \frac{\partial}{\partial x_i} \ln(f_2^1/f_1^1)\right) \mathrm{d}\mathbf{X}, \tag{47}$$

and with Eq. (19), $\theta_i(\psi)$ becomes

$$\theta_i(\psi) = -\frac{d_p}{2} g_0(\mathbf{x}) \int_{\mathbf{g}\cdot\mathbf{k}>0} [\psi_1' - \psi_1] k_i f_1^1 f_2^1 \times \left(1 + \frac{d_p}{2} k_j \frac{\partial}{\partial x_j} \ln(f_2^1/f_1^1)\right) \mathrm{d}\mathbf{X}. \tag{48}$$

These two integrals can now be written in their final form using Grad's third-order approximation (see Eq. (36)). In Eq. (36), the derivative terms, $\partial f^0/\partial c_{2i}\partial c_{2j}\ldots\partial c_{2p}$, are denoted $f^0_{ij\ldots p}$ for the sake of simplicity. The product $f_1^1 f_2^1$ is given by

$$f_1^1 f_2^1 = f_1^0 f_2^0 + \frac{1}{2!} a_{ij}(f_1^0 f_{2ij}^0 + f_{1,ij}^0 f_2^0) - \frac{1}{3!} a_{ijm}(f_1^0 f_{2ijm}^0 + f_{1,ijm}^0 f_2^0). \tag{49}$$

To obtain Eq. (49), the non-linear terms have been neglected (non-linear in a_{ij} and a_{ijm}). Furthermore, if the terms a_{ij}/T_2 and $a_{ijm}/T_2^{3/2}$ are small (low level of anisotropy) and have the same order of magnitude, which means that only flows whose state is close to the uniform steady state are considered, the following approximation can be made: $\ln(f_2^1/f_1^1) \approx \ln(f_2^0/f_1^0)$. Using Eqs (47) and (49), Jenkins and Richman[12] proposed writing the following expressions for the source term of the collisional rate of change:

$$\chi(\psi) = E(\psi) + F(\psi) + a_{ij}F_{ij}(\psi) + a_{ijm}F_{ijm}(\psi), \tag{50}$$

where $E(\psi), F(\psi)$, $F_{ij}(\psi)$ and $F_{ijm}(\psi)$ are given by the following integrals:

$$E(\psi) = \frac{1}{2} g_0(\mathbf{x}) \int_{\mathbf{g}\cdot\mathbf{k}>0} \Delta\psi f_1^0 f_2^0 \mathrm{d}\mathbf{X}, \tag{51}$$

$$F(\psi) = \frac{d_p}{4} g_0(\mathbf{x}) \int_{\mathbf{g}\cdot\mathbf{k}>0} \Delta\psi f_1^0 f_2^0 k_i \frac{\partial}{\partial x_i} \ln(f_2^0/f_1^0) \mathrm{d}\mathbf{X}, \tag{52}$$

$$F_{ij}(\psi) = \frac{1}{4} g_0(\mathbf{x}) \int_{\mathbf{g}\cdot\mathbf{k}>0} \Delta\psi (f_1^0 f_{2,ij}^0 + f_{1,ij}^0 f_2^0) \mathrm{d}\mathbf{X}. \tag{53}$$

$$F_{ijm}(\psi) = -\frac{1}{12} g_0(\mathbf{x}) \int_{\mathbf{g}\cdot\mathbf{k}>0} \Delta\psi (f_1^0 f_{2,ijm}^0 + f_{1,ijm}^0 f_2^0) \mathrm{d}\mathbf{X}. \tag{54}$$

In Eq. (50), some terms have been neglected. These terms are the products of a_{ij} and a_{ijm}, with integrals similar to Eq. (52). One of these terms is

$$a_{ij} \frac{d_p}{4} g_0(\mathbf{x}) \int_{\mathbf{g}\cdot\mathbf{k}>0} \Delta\psi (f_1^0 f_{2,ij}^0 + f_{1,ij}^0 f_2^0) k_m \frac{\partial}{\partial x_m} \ln(f_2^0/f_1^0) \mathrm{d}\mathbf{X}. \tag{55}$$

In order to understand when this approximation is valid, let us define the following dimensionless quantities: U_0, L_0 and T_0, which are characteristic values of velocity, length and granular temperature. If integral (52) is an order of magnitude less than integral (51), then integral (55) will be a term of second order. The previous assumption is true if the ratio d_p/L_0 is small and the ratio $\sqrt{T_0}/U_0$, the non-dimensionalized spatial gradients of the granular temperature and the mean velocity are all of the order of unity.

Applying a similar reasoning and with Eqs (48) and (49), Jenkins and Richman[12] propose for the flux term of the collisional rate of change:

$$\theta_i(\psi) = A_i(\psi) + B_i(\psi) + a_{jm}B_{jm}(\psi) + a_{jmn}B_{ijmn}(\psi), \tag{56}$$

where $A_i(\psi)$, $B_i(\psi)$, $B_{jm}(\psi)$ and $B_{ijmn}(\psi)$ are given by the following expressions:

$$A_i(\psi) = -\frac{d_p}{2} g_0(\mathbf{x}) \int_{\mathbf{g}\cdot\mathbf{k}>0} \delta\psi f_1^0 f_2^0 k_i \mathrm{d}\mathbf{X}, \tag{57}$$

$$B_i(\psi) = -\frac{d_p^2}{4} g_0(\mathbf{x}) \int_{\mathbf{g}\cdot\mathbf{k}>0} \delta\psi f_1^0 f_2^0 k_i k_j \frac{\partial}{\partial x_j} \ln(f_2^0/f_1^0) \mathrm{d}\mathbf{X}, \tag{58}$$

$$B_{ijm}(\psi) = -\frac{d_p}{4} g_0(\mathbf{x}) \int_{\mathbf{g}\cdot\mathbf{k}>0} \delta\psi k_i (f_1^0 f_{2,jm}^0 + f_{1,jm}^0 f_2^0) \mathrm{d}\mathbf{X}, \tag{59}$$

$$B_{ijmn}(\psi) = -\frac{d_p}{12} g_0(\mathbf{x}) \int_{\mathbf{g}\cdot\mathbf{k}>0} \delta\psi k_i (f_1^0 f_{2,jmn}^0 + f_{1,jmn}^0 f_2^0) \mathrm{d}\mathbf{X}. \tag{60}$$

These integrals can be evaluated analytically by means of known integrals and the corresponding expression in Eqs (23) and (24).[12] By definition, the source term in the momentum equation is equal to zero, $\chi_i = 0$ (Eqs (24) and (47)). The source term in the second-order moment equation is

$$\chi_{ij} = -\frac{8}{d_p} \alpha_2^2 \rho_2 g_0 (1 - e^2) \sqrt{\frac{T_2}{\pi}} T_2 \delta_{ij}$$

$$- \frac{24}{5}\alpha_2^2\rho_2 g_0(1+e)(3-e)\sqrt{\frac{T_2}{\pi}}a_{ij} - \frac{6}{5}\alpha_2^2\rho_2 g_0(1+e)(2(e-2)S_{2ij} + (e-1/3)S_{2mm}\delta_{ij})T_2. \quad (61)$$

The source term in the third-order moment equation is

$$\chi_{ijm} = \frac{1}{5}\alpha_2^2\rho_2 g_0(1+e)(13-9e)T_2 T_{2(,i}\delta_{jm)} + \frac{2}{5d_p}\alpha_2^2\rho_2 g_0(1+e)(33e-49)\sqrt{\frac{T_2}{\pi}}a_{ijm}. \quad (62)$$

The source term in the granular temperature equation is

$$\chi_{mm} = -\frac{12}{d_p}\alpha_2^2\rho_2 g_0 \times (1-e^2)\sqrt{\frac{T_2}{\pi}}T_2 + 3\alpha_2^2\rho_2 g_0(1-e^2)T_2 S_{2mm}. \quad (63)$$

The flux term in the momentum equation is

$$\theta_{ij} = 2\alpha_2^2\rho_2 g_0(1+e)T_2\delta_{ij} - \frac{4}{5}\alpha_2^2\rho_2 d_p g_0(1+e) \times \sqrt{\frac{T_2}{\pi}}(2S_{2ij} + S_{2mm}\delta_{ij}) + \frac{4}{5}\alpha_2^2\rho_2 g_0(1+e)a_{ij}. \quad (64)$$

The flux in the second-order moment equation is

$$\theta_{ijm} = \frac{1}{5}\alpha_2^2\rho_2 g_0(1+e)(4a_{ijm} + a_{inn}\delta_{jm} + a_{jnn}\delta_{im}) - \frac{4}{5}\alpha_2^2\rho_2 d_p g_0(1+e)\left(\frac{T_2}{\pi}\right)^{1/2} T_{2(,i}\delta_{jm)}. \quad (65)$$

The flux in the granular temperature equation is

$$\theta_{ijj} = \frac{6}{5}\alpha_2^2\rho_2 g_0(1+e)a_{ijj} - 4\alpha_2^2\rho_2 d_p g_0(1+e)\sqrt{\frac{T_2}{\pi}}T_{2,i}. \quad (66)$$

2.8. *Determination of the Moments*

The moments a_{ij} and a_{ijj} are fully determined by a numerical solution of the set of non-linear equations given by Eqs (43) and (44), or Eqs (30) and (32). However, simplified forms of a_{ij} and a_{ijj} can be obtained employing the assumptions already made and a term-by-term order of magnitude analysis,[12] and also other closure assumptions to simplify the coupling terms (see Eqs (43) and (44)). The derivation begins by defining some additional dimensionless quantities, ρ_0, a_2 and a_3, which are typical values for ρ_2, a_{ij} and a_{ijj}. A preliminary remark is that the time derivatives in Eqs (43) and (44) can be neglected if $d_p U_0/L\sqrt{T_0}$ is small.[12] This is consistent with the previous assumptions. Let us rewrite Eqs (43) and (44) in a dimensionless form as multiples of $d_p U_0/L\sqrt{T_0}$, a_2/T_0, $a_3/T_0\sqrt{T_0}$ and d_p/L. These terms are all small. If it can be assumed that they have the same order of magnitude, only terms which are linear in these quantities will be kept (first-order approximation).

2.8.1. *Determination of a_{ij}*

The present determination of a_{ij} is different from the original work of Jenkins and Richman, because of the coupling term which appears in Eq. (43),

$$\frac{2\alpha_2\rho_2}{\tau_{12}^x}(a_{ij} - (M_{12ij} - M_{12mm}\delta_{ij}/3)). \quad (67)$$

The second-order moment is written using a Boussinesq approximation[27] as

$$-M_{2ij} = 2\nu_2^t\hat{S}_{2ij} - T_2\delta_{ij} \Rightarrow a_{ij} = -2\nu_2^t\hat{S}_{2ij}. \quad (68)$$

The turbulent viscosity is denoted ν_2^t. The Boussinesq hypothesis is valid when $\tau_2^c|\partial U_{2i}/\mathrm{d}x_j| \ll 1$, which means that the stresses react rapidly to a change in the mean flow.[29] In a similar way, the fluid–particle velocity correlation tensor is expressed with a Boussinesq approximation consistent with the limit tracer case[27] as

$$-M_{12ij} = \nu_{12}^t\hat{S}_{12ij} - \frac{1}{3}k_{12}\delta_{ij}, \quad (69)$$

where $\hat{S}_{12ij} = S_{12ij} - S_{12mm}\delta_{ij}/3$ is the deviatoric part of the strain rate tensor S_{12ij}, which is defined by $S_{12ij} = U_{1i,j} + U_{2j,i}$. The turbulent fluid–particle viscosity is given by $\nu_{12}^t = k_{12}\tau_{12}^t/3$. If the assumption of equal mean velocity gradients in both phases can be made, $U_{1i,j} \simeq U_{2i,j}$, the previous equation can be rewritten as

$$-M_{12ij} = 2\nu_{12}^t\hat{S}_{2ij} - \frac{1}{3}k_{12}\delta_{ij}. \quad (70)$$

The coupling term (Eq. (67)) can then be written as

$$\frac{2\alpha_2\rho_2}{\tau_{12}^x}(a_{ij} + 2\nu_{12}^t\hat{S}_{2ij}). \quad (71)$$

With Eq. (71) in Eq. (43), in the frame of the order of magnitude analysis defined above, Eq. (43) reduces to Eq. (68), where the turbulent viscosity, ν_2^t, is given by

$$\nu_2^t = \left(\frac{2}{3}\frac{\tau_{12}^t}{\tau_{12}^x}k_{12} + T_2(1+\alpha_2 g_0 A)\right)\Big/\left(\frac{2}{\tau_{12}^x} + \frac{B}{\tau_2^c}\right). \quad (72)$$

The constants A and B are defined in terms of the restitution coefficient, e, as $A = \frac{2}{5}(1+e)(3e-1)$ and $B = \frac{1}{5}(1+e)(3-e)$. This derivation, proposed by Boëlle *et al.*,[30] is very similar to that of Jenkins and Richman, but two additional terms appear. The first term in the numerator represents the contribution of the fluctuating motion of the continuous phase, while the first term in the denominator represents the contribution of particle inertia to the turbulent viscosity. The latter parameter is important; when particle motion is controlled by the aerodynamic forces, $\tau_{12}^x \ll \tau_2^c$, the behavior of the kinetic and granular stresses is significantly affected.[31] When there is no interstitial gas, Eq. (72) is identical to the results of Jenkins and Richman. With Eqs (64), (68) and (72), the collisional stress tensor can then be expressed in terms of a collisional viscosity, ν_2^c, as

$$\theta_{ij} = \frac{\theta_{mm}}{3}\delta_{ij} - 2\alpha_2\rho_2\nu_2^c\hat{S}_{2ij}, \quad (73)$$

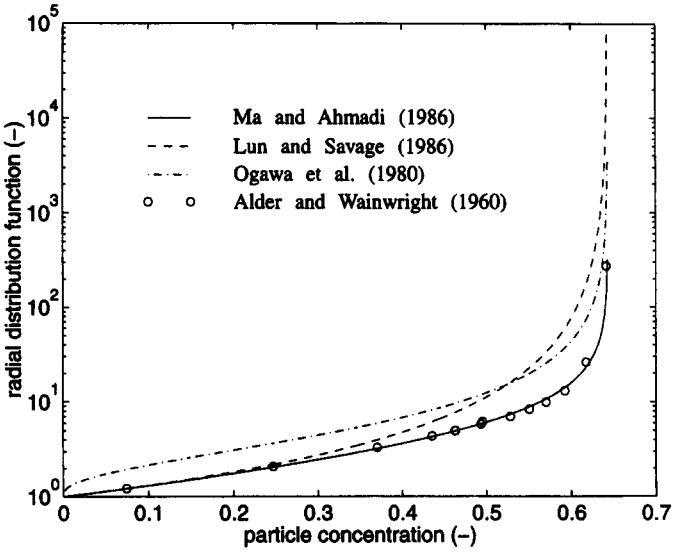

Fig. 3. Comparison of radial distribution functions.

where the collisional viscosity is given by

$$\nu_2^c = \frac{4}{5}\alpha_2 g_0(1+e)\left(\nu_2^t + d_p\sqrt{\frac{T_2}{\pi}}\right). \tag{74}$$

These results can be summarized writing the definition of the effective stress tensor, Σ_{2ij} (Eq. (29)). It can be written in the conventional form $\Sigma_{2ij} = (P_2 - \xi_2 S_{mm})\,\delta_{ij} - 2\mu_2 \hat{S}_{2ij}$,[29] where the so-called particle pressure is defined by

$$P_2 = \alpha_2\rho_2(1 + 2\alpha_2 g_0(1+e))T_2, \tag{75}$$

and the bulk viscosity is given by

$$\xi_2 = \frac{4d_p}{3}\alpha_2^2\rho_2 g_0(1+e)\sqrt{\frac{T_2}{\pi}}. \tag{76}$$

The dynamic viscosity is expressed as $\mu_2 = \alpha_2\rho_2(\nu_2^t + \nu_2^c)$.

2.8.2. *Determination of a_{ijj}*

The coupling term in Eq. (44) is defined by

$$\frac{3\alpha_2\rho_2}{\tau_{12}^r}(a_{ijj} - M_{12ijj}). \tag{77}$$

A similar analysis, as done in the previous section, can be applied to Eq. (44). Retaining the linear terms and neglecting the terms proportional to the mean concentration of solids, $\partial\alpha_2/\partial x_i$, the contracted third-order moment can be written as

$$a_{ijj} = -2K_2^t\frac{\partial k_2}{\partial x_i}, \tag{78}$$

where the turbulent diffusion coefficient, K_2^t, is given by

$$K_2^t = \left(\frac{3\tau_{12}^t}{5\tau_{12}^r}k_{12} + T_2(1+\alpha_2 g_0 C)\right)\Big/\left(\frac{9}{5\tau_{12}^r} + \frac{D}{\tau_2^c}\right). \tag{79}$$

The constants C and D are given by $3(1+e)^2(2e-1)/5$and $(1+e)(49-33e)/100$, respectively. The influence of the interstitial gas can be observed in Eq. (79) as in Eq. (72). When there is no interstitial gas, Eq. (79) is identical to the results of Jenkins and Richman. A simple shear flow analysis in the case of no interstitial gas shows that the terms proportional to the mean concentration of solids are negligible, provided that the quantity $1-e$ is small, i.e. nearly elastic particles. The collisional energy flux can be written in the form $\theta_{ijj} = -2\alpha_2\rho_2 K_2^c k_{2,i}$, where the collisional diffusion coefficient, K_2^c, is defined by

$$K_2^c = \alpha_2 g_0(1+e)\left(\frac{6}{5}K_2^t + \frac{4}{3}d_p\sqrt{\frac{T_2}{\pi}}\right). \tag{80}$$

The effective energy flux vector, E_{ijj}, can then be written $E_{ijj} = -2\alpha_2\rho_2(K_2^t + K_2^c)k_{2,i}$.

2.9. *Radial Distribution Function*

In the frame of the kinetic theory, the radial distribution function, g_0, accounts for the increase of the probability of collisions when the gas becomes denser (a deeper insight into the meaning of the radial distribution function can be found, for example, in Smith and Henderson[32]). In a rare gas, where molecular chaos can be assumed, g_0 is equal to unity, whereas g_0 tends to infinity when the molecules are closely packed, so that motion is almost impossible. For a rare uniform gas consisting of rigid spherical molecules, it can be shown (Ref. 24, Chap. 16) that the radial distribution function is given by

$$g_0(\alpha_2) = 1 + 2.5\alpha_2 + 4.59\alpha_2^2 + 7.06\alpha_2^3 + 9.88\alpha_2^4 + \ldots \tag{81}$$

Another classical expression for $g_0(\alpha_2)$ is given by Carnahan and Starling[33] for a fluid of identical hard, non-attracting spheres, $g_0 = (2-\alpha_2)/2(1-\alpha_2)^3$. Other equations for the radial distribution function (expressed

as a function of the volume fraction and the compressibility factor) can be found in Carnahan and Starling.[33]

However, these equations are not consistent with the asymptotic behavior of dense gases at extreme high concentration ($\alpha_2 \rightarrow \alpha_m$). An improved equation of state is given by Ma and Ahmadi,[34] based on the results of Ree and Hoover[35] (numerator) and a correction factor for highly dense cases (denominator):

$$g_0(\alpha_2) = \frac{(1 + 2.5\alpha_2 + 4.5904\alpha_2^2 + 4.515439\alpha_2^3)}{(1 - (\alpha_2/\alpha_m)^3)^{0.678021}}, \quad (82)$$

where the maximum solid fraction for a random packing, α_m, is given by $\alpha_m = 0.64356$. Equation (82) is in very good agreement with the numerical simulations of Alder and Wainwright,[36] involving 500 elastic spheres at equilibrium conditions using periodic boundary conditions (Fig. 3).

Lun and Savage[37] proposed an empirical expression:

$$g_0 = (1 - \alpha_2/\alpha_m)^{-2.5\alpha_m}. \quad (83)$$

This equation is believed to give good results for shearing of small finite systems at high concentration. A similar expression is the one of Ogawa *et al.*:[38]

$$g_0 = (1 - (\alpha_2/\alpha_m)^{1/3})^{-1}. \quad (84)$$

Ding and Gidaspow[14] proposed multiplying this equation by a factor 3/5 for a better fit of the numerical data of Alder and Wainwright. This correction is not valid (1) because the expression is not consequent for the dilute case, $g_0(0) = 3/5$, and (2) the data of Alder and Wainwright are given for equilibrium conditions. Figure 3 displays Eqs (83) and (84).

2.10. *Concluding Remarks*

Expressions have been given for the momentum and energy fluxes as functions of the granular temperature provided that certain assumptions are fulfilled. Before summing up these assumptions, the dissipation rate of energy due to collisions will be written under the assumptions made previously. Using Eq. (63), the dissipation rate of energy due to collisions reduces to

$$\frac{1}{2}\chi_{mm} = \alpha_2\rho_2\frac{(e^2 - 1)}{2\tau_2^c}T_2. \quad (85)$$

All results obtained so far are valid for flows with small spatial gradients of mean velocity and granular temperature, nearly elastic particles ($1 - e$ small) and low level of anisitropy (a_{ij}/T_2 small). In the case of a restitution coefficient for which $1 - e$ is not small, terms such as $\partial\alpha_2/\partial x_i$ should appear in the expression of the energy flux.

As far as the particle velocity probability density function is concerned, Boëlle *et al.*[31] showed, by comparing the present theory (Eqs (36) and (37)) with numerical results of the isovalues of the distribution function, obtained by a Lagrangian simulation, that the third-order truncation does not give a correct shape in the case of high anisotropy. In this case, a generalized distribution function proposed by Richman,[39]

$$f^1(\mathbf{x}, \mathbf{c}, t) = (n/(2\pi K^{1/3})^{3/2}) \exp\left(-\frac{1}{2}C_i(M_{ij})^{-1}C_j\right), \quad (86)$$

where $K = \det(M_{2ij})$, shows a shape which is similar to the numerical distribution function. Boëlle *et al.*[31] tried to recalculate the expressions of Jenkins and Richman[12] with such a distribution function, but no results could be derived in the general case. An expression for the source term of the collisional rate of change is given for a simple case by Richman.[39]

The difficulty in rendering the present theory more general illustrates, for gas–solid suspensions, the superiority of Lagrangian simulations to model particle collisions.[40] Lagrangian models allow more general collision models; for example, one can introduce a friction coefficient and consider particle rotation,[41] or a variable normal force during collision,[42] or a restitution coefficient which depends on the particle impact velocity.[37] In the present work, only smooth spheres in translational motion are considered, and therefore collisions are described with a single constant coefficient, e. In reality, particles are rough and are rotating. This implies that an accurate model should be based on at least three coefficients, normal and tangential restitution coefficients and Coulomb friction, in order to be valid for a large number of incident angles (sticking and/or sliding contacts).[43] Foerster *et al.*[43] also give some values of these coefficients for two types of particles for particle–particle and wall–particle collisions. Other measurements of particle–particle and wall–particle collisional properties can be found in Dave and Rosato[44] and Massah *et al.*[45] Lagrangian simulations involving collisions, in the case of simple dry (a granular flow without an intertitial gas) granular flow (simple shear flow), are discussed by Lun[46] and Lun and Bent.[41] From these simulations, several observation can be made. (1) When the particle concentration is high, the binary collision model might not be accurate, as multiple collisions are likely to occur. High density microstructures are formed, and the correlation in particle velocity increases (influence of g_0). Indeed, at a critical solid concentration, about 0.52 for smooth inelastic spheres, abrupt changes in the flow properties are observed. This matter is discussed by Lun and Bent. (2) Anisotropy of the normal stresses increases with decreasing e. (3) Formation of inelastic microstructures at low solid concentrations with a low restitution coefficient is consistent with the observations of Hopkins and Louge.[40] The previous observations suggest that the major drawbacks of the kinetic theory of granular flow, presented in this work, are due to the simple collision model (no particle rotation, no friction) and the moment method, $f^1 = f^0(1 + \varepsilon)$, where ε is small (low level of anisotropy).

However, it is possible to generalize the theory presented here by removing one of these limitations. Such an improvement is due to Lun,[46] following the work of Jenkins and Richman.[47] In this work, collisions between slightly inelastic, slightly rough spheres are modeled, and therefore additional transport equations are given for the angular momentum and rotational kinetic energy. Applying the moment method presented in this paper with a modified normal distribution function, expressions for the rotational energy flux, the rotational energy dissipation and the spin viscosity can be added to the quantities defining translational motion. Moreover, particle rotation is important in dry granular flow, but it might also be important in turbulent gas–solid flows, as a result of aerodynamic forces.[10] More research is needed to render the kinetic theory of granular flow more general for an improvement of the Eulerian/Eulerian formulation.

3. FLUID–PARTICLE FLUCTUATIONS

In the previous sections, it has been demonstrated that the closure problem formulated in Section 1.1 is not limited to the interfacial terms, the stress tensors and the second-order velocity moments. Indeed, in the formulation of the interfacial momentum transfer term, a closure model has to be found for the "**drift velocity**", $<u_{1i}'>_2$, and, in the formulation of the transport equation for the second-order velocity moment of the particle phase, a closure model has to be found for the "**fluid–particle velocity correlation tensor**", M_{12ij}. The drift velocity[11,16] is defined by Eq. (9) using $\psi(c)=u_{1i}'$. In the following sections, various proposals for closure equations are given for this velocity and for the fluid–particle velocity correlation tensor (Eq. (30)).

3.1. *Closure Model Based on Tchen's Theory*

3.1.1. *Dispersion in homogeneous turbulence*

According to the general definition of a diffusion coefficient,[48] the transport (or flux) of particles (fluid or solid particles) is defined as the product of a coefficient and the concentration gradient. Since particles are transported by the mean flow and are dispersed by the turbulent motion, the dispersion (or diffusion tensor), D_{kij}^t, is defined by

$$\alpha_k U_{ki} = -D_{kij}^t \frac{\partial \alpha_k}{\partial x_j}. \tag{87}$$

D_{kij}^t is given by the displacement tensor $<y_{ki}y_{ki}>_k$ as $D_{kij}^t = \frac{1}{2}\,\mathrm{d}/\mathrm{d}t <y_{ki}y_{kj}>_k$, where y_{ki} is the displacement of a particle in direction i. For long-time diffusion, the dispersion tensor is written in terms of the Lagrangian correlation tensor,

$$R_{kij}(\tau) = <u_{ki}'(t)u_{kj}'(t+\tau)>_k \Big/ (<u_{ki}'^2>_k <u_{kj}'^2>_k)^{1/2}, \tag{88}$$

and the Lagrangian integral time scale, $\tau_{kij}^t = \int_0^\infty R_{kij}(\tau)\mathrm{d}\tau$, as

$$D_{kij}^t = (<u_{ki}'^2>_k <u_{kj}'^2>_k)^{1/2}\tau_{kij}^t. \tag{89}$$

3.1.2. *Eulerian model*

We now study "**steady homogeneous turbulence**", where the mean velocity of the gas phase satisfies $U_{1i}=0$ for "**very dilute suspensions**", $\alpha_2 \ll 1$, so that two-way coupling and particle–particle collisions can be neglected. According to Simonin,[11] the particle flux can then be written as

$$\alpha_2 U_{2i} = \alpha_2(U_{ri} + U_{di}). \tag{90}$$

For very dilute suspensions, when the collisional effects may be neglected, the interfacial momentum transfer term can be obtained by averaging the local force acting on a particle. The interfacial momentum transfer is $I_{2i} = <X_2 f_{2i}> = \alpha_2 <f_{2i}>_2$, where f_{2i} is the force exerted by the fluid on a particle per unit volume. This force can be written as[10] $f_{2i} = -\rho_2 u_{ri}/\tau_{12}^r + \rho_1 \mathrm{d}\tilde{u}_{1i}/\mathrm{d}t - \rho_1 g_i$. Inserting this expression in the Eulerian momentum equation and noticing that $\mathrm{d}/\mathrm{d}t$ is the Lagrangian derivative, following a particle, an expression can be found for the mean relative velocity:[16]

$$\alpha_2 U_{ri} = \tau_{12}^r(-<u_{2i}'u_{2j}'>_2 + b<u_{1i}'u_{2j}'>_2) \times \frac{\partial \alpha_2}{\partial x_j}, \tag{91}$$

where $b = \rho_1/\rho_2$. This expression is valid if the the buoyancy force is equal to the mean aerodynamic force (drag force based on the free fall velocity, $\mathbf{U}_1 - \mathbf{U}_2$). In other words, the mean relative velocity is the sum of two mechanisms: a free fall velocity and a dispersion velocity (drift velocity). The free fall velocity can be found from the Lagrangian equation of motion with an average over the particle cloud, and is defined by $\tau_{12}^r(1-\rho_1/\rho_2)g_i$. An expression for the drift velocity can be found using the following procedure.[16] A conservation equation for the mass fraction of particles per unit volume, $Y_2 = \alpha_2\rho_2/\rho_m$, can be written from the discrete phase continuity equation and Eq. (90) as

$$\frac{\partial}{\partial t}(\rho_m Y_2) + \frac{\partial}{\partial x_i}(\rho_m Y_2 U_{mi}) = -\frac{\partial}{\partial x_i}\left(\frac{\alpha_1\rho_1\alpha_2\rho_2}{\rho_m}(U_{ri}+U_{di})\right), \tag{92}$$

where the mixture density is $\rho_m = \alpha_1\rho_1 + \alpha_2\rho_2$ and the mixture velocity is $\rho_m U_{mi} = \alpha_1\rho_1 U_{1i} + \alpha_2\rho_2 U_{2i}$. In the limiting case of particles whose diameter converges to zero, the relative velocity converges to zero. In such a case and with stationary conditions, the drift velocity can be written using Eq. (92) as

$$U_{di} = D_{12ij}^t\left(\frac{1}{\alpha_1\rho_1}\frac{\partial \alpha_1\rho_1}{\partial x_i} - \frac{1}{\alpha_2\rho_2}\frac{\partial \alpha_2\rho_2}{\partial x_i}\right), \tag{93}$$

where the binary dispersion coefficient or turbulent

fluid–particle interaction dispersion coefficient is defined in analogy with Eq. (87),

$$Y_2 U_{mi} = -D^t_{12ij}\frac{\partial Y_2}{\partial x_j}. \quad (94)$$

With Eqs (87), (91) and (93), the discrete phase dispersion coefficient can be expressed as

$$D^t_{2ij} = D^t_{12ij} + \tau^x_{12}(< u_{2i}'u_{2j}' >_2 - b < u_{1i}'u_{2j}' >_2). \quad (95)$$

The dispersion coefficient of the discrete phase is therefore the sum of two terms. The first term is the binary dispersion coefficient and the second term is the sum of two mechanisms: one due to the random motion of particles and the other due to the fluid–particle velocity correlation tensor. In the case of small particles, the relaxation time converges to zero and the discrete phase dispersion coefficient reduces to the binary dispersion coefficient.

3.1.3. *Tchen's theory*

The work of Tchen[49] is one of the first attempts to study the diffusion (or dispersion) of discrete particles in a turbulent flow field. Tchen showed that it is possible to express the particle turbulence intensity, the particle diffusion coefficient and the particle Lagrangian correlation function in terms of the fluid turbulent motion (the fluid Lagrangian correlation function, $R_{1ij}(\tau)$). With a given expression for the Lagrangian correlation function of the fluid turbulent motion, an analytical expression for the characteristics of particle motion can be obtained. Tchen made the following assumptions in his derivations: (1) turbulence is steady and homogeneous, (2) particles are spherical and follow Stokes' law of resistance, (3) particles are small compared to the smallest length scales of the fluid flow, and (4) during the motion of the particles, their neighborhood is formed by the same fluid. As pointed out by Hinze[48] and later by Deutsch and Simonin,[16] the last assumption is the most questionable. It is known that, in a turbulent flow, the fluid elements are distorted and stretched, so that a given fluid element should not always contain the same particle(s). This remark is enhanced when considering heavy particles which do not follow Stokes' law of resistance and therefore have a significant relative velocity. Consequently, as stated by Deutsch and Simonin, the Lagrangian correlation function of the fluid turbulent motion must be expressed in terms of the fluid velocity fluctuations seen by the particles, which means it must be computed along particle trajectories:

$$\Re_{1ij}(\tau) = < u_{1i}'(t)u_{1j}'(t+\tau) >_2 / (< u_{1i}'^2 >_2 < u_{1j}'^2 >_2)^{1/2}, \quad (96)$$

where the integral scale of the fluid fluctuation seen by a particle is (see Eq. (3))

$$\tau^t_{12ij} = \int_0^\infty \Re_{1ij}(\tau)\mathrm{d}\tau. \quad (97)$$

With these definitions, it is possible to generalize Tchen's theory by eliminating assumptions (2) and (4).[16] The discrete phase dispersion tensor, D^t_{2ij}, can be defined in terms of the Lagrangian correlation function of the fluid turbulent motion as

$$D^t_{2ij} = \tau^t_{12ij}(< u_{1i}'^2 >_2 < u_{1j}'^2 >_2)^{1/2}. \quad (98)$$

If the the buoyancy force is equal to the mean aerodynamic force (see Eq. (91)), the equation for the discrete phase fluctuating velocity is

$$\frac{\mathrm{d}u_{2i}'}{\mathrm{d}t} + au_{2i}' = a\tilde{u}_{1i}' + b\frac{\mathrm{d}\tilde{u}_{1i}'}{\mathrm{d}t}, \quad (99)$$

where the coefficients are given by $a = 1/\tau^x_{12}$ and $b = \rho_1/\rho_2$. Let us find a suitable form for the Lagrangian correlation function of the fluid turbulent motion. The displacement of particles is controlled by the mean flow, while the dispersion is controlled by the turbulent motion. Furthermore, if the mean flow velocity is large enough, the eddy decay mechanism is negligible compared to the spatial change of correlations, and thus the Lagrangian correlation tensor becomes a spatial Eulerian tensor:

$$\Re_{1ij}(\tau) = < u_{1i}'(\mathbf{x})u_{1j}'(\mathbf{x}+\tau\mathbf{U}_\mathbf{r}) >_1 / (< u_{1i}'^2 >_1 < u_{1j}'^2 >_1)^{1/2}, \quad (100)$$

where the assumption $< u_{1i}'^2 >_1 = < u_{1i}'^2 >_2$ can be made, provided that the displacement of the particles is governed by the mean flow, and thus the turbulent kinetic energy of the continuous phase and the local instantaneous distribution of the discrete phase must be uncorrelated. According to Csanady[17] and Deutsch and Simonin,[16] for "**homogeneous isotropic turbulence**", $R_1(\tau)$ can be written, in the direction of the mean flow, as $R_1(\tau) = \exp(-t/\tau^t_{12})$, where τ^t_{12} is defined by Eq. (3). Using a Fourier transform of Eq. (99) and the classical results of turbulence (Hinze,[48] pp. 464–467), the following equation is obtained in the direction of the mean flow, for the particle correlation function:

$$< u_2'u_2' >_2 = < u_1'u_1' >_2 (b^2+\eta)/(1+\eta), \quad (101)$$

where $\eta = \tau^t_{12}/\tau^x_{12}$. The fluid–particle correlation function (Hinze,[48] pp. 62–64) is obtained with the same procedure:

$$< u_1'u_2' >_2 = < u_1'u_1' >_2 (b+\eta)/(1+\eta). \quad (102)$$

A direct consequence of the previous results and assumptions is

$$D^t_2/D^t_1 = \tau^t_{12}/\tau^t_1. \quad (103)$$

When the relative mean velocity is very small, $\tau^t_{12} = \tau^t_1$, the original result of Tchen can be expressed: the long-term dispersion coefficients of the discrete particles and the fluid particles are the same. In addition, from Eqs (98), (101) and (102) inserted in Eq. (95),

$$D^t_{12} = \tau^t_{12} < u_1'u_2' >_2. \quad (104)$$

The results derived so far for the direction of the mean flow can be generalized to the other directions if one accounts for the continuity effects. According to

Csanady,[17] this can be achieved by Eq. (3), where the coefficient C_β depends on the direction which is considered. Possible numerical values for this coefficient can be found in Wells and Stock.[50] If the above expression is generalized to non-isotropic cases, $D^t_{12ij} = \tau^t_{12ij} < u_{1i}' u_{2j}' >_2$ and Eq. (93) give a closure equation for the drift velocity.

The results presented in this section have been tested by numerical simulations using large eddy simulation with a particle tracking algorithm.[16] In these simulations, one-way coupling was assumed. The results showed good agreement with Tchen's theory for heavy particles ($\rho_2 \gg \rho_1$). The results also showed that, for heavy particles, there is an optimal ratio τ^t_1/τ^x_{12} or Stokes number $St = \tau^x_{12}/\tau^t_1$, which gives a maximal dispersion of the particles, where $D^t_2 \geq D^t_1$. Furthermore, the results of Deutsch and Simonin show that, even for heavy particles, there is an intermediate time scale domain for τ^x_{12}/τ^t_1, where particles gather in low vorticity regions. Outside this time scale domain, small particles follow the fluid turbulence and coarse particles have a random motion (scalar and coarse cases). This phenomenon has been observed by Squires and Eaton,[51] who found a concentration of particles in regions of low vorticity and high strain rate in an intermediate range of Stokes numbers ($St = 0.15$), but their observations also showed sensitivity to the volume fraction of particles. Heavy particle concentration in regions of low vorticity and high strain rate has also been observed by Maxey.[52]

In the following section, attention is paid to other closure models which give results similar to the ones of the generalized Tchen theory.

3.2. *Closure Model of Derevich and Zaichik*

Assuming that the velocity fluctuations in the continuous phase are represented by a Gaussian random field, Derevich and Zaichik[53] gave an expression for the probable net acceleration of a particle from interactions with turbulent eddies. This expression is

$$\frac{1}{\tau^x_{12}} u_{1i}' f^1 = -\frac{1}{\tau^x_{12}} f_u M_{1ij} \frac{\partial f^1}{\partial c_j} - g_u M_{1ij} \frac{\partial f^1}{\partial x_j}, \tag{105}$$

where the second-order moment in the continuous phase is $M_{1ij} = < u_{1i}' u_{1j}' >_1$. The functions f_u and g_u are defined as functions of the integral of the fluid Lagrangian integral time scale measured along a particle path, τ^t_{12}, and the Lagrangian correlation tensor of the continuous phase computed along particle trajectories, $\Re_{1ij}(\tau)$,

$$f_u = \frac{1}{\tau^x_{12}} \int_0^t \Re_{1ij}(\tau) \exp(-\tau/\tau^t_{12}) \mathrm{d}\tau,$$

$$g_u = \frac{1}{\tau^x_{12}} \int_0^t \Re_{1ij}(\tau) \mathrm{d}\tau - f_u. \tag{106}$$

Using Eq. (9) with $\psi = u_{1i}'$, in combination with Eqs (105) and (106), a closure equation for the drift velocity is obtained:

$$U_{di} = -\tau^x_{12} g_u M_{1ij} \frac{1}{\alpha_2} \frac{\partial \alpha_2}{\partial x_j}. \tag{107}$$

If the Lagrangian correlation tensor is written $\exp(-t/\tau^t_{12})$, for long diffusion time, the function g_u is given by $1/(1+\eta)$. Tchen's theory for heavy particles, $\rho_1/\rho_2 \ll 1$, inserted into Eqs (93) and (107), gives a result consistent with Eq. (104).

Inserting $\psi = u_{1i}' u_{2j}'$ in Eq. (9), in combination with Eqs (105) and (106), a closure equation for the fluid–particle velocity correlation tensor is obtained:

$$< u_{1i}' u_{2j}' >_2 = f_u M_{1ij} - \tau^x_{12} g_u M_{1im} \frac{\partial U_{2j}}{\partial x_m}. \tag{108}$$

If the Lagrangian correlation tensor is written as $\exp(-t/\tau^t_{12})$, for a long diffusion time, the function f_u is given by $\eta/(1+\eta)$. If the term involving the gradient of the mean velocity of the discrete phase can be neglected, Eq. (108) is consistent with Tchen's theory for heavy particles, $\rho_1/\rho_2 \ll 1$. Simonin[27] pointed out that, in the case of a simple stationary shear flow, Eq. (108) is not consistent with the asymptotic scalar case.

3.3. *Closure Model of Koch*

Koch[23] gave algebraic expressions for the fluid–particle velocity correlation tensor and its trace if isotropy can be assumed. These expressions are based on the kinetic theory applied to a monodisperse gas–solid suspension under the following assumptions: collisions are elastic ($e = 1$), very dilute suspensions so that the hypothesis of molecular chaos is valid ($g_0 = 1$) and small particle Reynolds number, $Re \ll 1$. For very massive particles, $St \gg \alpha_2^{-3/2}$, where the Stokes number is $St = 2mU_1/3\pi\mu_1 d_p^2$, the velocity distribution is dominated by collisions, so that the fluid–particle velocity covariance reads

$$< u_{1i}'' u_{2j}' >_2 = \frac{d_p}{4\tau^x_{12,St}} \frac{1}{\sqrt{\pi T_2}} \mathrm{U}_r^2, \tag{109}$$

where $\tau^x_{12,St}$ is the particle relaxation time based on Stokes flow, $\tau^x_{12,St} = \rho_2 d_p^2/18\mu_1$. When the particle Reynolds number is greater than one, Louge *et al.*[54] proposed the use of Eq. (109) with the corresponding particle relaxation time, τ^x_{12}. For moderately massive particles, $\alpha_2^{-3/4} \ll St \ll \alpha_2^{-3/2}$, the velocity distribution is determined by fluid–particle interactions. In the present case, a gas–solid suspension in a vertical column (z direction), the velocity distribution is anisotropic, whereas for very massive particles it is modeled by the Maxwellian distribution function. The velocity fluctuations in the vertical direction are defined by $< u_{2z}' u_{2z}' >_2 = M_{2\|}$, and in the directions normal to the vertical one by $< u_{2x}' u_{2x}' >_2 = < u_{2y}' u_{2y}' >_2 = M_{2\perp}$, where the turbulent stress tensor is determined by $< u_{2i}' u_{2j}' >_2 = M_{2\perp}\delta_{ij} + (M_{2\|} - M_{2\perp}) I_i I_j$. I_i is the unit vector in the vertical direction. According to Koch's analysis, the distribution

function is

$$f(\mathbf{c}) = (1/(2\pi)^{3/2} M_{2\perp} M_{2\parallel}^{1/2}) \exp(-C_z^2/2M_{2\parallel} - (C_x^2 + C_y^2)/2M_{2\perp}). \quad (110)$$

With this distribution function, Koch[23] gave algebraic expressions for the fluid–particle velocity correlation tensor, $< u_{1i}'' u_{2j}' >_2 = F_\parallel \delta_{ij} + (F_\parallel - F_\perp) I_i I_j$, where $F_\parallel$ is defined by $F_\parallel = A f_\parallel(\beta)$, where $A = (3 d_p / 32 \tau_{12,St}^x) U_r^2 / \sqrt{\pi M_{2\parallel}}$, and $F_\perp$ is given by $F_\perp = A f_\perp(\beta)$. The functions $f_\parallel(\beta)$ and $f_\perp(\beta)$ are functions of the dimensionless parameter $\beta^2 = M_{2\parallel}/(M_{2\parallel} - M_{2\perp})$,

$$f_\parallel(\beta) = (\beta^5 + \beta)\ln((\beta+1)/(\beta-1)) - 2\beta^2/3 - 2\beta^4,$$

$$f_\perp(\beta) = (\beta^3 - \beta^5)\ln((\beta+1)/(\beta-1))/2 - 2\beta^2/3 + \beta^4. \quad (111)$$

These expressions are limited to small Reynolds numbers and large Stokes numbers, but they are algebraic. Therefore, for suspensions where these conditions are fulfilled, one does not need to solve a transport equation for the fluid–particle velocity correlation tensor.

3.4. *Closure Model of Reeks*

Before discussing transport equations for the fluid–particle velocity correlation tensor and its trace, another model similar to the previous ones is presented. Reeks[55,56] proposed a closure model describing the net acceleration of a particle from interactions with turbulent eddies. This acceleration is based on the Lagrangian history direct interaction approximation (LHDI),[57] and can be written as

$$\frac{1}{\tau_{12}^x} u_{1i}' f^1 = -\frac{\partial}{\partial c_j}(\mu_{ji} f^1) - \frac{\partial}{\partial x_j}(\lambda_{ji} f^1) - \gamma_i f^1, \quad (112)$$

where μ_{ji}, λ_{ji} and γ_i are diffusion tensors, which are functions of x_i, c_i and t.[55,56] Using a reasoning similar to that of the closure model of Derevich and Zaichik[58] and neglecting the dependency on local particle velocity, a closure equation for the drift velocity can be derived. This expression reads

$$U_{di} = -\tau_{12}^x \left(\lambda_{ji} \frac{1}{\alpha_2} \frac{\partial \alpha_2}{\partial x_j} + \frac{\partial \lambda_{ji}}{\partial x_j} + \gamma_i \right). \quad (113)$$

The fluid–particle velocity correlation tensor is defined by

$$< u_{1i}' u_{2j}' >_2 = \tau_{12}^x \left(\mu_{ji} - \lambda_{mi} \frac{\partial U_{2j}}{\partial x_m} \right). \quad (114)$$

For stationary homogeneous turbulence, it can be shown that[27] $\gamma_i = 0$ and that the tensors can be written $\mu_{ji} = < u_{1i}' u_{1j}' >_1 f_u / \tau_{12}^x$ and $\lambda_{ji} = < u_{1i}' u_{1j}' >_1 g_u$ provided that $< u_{1i}' u_{1j}' >_2 = < u_{1i}' u_{1j}' >_1$. Equations (113) and (114) are then equivalent to Eqs (107) and (108), respectively.

3.5. *Final Remarks on the Closure Models*

Closure equations based on different physical considerations have been presented to model the drift velocity and the fluid–particle velocity correlation tensor. These algebraic expressions are derived for specific cases and their validity should be tested against experimental data if possible. It is worthwhile noticing that, in the case of stationary homogeneous turbulence, the models of Tchen, Derevich and Zaichik, and Reeks are equivalent. In the case of practical gas–solid flows, most assumptions of the previous models are too restrictive and a more general formulation is necessary.

This general formulation, transport equations for the drift velocity and the fluid–particle velocity correlation tensor, is now given. In the following, a transport equation for the fluid–particle velocity covariance will first be derived, with a mathematical derivation which is analogous to the single-phase flow derivation for the transport equation of the second-order velocity moment. Secondly, transport equations for the drift velocity and the fluid–particle velocity correlation tensor will be expressed from a formulation of the fluid–particle joint probability density function. In this formulation, an equation of the Maxwell–Boltzmann type is derived with a method similar to the one adopted in the kinetic theory of granular flow. To close this model, the acceleration of a virtual fluid particle along the discrete particle trajectory is needed. This is done with a generalized form of the Langevin equation.

3.6. *Transport Equations*

3.6.1. *Fluid–particle velocity covariance*

A transport equation for the fluid–particle velocity correlation tensor can be derived from a procedure similar to the one used in single-phase flows.[59] Let $N_1(u_{1i}) = 0$ symbolize the local instantaneous momentum equation for the continuous phase, where N_1 denotes the Navier–Stokes operator. Accordingly, the local instantaneous momentum equation for the discrete phase can be written as $N_2(u_{2i}) = 0$, where N_2 is the corresponding Navier–Stokes operator. The local instantaneous momentum equations are, for the continuous phase,

$$X_2 \rho_2 \left(\frac{\partial}{\partial t} + u_{1j} \frac{\partial}{\partial x_j} \right) u_{1i} = \frac{X_2 \rho_2}{X_1 \rho_1} \left(\frac{\partial}{\partial x_j}(X_1 \sigma_{1ij}) + \sigma_{1ij} n_{1j} \delta_1 + X_1 \rho_1 g_i \right), \quad (115)$$

and for the discrete phase,

$$X_2 \rho_2 \left(\frac{\partial}{\partial t} + u_{2j} \frac{\partial}{\partial x_j} \right) u_{2i} = -X_2 \frac{\partial \bar{p}_1}{\partial x_i} + X_2 \rho_2 \frac{1}{\tau_{12}^x} u_{ri} + X_2 \rho_2 g_i. \quad (116)$$

In this formulation, Eq. (115) has been rearranged for the derivation of the transport equation of the fluid–particle velocity correlation tensor. The local instantaneous

momentum equation for the discrete phase (Eq. (116)) is written without particle–particle interaction terms. This means that, strictly speaking, only "**dilute suspensions**" are considered, $\alpha_2 \ll 1$, and the effect of particle–particle collisions on the fluid–particle velocity correlation tensor is not included. The derivation of Eqs (115) and (116) can be found in Peirano.[10] In order to derive the transport equation of the fluid–particle velocity correlation tensor, the quantity $< u_{1i}''N_2(u_{2j}) + u_{2j}'N_1(u_{1i}) > = 0$ is evaluated. Emphasizing the transport by the particulate phase, we obtain, after some algebra,

$$\alpha_2\rho_2 \frac{D_2}{Dt} < u_{1i}''u_{2j}' >_2 = \frac{\partial}{\partial x_m} D_{12ijm} + P_{12ij} + \phi_{12ij} + \prod_{12ij} - E_{12ij}, \tag{117}$$

where the terms on the RHS are similar to the single-phase flow case: diffusion, production, pressure strain, phase interaction (specific to two-phase flows) and destruction. The detailed expression of these terms can be found in Peirano.[60] The fluid–particle velocity covariance is defined as $k_{12} = < u_{1i}''u_{2i}' >_2$. A transport equation for fluid–particle velocity covariance can be obtained from Eq. (117) with $i = j$, modeling the diffusion term as

$$D_{12iim} = \alpha_2\rho_2 \left(\frac{\nu_{12}^t}{\sigma_{k1}} \right) \frac{\partial k_{12}}{\partial x_m}, \tag{118}$$

and the destruction term as $E_{12ii} = \alpha_2\rho_2\epsilon_{12}$, where $\epsilon_{12} = k_{12}/\tau_{12}^t$ contains the eddy–particle interaction time. Destruction is caused by viscous effects in the continuous phase and by crossing trajectories effects. Neglecting the trace of the pressure strain (this term is not traceless as for single-phase flows), the fluid–particle velocity covariance transport equation reads

$$\begin{aligned} \alpha_2\rho_2 \frac{D_2}{Dt} k_{12} = & \frac{\partial}{\partial x_j} \left(\alpha_2\rho_2 \frac{\nu_{12}^t}{\sigma_{k1}} \frac{\partial k_{12}}{\partial x_j} \right) \\ & - \alpha_2\rho_2 < u_{1i}''u_{2j}' >_2 \frac{\partial U_{2i}}{\partial x_j} \\ & - \alpha_2\rho_2 < u_{1j}''u_{2i}' >_2 \frac{\partial U_{1i}}{\partial x_j} \\ & + \prod_{12} - \alpha_2\rho_2\epsilon_{12}, \end{aligned} \tag{119}$$

where the phase interaction term, Π_{12}, is given by

$$\prod_{12} = -\frac{\alpha_2\rho_2}{\tau_{12}^r} ((1 + X_{12})k_{12} - 2X_{12}k_2 - 2k_1). \tag{120}$$

The quantity X_{12} is defined by $X_{12} = \alpha_2\rho_2/\alpha_1\rho_1$. Equation (120) is obtained by assuming statistical independence between the local instantaneous spatial distribution of particles and the turbulent kinetic energy of the continuous phase, so that one can write $< u_{1i}''u_{1i}'' >_2 = <_{1i}' u_{1i}' >_1$. The transport equation is closed using a Boussinesq approximation consistent with the limit tracer case:

$$< u_{1i}''u_{2j}' >_2 = \frac{1}{3} k_{12}\delta_{ij} - \nu_{12}^t \hat{S}_{12ij}, \tag{121}$$

where $\hat{S}_{12ij} = S_{12ij} - \frac{1}{3} S_{12mm}\delta_{ij}$ is the deviatoric part of the strain rate tensor S_{12ij} which is defined by $S_{12ij} = U_{1i,j} + U_{2j,i}$. The turbulent fluid–particle viscosity is given by $\nu_{12}^t = k_{12}\tau_{12}^t/3$.

3.6.2. *Maxwell–Boltzmann type equation*

Transport equations for the drift velocity and the fluid–particle velocity correlation tensor can be obtained using a method similar to the one adopted in the kinetic theory of granular flow. This can be done[27] by introducing the fluid–particle joint probability density function, $f_{12}(\mathbf{c}, \mathbf{u_1}, \mathbf{x}, t)$, where $f_{12}(\mathbf{c}, \mathbf{u_1}, \mathbf{x}, t)\mathrm{d}\mathbf{c}\mathrm{d}\mathbf{u}_1\mathrm{d}\mathbf{x}$ represents the probable number of particles located in the volume $\mathrm{d}\mathbf{x}$ centered at $\mathbf{x}$, having a velocity in the velocity space $\mathbf{c} + \mathrm{d}\mathbf{c}$ and viewing a locally undisturbed fluid velocity in the velocity space $\mathbf{u}_1 + \mathrm{d}\mathbf{u}_1$. A corresponding fluid–particle Maxwell–Boltzmann equation can be written as was done for the kinetic theory of granular flow:

$$\begin{aligned} & \frac{\partial f_{12}}{\partial t} + \frac{\partial}{\partial x_i}(c_{2i} f_{12}) + \frac{\partial}{\partial c_{2i}} \left(\frac{\mathrm{d}u_{2i}}{\mathrm{d}t}\Big|_{\mathbf{c}_1, \mathbf{c}_2} f_{12} \right) \\ & \quad + \frac{\partial}{\partial c_{1i}} \left(\frac{\mathrm{d}u_{1i}}{\mathrm{d}t}\Big|_{\mathbf{c}_1, \mathbf{c}_2} f_{12} \right) = \frac{\partial f_{12}}{\partial t}\Big|_{\mathbf{c}}, \end{aligned} \tag{122}$$

where the term $\partial f_{12}/\partial t|_{\mathbf{c}}$ is the rate of change of the fluid–particle joint probability density function due to particle–particle collisions. The notation $\mathrm{d}u_i/\mathrm{d}t|_{\mathbf{c}_1, \mathbf{c}_2}$ represents the acceleration along the particle trajectory with a conditional expectation that $c_{1i} = \tilde{u}_{1i}$ and $c_{2i} = u_{2i}$. The term $\mathrm{d}u_{2i}/\mathrm{d}t|_{\mathbf{c}_1, \mathbf{c}_2}$ equals the force acting on the particle per unit mass, F_i (Eq. (7)). The term $\mathrm{d}u_{1i}/\mathrm{d}t|_{\mathbf{c}_1, \mathbf{c}_2}$ is more difficult to evaluate. It represents the acceleration of a virtual fluid particle along the discrete particle trajectory, which is the force per unit mass exerted on the virtual fluid particle following the discrete particle trajectory. According to Simonin,[27] this acceleration can be evaluated by a generalized form of the Langevin equation.

The increment over a time $\mathrm{d}t$ of the virtual fluid particle velocity following the particle trajectory is

$$\begin{aligned} \tilde{u}_{1i}(\mathbf{x}_2(t + \mathrm{d}t), t + \mathrm{d}t) = & \tilde{u}_{1i}(\mathbf{x}_1(t), t) \\ & + \tilde{u}_{1i}(\mathbf{x}_1(t + \mathrm{d}t), t + \mathrm{d}t) - \tilde{u}_{1i}(\mathbf{x}_1(t), t) \\ & + U_{1i}(\mathbf{x}_2(t + \mathrm{d}t), t + \mathrm{d}t) - U_{1i}(\mathbf{x}_1(t + \mathrm{d}t), t + \mathrm{d}t) \\ & + u_{1i}'(\mathbf{x}_2(t + \mathrm{d}t), t + \mathrm{d}t) - u_{1i}'(\mathbf{x}_1(t + \mathrm{d}t), t + \mathrm{d}t), \end{aligned} \tag{123}$$

where the terms on the second line represent the trajectory of the virtual fluid particle in the turbulent field, which is the solution to the Navier–Stokes equation for the undisturbed turbulent flow field of the continuous phase. The terms on the third line represent the increment of the mean fluid velocity due to the mean relative velocity between the virtual fluid particle and the discrete particle. Using a first-order approximation, this term can be written as $(u_{2m} - \tilde{u}_{1m})(\partial U_{1i}/\partial x_m)\mathrm{d}t$. The terms on the fourth line represent the increment of the fluctuation velocity due to the mean relative velocity between the virtual fluid particle and the discrete

particle, i.e. the crossing trajectories effect. The terms on the second line can be evaluated using the work of Pope,[61,62] and Haworth and Pope.[63] For single-phase flow, in an infinitesimal time interval dt, the velocity of a fluid particle changes by

$$\tilde{u}_{1i}(\mathbf{x}_1(t+dt),t+dt)=\tilde{u}_{1i}(\mathbf{x}_1,t)+\left(-\frac{1}{\rho_1}\frac{\partial P_1}{\partial x_i}+\frac{\partial}{\partial x_j}\left(\nu_1\frac{\partial U_{1i}}{\partial x_j}\right)\right)dt+\left(-\frac{1}{\rho_1}\frac{\partial \tilde{p}_1{}'}{\partial x_i}+\frac{\partial}{\partial x_j}\left(\nu_1\frac{\partial u_{1i}{}'}{\partial x_j}\right)\right)dt, \quad (124)$$

where the Navier–Stokes equation has been used with $\tilde{u}_{1i}=U_{1i}+u_{1i}'$ and $\tilde{p}_1=P_1+\tilde{p}_1'$. A generalized Langevin equation can then be written:

$$\tilde{u}_{1i}(\mathbf{x}_1(t+dt),t+dt)=\tilde{u}_{1i}(\mathbf{x}_1,t)+\left(-\frac{1}{\rho_1}\frac{\partial P_1}{\partial x_i}+\frac{\partial}{\partial x_j}\left(\nu_1\frac{\partial U_{1i}}{\partial x_j}\right)\right)dt+G_{1ij}(\tilde{u}_{1j}-U_{1j})dt+(C_0\epsilon_1)^{1/2}dW_{1i}. \quad (125)$$

Comparing Eq. (124) with Eq. (125) makes clear that G_{1ij} and C_0 account for the effects of viscosity and fluctuating pressure gradient. Haworth and Pope[63] give $C_0=2.1$. According to Haworth and Pope, the last term in Eq. (125) represents a random walk in velocity space. The random vector, dW_{1i}, is characterized by a zero mean, $<dW_{1i}>_1=0$, and a covariance defined by $<dW_{1i}dW_{1j}>_1=\delta_{ij}dt$. As stated by Haworth and Pope, there are limitations to Eq. (125): the infinitesimal time increment must be smaller than the dissipation time scale (actually it is sufficient that the time increment corresponds to the inertial range[64]), the turbulence structure is described only by local mean quantities (if G_{1ij} is modeled in terms of local mean quantities) and the small scales of the flow are isotropic. To close Eq. (125), an expression for G_{1ij} has to be found. Haworth and Pope[63] proposed the following closure model:

$$G_{1ij}=G_{1ij}\left(<u_{1m}'u_{1n}'>,\frac{\partial U_{1m}}{\partial x_n},\epsilon_1\right). \quad (126)$$

The study of such a closure expression in the general case is not given, but instead a model is proposed for "**homogeneous turbulent flows**". Haworth and Pope give

$$G_{1ij}=a_1\frac{1}{\tau_1'}\delta_{ij}+a_2\frac{1}{\tau_1'}b_{ij}+H_{ijmn}\frac{\partial U_{1m}}{\partial x_n}, \quad (127)$$

where $\tau_1'=k_1/\epsilon_1$, the normalized anisotropy tensor, b_{ij}, is defined by $b_{mn}=<u_{1m}'u_{1n}'>_1/<u_{1i}'u_{1i}'>_1-\delta_{mn}/3$ and the tensor H_{ijmn} is given in terms of the normalized anisotropy tensors and the Kronecker symbol. Equation (127) includes 11 model coefficients (a_1, a_2 and nine coefficients in the expression of H_{ijmn}). However, for practical applications, Haworth and Pope[65] simplified this model by introducing the simplified and intermediate models. These models are not presented here, but instead their extension to two-phase flows by Simonin[27] is given.

To carry on in a practical way, Simonin *et al.*[66] proposed generalizing Eq. (125) to two-phase flows. An equation was given for the infinitesimal increment of the local undisturbed velocity of a fluid particle along the particle trajectory. This equation reads

$$\tilde{u}_{1i}(\mathbf{x}_2(t+dt),t+dt)=\tilde{u}_{1i}(\mathbf{x}_2(t),t)+\left(-\frac{1}{\rho_1}\frac{\partial P_1}{\partial x_i}+\frac{\partial}{\partial x_j}\left(\nu_1\frac{\partial U_{1i}}{\partial x_j}\right)\right)dt+(u_{2j}-\tilde{u}_{1j}\frac{\partial U_{1i}}{\partial x_j}dt+G_{12ij}(\tilde{u}_{1j}-U_{1j}))dt+(C_0\epsilon_1)^{1/2}dW_{12i}, \quad (128)$$

where, as for the single-phase flow case, dW_{12i} is a random vector characterized by a zero mean, $<dW_{12i}>_2=0$. The form of this equation remains an open question.[67] Simonin *et al.*[66] and Simonin[27] gave models for the tensor G_{12ij} which account for the same effects as for single-phase flows, but also for the crossing trajectories effect. This extension of the Langevin equation is valid for "dilute" two-phase flows, otherwise Eq. (128) should include terms for the particle–particle collision mechanism and terms for the influence of the surrounding particles on the particle considered (two-way coupling). In other words, this expression is only valid for one-way coupling. In addition, the form of the mean velocity gradient of the continuous phase, $\partial U_{1i}/\partial x_j$, in Eq. (128) could well be replaced by the mean velocity gradient of the continuous phase seen by the particle, $\partial <u_{1i}>_2/\partial x_j$. In order to continue in a more practical way, Simonin *et al.*[66] proposed models for G_{12ij}. The first model, or simplified model,[66] is given by

$$G_{12ij}=-\frac{1}{\tau_{12\perp}'}\delta_{ij}-\left(\frac{1}{\tau_{12\|}'}-\frac{1}{\tau_{12\perp}'}\right)I_iI_j, \quad (129)$$

where I_i is the unit vector defined by $I_i=U_{ri}/|\mathbf{U}_r|$. The eddy–particle interaction time in the direction of the mean flow is $\tau_{12\|}'$, and the eddy–particle interaction time in the direction perpendicular to the mean flow is $\tau_{12\perp}'$. These interaction times are defined according to Eq. (3), where the constant C_β takes a value depending on the direction in the flow. The second model, or intermediate model,[27] is given by

$$G_{12ij}=-\frac{1}{\tau_{12}'}\delta_{ij}+0.6\frac{\partial}{\partial x_j}<\tilde{u}_{1i}>_2. \quad (130)$$

This model neglects the anisotropy caused by the crossing trajectories effect. To fully understand the form of these models, comparisons must be made with the single-phase flow models of Haworth and Pope.[63]

As was done in Eq. (9), an averaging operator, $<>_2$, is defined for a given function $\psi(\mathbf{c}_1,\mathbf{c}_2)$:

$$n<\psi(\mathbf{c}_1,\mathbf{c}_2)>_{12}=\int f_{12}\psi(\mathbf{c}_1,\mathbf{c}_2)d\mathbf{c}_1d\mathbf{c}_2. \quad (131)$$

The fluid–particle joint probability density function can be defined in terms of the conditional probability distribution function, $f_{1|2}$, as $f_{1|2}(\mathbf{c}_1|\mathbf{c}_2,\mathbf{x},t)=f_{12}$

$(\mathbf{c}_1, \mathbf{c}_2, \mathbf{x}, t)/f_2(\mathbf{c}_2, \mathbf{x}, t)$, where $f_2(\mathbf{c}_2,\mathbf{x},t)$ is the particle velocity probability density function (Section 2). As for the pair distribution function (Section 2), the fluid–particle joint probability density function is not the product of the particle velocity probability density function and the standard fluid velocity probability distribution function, $f_1(\mathbf{c}_1,\mathbf{x},t)$, and $f_12(x,c_1,\mathbf{c}_2,t)$ is different from $f_1(x,c_1,t)f_2(\mathbf{x},\mathbf{c}_2,t)$. This means that, along the particle path, the fluid velocity and the particle velocity are correlated variables. From the previous definitions, it is obvious that the particle velocity probability density function, f_2, and the fluid–particle joint probability density function, f_{12}, must satisfy

$$f_2 = \int f_{12} \mathrm{d}\mathbf{c}_1. \tag{132}$$

With these definitions, it can be shown that $<\psi(\mathbf{c}_1,\mathbf{c}_2)>_{12} = <\psi(\mathbf{c}_1,\mathbf{c}_2)>_2$. This is used for writing the transport equations for the drift velocity and the fluid–particle velocity correlation tensor. Multiplying Eq. (122) by the function $\psi(\mathbf{c}_1,\mathbf{c}_2)$ and applying the averaging operator $< >$, an averaged equation can be derived. This equation is written assuming a "**dilute suspension**", so that the rate of change of the fluid–particle joint probability density function (Section 2) can be neglected. The resulting equation is, using $\alpha_2\rho_2 = nm_2$,

$$\begin{aligned}
&\frac{\partial}{\partial t}(\alpha_2\rho_2 <\psi>_2) + \frac{\partial}{\partial x_i}(\alpha_2\rho_2 <c_{2i}\psi>_2) \\
&= \alpha_2+\rho_2+\left(\left\langle\frac{\partial\psi}{\partial t}\right\rangle_2 + \left\langle c_{2i}\frac{\partial\psi}{\partial x_i}\right\rangle_2 + \left\langle F_{2i}\frac{\partial\psi}{\partial c_{2i}}\right\rangle_2 \right. \\
&\quad \left. + \left\langle F_{1i}\frac{\partial\psi}{\partial c_{1i}}\right\rangle_2\right),
\end{aligned} \tag{133}$$

where F_{2i} is the external force per unit of mass acting on a discrete particle and F_{1i} is the external force per unit of mass acting on a virtual fluid particle following the trajectory of the corresponding discrete particle. F_{2i} is given by Eq. (7), whereas F_{1i} is given by the generalized Langevin equation (Eq. (128)). The equation for the external force per unit of mass acting on a virtual fluid particle which follows the trajectory of the corresponding discrete particle reads

$$\begin{aligned}
F_{1i} = &-\frac{1}{\rho_1}\frac{\partial P_1}{\partial x_i} + \frac{\partial}{\partial x_j}\left(\nu_1\frac{\partial U_{1i}}{\partial x_j}\right) \\
&+ (u_{2j}-\tilde{u}_{1j})\frac{\partial U_{1i}}{\partial x_j} + (\tilde{u}_{1j}-U_{1j})G_{12ij} \\
&+ (C_0\epsilon_1)^{1/2}\frac{\mathrm{d}W_{12i}}{\mathrm{d}t}.
\end{aligned} \tag{134}$$

3.6.3. *Drift velocity*

With Eq. (133) with $\psi = u_{1i}'$ and Eq. (134), a transport equation can be derived for the drift velocity. This equation reads

$$\begin{aligned}
\alpha_2\rho_2\frac{D_2}{Dt}U_{di} = &-\frac{\partial}{\partial x_j}(\alpha_2\rho_2 <u_{1i}'u_{2j}'>_2) \\
&- X_{12}\frac{\partial}{\partial x_j}(\alpha_1\rho_1 <u_{1i}'u_{1j}'>_1) - X_{12}I_{1i} \\
&- \alpha_2\rho_2 U_{di}\frac{\partial U_{1i}}{\partial x_j} + \alpha_2\rho_2 G_{12ij}U_{dj}.
\end{aligned} \tag{135}$$

The first and second terms on the RHS represent the transport of the drift velocity by velocity fluctuations. The third term is a result of the interaction of the discrete phase with the continuous phase. The fourth term is a production term caused by the mean velocity gradients of the continuous phase. The fifth term on the RHS accounts for the effects of the fluctuating pressure gradients, viscosity and crossing trajectories. A simplified expression of this transport equation was given by Simonin,[27] for "**dilute flows**" where the interfacial term, $X_{12}I_{1i}$, can be neglected as well as the gradient of the mean volume fraction, $\partial\alpha_1/\partial x_i$.

3.6.4. *Fluid–particle velocity correlation tensor*

From Eq. (133) with $\psi = u_{1i}'u_{2j}'$ and Eq. (134), a transport equation can be derived for the fluid–particle velocity correlation tensor. This equation reads

$$\begin{aligned}
&\alpha_2\rho_2\frac{D_2}{Dt}<u_{1i}''u_{2j}'>_2 \\
&= -\frac{\partial}{\partial x_m}(\alpha_2\rho_2 <u_{1i}''u_{2j}'u_{2m}'>_2) \\
&\quad - \alpha_2\rho_2\left(<u_{1i}''u_{2m}'>_2\frac{\partial U_{2j}}{\partial x_m} + <u_{1m}'u_{2j}'>_2\right. \\
&\quad \left.\times\frac{\partial U_{1i}}{\partial x_m} + <u_{2j}'u_{2m}'>_2\frac{\partial U_{di}}{\partial x_m}\right) \\
&\quad - \frac{\alpha_2\rho_2}{\tau_{12}^x}(<u_{1i}''u_{2j}'>_2 - <u_{1i}''u_{1j}''>_2) \\
&\quad + \alpha_2\rho_2 G_{12im}<u_{1m}''u_{2j}'>_2.
\end{aligned} \tag{136}$$

The first term on the RHS represents the transport of the fluid–particle velocity correlation tensor by the particle velocity fluctuations. The second term on the RHS represents the production caused by the mean velocity gradients of the discrete and the continuous phase, and the interaction between the second-order velocity moment in the discrete phase and the gradient of the drift velocity. The third term is a production or destruction term caused by the interaction of the discrete phase with the continuous phase. The fourth term on the RHS accounts for the effects of the fluctuating pressure gradient, viscosity and crossing trajectories.

3.6.5. *Final remarks on the transport equations*

Equations (119) and (136), taking $i = j$, should be equivalent as they both give the transport equation for

the fluid–particle velocity covariance. It is quite straightfoward to observe that these two equations are not equivalent for two reasons: the production and interaction terms differ. However, two points must be emphasized (Simonin, personal communications). (1) In the generalized Langevin equation (Eq. (128)), the term $(u_{2j}-\tilde{u}_{1j})\partial U_{1i}/\partial x_j$ should rather be written $(u_{2j}-\tilde{u}_{1j})\,\partial < u_{1i} >_2 /\partial x_j$. (2) In the formulation of Eq. (134), two-way coupling is neglected. To account for the effect of the surrounding particles, an additional drag term must be included. This term reads

$$\frac{\mathrm{d}}{\mathrm{d}t}u_{1i}(\mathbf{x}_2,t)=\alpha_2^*\frac{\rho_2}{\rho_1}\frac{1}{\tau_{12}^r}(u_{2i}^*(\mathbf{x}_2,t)-u_{1i}(\mathbf{x}_2,t)), \qquad (137)$$

where α_2^* is the local concentration of the surrounding particles and $u_{2i}^*(x_2,t)$ is the characteristic velocity of the surrounding particles. Using Eq. (133) with $\psi=u_{1i}'u_{2j}'$ and the modified form of Eq. (134), a transport equation can be derived for the fluid–particle velocity correlation tensor and the fluid–particle velocity covariance, taking $i=j$. For dilute flows, this equation is then almost equivalent to Eq. (119). The interaction term is the same, the production terms differ by the mean gas velocity gradient, $\partial < u_{1i} >_2/\partial x_j$ instead of $\partial U_{1i}/\partial x_j$, and the dissipation term $\alpha_2\rho_2 G_{12im} < u_{1m}''u_{2i}' >_2$ becomes $\alpha_2\rho_2 k_{12}/\tau_{12}^t$ using a simplified Langevin model (Eq. (129)).

The form of the transport equation for the fluid–particle velocity correlation tensor is a key point in the formulation of the models. Indeed, when solving the transport equations for the second-order velocity moment, the fluid–particle velocity correlation tensor appears in the coupling term (Eqs (30) and (139)). In the present section, all derivations were made assuming dilute suspensions, so that the collisional term,

$$C_{12}(\psi)=\int\psi\left.\frac{\partial f_{12}}{\partial t}\right|_c \mathrm{d}\mathbf{c}_1\mathrm{d}\mathbf{c}_2, \qquad (138)$$

could be neglected in the transport equation of the drift velocity ($\psi=u_{1i}'$) and the fluid–particle velocity correlation tensor ($\psi=u_{1i}'u_{2j}'$). We shall see later that the models can be extended to dense suspensions by treatment of the collisional term (Section 7).

4. CONTINUOUS PHASE FLUCTUATIONS

In the previous sections, various closure models for the stress tensor and the second-order velocity moments in the particle phase, the drift veloicty and the fluid–particle velocity correlation tensor have been given. To complete the closure problem, the second-order velocity moment of the gas phase, $M_{1ij}=< u_{1i}'u_{1j}' >_1$, has to be modeled. In this section, we start by giving a deeper insight into two-way coupling and discuss models which can describe gas phase turbulence. Then, we formulate a transport equation for M_{1ij} and a complete closure for a two-equation model (k–ϵ model). Problems specific to the k–ϵ model are discussed.

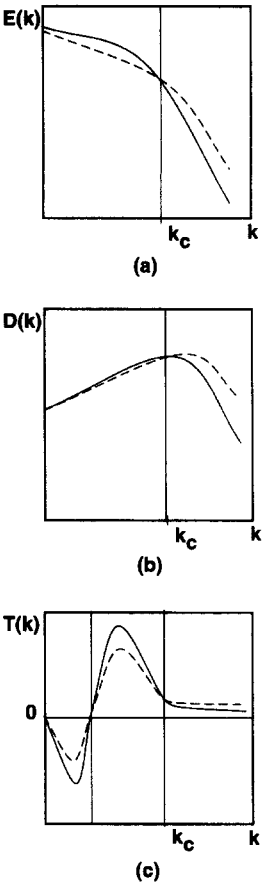

Fig. 4. Spectral distributions for $E(k)$, $D(k)$ and $T(k)$ without gravity field. Solid line: without particles; dashed line: with particles.

4.1. *Two-way Coupling*

Two-way coupling was briefly mentioned in Section 1, where some basic principles and explanations on the nature and the mechanisms of two-way coupling were presented, based on semi-empirical models and well-known experiments. This description is, however, insufficient and needs to be discussed together with direct numerical simulation (DNS) results. Indeed, it is generally considered[68] that particles with a small Reynolds number damp turbulence, whereas particles with large Reynolds numbers enhance turbulence due to vortex shedding. As a matter of fact, it has been shown by Elgobashi and Truesdell,[69] using direct numerical simulation of grid turbulence (homogeneous isotropic turbulence), that small particles (smaller than the Kolmogorov scale) could enhance turbulence in a specific range of wavenumbers. As stated by Elgobashi and Truesdell, the modulation by particles of $E(k)$, the three-dimensional spectrum of energy, and $D(k)$, the three-dimensional spectrum of energy dissipation, follows a pattern of selective "**spectral redistribution**" rather than a uniform attenuation or augmentation.

A first set of results was presented by Elgobashi and Truesdell for zero gravity (no crossing trajectories effect). It is observed that, at low wavenumbers (large

scales), the values of $E(k)$ and $D(k)$ for a turbulent field with particles are smaller than the corresponding quantities of a turbulent field without particles below a critical wavenumber, k_c, above which the contrary is seen (Fig. 4(a, b)). As a decrease of the time-dependent turbulent kinetic energy and an increase of the time-dependent dissipation were observed, it can be concluded that, globally, for the kinetic energy, the production at high wavenumbers is dominated by the destruction at low wavenumbers. For the dissipation, attenuation at low wavenumbers is dominated by enhancement at large wavenumbers. According to Elgobashi and Truesdell, a possible explanation for this spectral redistribution is that particles transfer their energy to the small scales, with a corresponding increase in dissipation. This rise in dissipation is detected by the large scales, which increase their supply of energy to the small scales (Fig. 4(c)), and this results in the reduction of $E(k)$ at large scales. The detection by the large scales is due to non-local triadic interaction of $T(k)$, illustrated in Fig. 4(c), the rate of energy transfer to wavenumbers of magnitude k. A discussion of these mechanisms can be found, for example, in McComb[70] and Domaradzki and Rogallo.[71] A second set of results was given by Elgobashi and Truesdell for non-zero gravity. A similar behavior for the spectral redistribution was observed, but the critical wavenumber, k_c, decreased with time. This seems to indicate that energy transfer from particles starts at high wavenumbers and propagates to lower wavenumbers, which gives a reverse cascade phenomenon. The main feature of gravity is to produce anisotropy at high wavenumbers. The excess of energy in the gravity component is transferred to the other directions at the same wavenumber by the pressure strain term, and to other wavenumbers by triadic interactions.

The results of Elgobashi and Truesdell were confirmed experimentally by Tsuji *et al.*[72] for dilute suspensions in the case of homogeneous isotropic turbulence. The measurements of Tsuji *et al.* for the one-dimensional spectrum showed the same trend as in Fig. 4(a); the energy spectrum of the turbulent field with particles takes smaller values than the energy spectrum of the turbulent field without particles below a critical wavenumber, above which the contrary is observed. The measurements of Tsuji *et al.* were done for very dilute suspensions in pipe flows and the smallest particle size used in this experiment was greater than the Kolmogorov scale by a factor of two. In the experiment, the existence of the critical wavenumber is more pronounced in the core region, where turbulence can be assumed to be isotropic, than in the wall region. In addition, the experiment showed that for large particles (3 mm), turbulence is increased throughout the whole cross-section, while for small particles (200 μm), the contrary is observed. For medium-sized particles (500 μm and 1 mm), turbulence is enhanced in the core region but damped near the walls. Moreover, the tendencies observed by Tsuji *et al.*[72] have been predicted theoretically by Derevich,[58] whose model compares favorably with the measurements of Tsuji *et al.* The computations of Elgobashi and Truesdell, together with the theoretical results of Derevich and the measurements of Tsuji *et al.*, seem to prove the uncertainty of the early measurements of Hetsroni and Sokolov[73] and the theoretical results of Baw and Peskin,[74] which predict a decrease of the spectral components at high wavenumbers due to the presence of particles.

As a conclusion, three-dimensional spectra of turbulent kinetic energy and energy dissipation in dilute suspensions are governed by "**spectral redistribution**" mechanisms rather than by uniform mechanisms over the whole range of wavenumbers.

4.2. *Choice of a Model*

The purpose is to describe the motion of the continuous phase turbulence for "confined" turbulent two-phase flows, with application to fluidization. In turbulent single-phase flows, two-equation models, and especially the k–ϵ model,[75] are commonly used. However, it is known in single-phase flow modeling that the Boussinesq approximation yields an unsatisfactory description for certain types of flows, such as flows over curved surfaces, three-dimensional flows, flows with boundary layer separation and flows with secondary motions. Alternatives are possible with, on the one hand, an increase of the mathematical and physical complexity and, on the other, with powerful computers. Models increasing mathematical and physical complexity are non-linear models,[76] Reynolds stress models (RSMs)[77] and algebraic stress models (ASMs).[78] Models requiring computer capacity are large eddy simulation (LES)[79] and direct numerical simulation (DNS).[80] In this study, because of the complexity generated by the two-phase problem, it is considered that the Boussinessq approximation is valid in the applications to fluidization. Therefore, the study is limited to the k–ϵ model. The reasons why the k–ϵ model is preferred to the other two-equation models can be found in Launder and Spalding.[81] Advantages of the low Reynolds number k–ϵ model over ASMs and RSMs for prediction of pipe flow have been shown by Martinuzzi and Pollard.[82] Their study[82] does not give any indications on two-phase flow prediction, but it provides an argument which can strengthen the choice of a low Reynolds number k–ϵ model. In dilute two-phase flows, DNS has been tested by Elgobashi and Truesdell[69] and LES by Simonin *et al.*[83]

4.3. *Second-order Velocity Moment Transport Equation*

The transport equations for the second-order velocity moment of the continuous phase, $M_{1ij} = < u_{1i}' u_{1j}' >_1$ can be obtained as for the single-phase flow equations.[59] Let $N(u_{1i}) = 0$ symbolize the local instantaneous momentum equation for the continuous phase, where N denotes the Navier–Stokes operator. To derive the transport equations for the second-order velocity moment of the continuous phase, the quantity $< u_{1i}' N(u_{1j}) + u_{1i}' N(u_{1j}) > = 0$ is evaluated. After

some algebra, this expression becomes

$$\alpha_1\rho_1\frac{D_1}{Dt}M_{1ij}=\frac{\partial D_{1ijm}}{\partial x_m}+P_{1ij}+\phi_{1ij}+\prod_{1ij}-E_{1ij}. \tag{139}$$

The first term on the RHS, $\partial D_{1ijm}/\partial x_m$, is a diffusion term. It is the sum of two terms, $D^t_{1ijm}+D^t_{1ijm}$, where D^t_{1ijm} represents the transport related to the local instantaneous viscous stress tensor which can be compared to the molecular transport term in single-phase flows,

$$D^t_{1ijm}=<X_1\tau_{1jm}u_{1i}'+X_1\tau_{1im}u_{1j}'>. \tag{140}$$

This term is negligible compared to D^t_{1ijm}, the turbulent transport and pressure diffusion term:

$$D^t_{1ijm}=-\alpha_1\rho_1<u_{1i}'u_{1j}'u_{1m}'>_1-\alpha_1<p_1'u_{1i}'\delta_{jm}>_1 -\alpha_1<p_1'u_{1j}'\delta_{im}>_1. \tag{141}$$

The second term on the RHS of Eq. (139), P_{1ij}, is the production term due to the interaction between the velocity fluctuations and the spatial gradients of the mean velocity:

$$P_{1ij}=-\alpha_1\rho_1\left(<u_{1i}'u_{1m}'>_1\frac{\partial U_{1j}}{\partial x_m}+<u_{1j}'u_{1m}'>_1\frac{\partial U_{1i}}{\partial x_m}\right). \tag{142}$$

The third term on the RHS, ϕ_{1ij}, is the pressure strain term. It is mostly responsible for the redistribution of energy between the different terms of the turbulent stress tensor. This term is

$$\phi_{1ij}=\left\langle p_1'\frac{\partial}{\partial x_j}X_1u_{1i}'+p_1'\frac{\partial}{\partial x_i}X_1u_{1j}'\right\rangle. \tag{143}$$

The trace of this tensor is not zero as in the case of single-phase flows. The fourth term on the RHS, Π_{1ij}, represents the work of the forces exerted on the particles, as the particles move in the turbulent flow field. This term can be a production term or destruction term and is written as

$$\prod_{1ij}=\frac{\alpha_2\rho_2}{\tau^x_{12}}(-2<u_{1i}''u_{1j}''>_2+<u_{1i}''u_{2j}''>_2 +<u_{1j}''u_{2i}''>_2+U_{ri}U_{dj}+U_{rj}U_{di}), \tag{144}$$

where the mean relative velocity is $U_{ri}=<u_{2i}-u_{1i}>_2$ and the drift velocity is $U_{di}=<u_{1i}'>_2$. The fluctuating velocity of the gas phase seen by the particles is denoted $u_{1i}''=u_{1i}-<u_{1i}>_2$. Using this definition, it is also shown, as in Section 3, that $<u_{1i}'u_{1i}''>_2=<u_{1i}''u_{1i}''>_2$. The fifth term on the RHS, E_{1ij}, represents the viscous dissipation at the small scales of the turbulent flow field, as in single-phase flows, but also the production or dissipation of energy due to the presence of the particles (wake effects):

$$E_{1ij}=\alpha_1\left\langle\tau_{1jm}\frac{\partial u_{1i}'}{\partial x_m}+\tau_{1im}\frac{\partial u_{1j}'}{\partial x_m}\right\rangle_1. \tag{145}$$

In this expression, additional terms which come from compressibility effects have been neglected. These terms are equivalent to the ones found in the Favre- averaged Reynolds stress equation in single-phase flow.[59] This terms are $-<X_1u_{1i}'>\partial P_1/\partial x_j-<X_1u_{1j}'>\partial P_1/\partial x_i$.

4.4. *Two-equation Model (k_1–ϵ_1)*

The second-order velocity moment is given by the Boussinesq approximation,

$$M_{1ij}=\frac{2}{3}k_1\delta_{ij}-2\nu^t_1\hat{S}_{1ij}, \tag{146}$$

where the turbulent viscosity reads $\nu^t_1=C_\mu k_1^2/\epsilon_1$ and ϵ_1 is the dissipation of turbulent kinetic energy. The Boussinesq approximation is valid provided that $\nu^t_1|\partial U_{1i}/\partial x_j|\ll k_1$ (first-order approximation). This condition states that the characteristic time scale of the fluctuating motion must be much smaller that the time scale of the mean flow, $\tau^t_1|\partial U_{1i}/\partial x_j|\ll 1$. The equation for the turbulent kinetic energy of the continuous phase, $k_1=<u_{1i}'u_{1i}'>/2$, is obtained from Eq. (139) setting $i=j$:

$$\alpha_1\rho_1\frac{D_1}{Dt}k_1=\frac{1}{2}\left(\frac{\partial}{\partial x_m}D_{1iim}+P_{1ii}+\phi_{1ii}+\prod_{1ii}-E_{1ii}\right). \tag{147}$$

The transport term is modeled as for single-phase flows,[59] as

$$D_{1iim}=D_{k_1}\frac{\partial k_1}{\partial x_m}, \tag{148}$$

where $D_{k_1}=\alpha_1\rho_1(\nu_1+\nu^t_1/\sigma_{k_1})$ and σ_{k_1} is the effective Prandtl number which relates the eddy diffusion of k_1 to the momentum eddy viscosity. Neglecting the trace of the pressure strain term, the equation for the turbulent kinetic energy reads

$$\alpha_1\rho_1\frac{D_1}{Dt}k_1=\frac{\partial}{\partial x_m}\left(D_{k_1}\frac{\partial k_1}{\partial x_m}\right)-\alpha_1\rho_1<u_{1i}'u_{1m}'>_1\frac{\partial U_{1i}}{\partial x_m}+\alpha_1\rho_1\prod_1-\alpha_1\rho_1\epsilon_1. \tag{149}$$

The interface term, Π_1, is given by

$$\prod_1=\frac{X_{12}}{\tau^x_{12}}(-2<k_1>_2+k_{12}+U_{ri}U_{di}), \tag{150}$$

where $2<k_1>_2=<u_{1i}''u_{1i}''>_2$ represents the turbulent kinetic energy of the continuous phase seen by the particles. As in Section 3, if statistical independence is assumed between the local instantaneous spatial distribution of particles and the turbulent kinetic energy of the continuous phase, one can write $<k_1>_2=k_1$. A transport equation must now be written for the dissipation, ϵ_1. This equation is obtained with a similar procedure as for single-phase flows.[59] After some algebra, the differential equation for dissipation of turbulent kinetic energy, ϵ_1, is

given by

$$\alpha_1\rho_1\frac{D_1}{Dt}\epsilon_1=\frac{\partial}{\partial x_m}\left(D_{\epsilon_1}\frac{\partial\epsilon_1}{\partial x_m}\right)-\alpha_1\rho_1\frac{\epsilon_1}{k_1}\left(C_{\epsilon_1}M_{1ij}\frac{\partial U_{1i}}{\partial x_j}+C_{\epsilon_2}\epsilon_1\right)+\prod_{11},\tag{151}$$

where $D_{\epsilon_1}=\alpha_1\rho_1(\nu_1+\nu_1^t/\sigma_{\epsilon_1})$ and σ_{ϵ_1} is the effective Prandtl number which relates the eddy diffusion of ϵ_1 to the momentum eddy viscosity. The interaction term, Π_{11}, is modeled according to Elgobashi *et al.*[84] as

$$\prod_{11}=C_{\epsilon_3}\frac{\epsilon_1}{k_1}\prod_1.\tag{152}$$

This term expresses the work of the forces exerted on the particles divided by the characteristic time of turbulence. The system of equations is closed if the constants σ_{k_1}, σ_{ϵ_1}, C_μ, C_{ϵ_1}, C_{ϵ_2} and C_{ϵ_3} are defined. The effective Prandtl numbers are $\sigma_{k_1}=1.0$ and $\sigma_{\epsilon_1}=1.3$. The other constants have been determined by applying the model to simple turbulent flows: $C_\mu = 0.09$, $C_{\epsilon_1}=1.44$, $C_{\epsilon_2}=1.92$. The constant in the term specific to two-phase flows was given by Elgobashi *et al.*[84] as $C_{\epsilon_3}=1.2$. The constants defined above and in Eqs (149)–(152) define the k_1–ϵ_1 model derived by He and Simonin.[85] In this formulation (Eqs (149) and (151)), the effect of the velocity fluctuations produced by the wakes is not considered. Such effects are assumed to be in local equilibrium with the viscous dissipation (the particle diameter is smaller than the Kolmogorov scale in the gas phase, so that wake effects are directly dissipated into heat). Therefore, turbulence is modeled for the length scales of the flow which are much larger than the particle diameter, $d_p \ll L_1^t$. A k–ϵ model which accounts for the wake effects was presented by Yokomine and Shimizu.[86]

Moreover, the present k–ϵ model, expressed by Eqs (149) and (151), is only valid for dilute, turbulent, fully developed two-phase flows: the "**high Reynolds number**" k–ϵ model. The subject of interest in this study is applications to fluidization, which means confined flows. Near walls, regions exist where the local Reynolds number of turbulence, $Re_t=C_\mu k_1^2/\epsilon_1\nu_1$, is small and viscous effects dominate over the turbulent ones. There are two methods to deal with this problem, "**wall functions**" and "**low Reynolds number**" k–ϵ models. Wall functions have been extensively treated for single-phase flows, but there are few results concerning two-phase flows. Rizk and Elgobashi[87] showed by means of a low Reynolds number model, that, even for dilute suspensions, the use of the law of the wall is questionable and that a significant deviation from single-phase flow can occur with a relatively low particle volume fraction, for example a deviation of U^+ of 16% at $y^+ = 30$, for $\alpha_2 = 0.004$. Bolio *et al.*[88] used a low Reynolds number model, the k–ϵ model of Myong and Kasagi,[89] a choice motivated by a comparative study of low Reynolds number k–ϵ models.[90] The model presented by Bolio *et al.* rises fundamental questions concerning the universality of the constants σ_{k_1}, σ_{ϵ_1}, C_{ϵ_1} and C_{ϵ_2}. Bolio *et al.* made a sensitivity analysis on their k–ϵ model by varying the model constants σ_{k_1}, σ_{ϵ_1}, C_{ϵ_1} and C_{ϵ_2} over an interval $\pm$ 0.1 and found that their predictions did not exhibit a significant sensitivity to these variations. However, this does not give any indication of the modification of the constants due to the presence of particles.

A more systematic investigation was done by Squires and Eaton[91] based on their DNS database.[51] The DNS database is generated from particle-laden "**homogeneous isotropic turbulence**" and therefore the influence of the presence of particles is investigated only for C_{ϵ_2} and C_{ϵ_3}. Results are presented for the following cases: a ratio of particle relaxation time to time scale of turbulence, τ_{12}^x/τ_1^t, ranging from 0.14 to 1.5, and a loading, X_{12}, ranging from 0 to 1.0. The results show that, for example, for $\tau_{12}^x/\tau_1^t=0.14$ and $X_{12}=1.0$, C_{ϵ_2} increases by a factor of 6 and C_{ϵ_3} decreases by a factor of 4 compared to the single-phase flow values. For $\tau_{12}^x/\tau_1^t=1.5$, the influence of particles does not depend very much on the loading.

An attempt to account for particle effects on C_μ was made by Cao and Ahmadi,[92] who proposed correcting the turbulent viscosity by modifying C_μ as $C_\mu=0.09C_\mu^*$, where C_μ^* is given by $C_\mu^{*-1}=1+(\tau_{12}^x/\tau_1^t)(1-\alpha_2/\alpha_m)^3$. In summary, more research is needed in this field.

4.5. *Low Reynolds Number k_1–ϵ_1 Model*

There are several low Reynolds number k–ϵ models for single-phase flows. Reviews of these models can be found in Patel *et al.*[93] and Wilcox.[59] In low Reynolds number k–ϵ models, the entire boundary layer is solved and the viscous effects at the wall are accounted for by means of damping functions. The study of the limiting behavior of the fluctuating velocities near the wall leads to two implementations of the low Reynolds number k–ϵ model.

The first implementation is to modify the ϵ_1 equation and solve it instead for $\tilde{\epsilon}_1$, defined by $\tilde{\epsilon}_1=\epsilon_1-\epsilon_w$. Here, ϵ_w represents the dissipation rate at the wall, which can be defined in several ways, the most famous being $\epsilon_w=2\nu_1(\partial\sqrt{k_1}/\partial y)^2$.[75] This solution has the advantage of having a Dirichlet boundary condition, which reads $\tilde{\epsilon}(y=0)=0$. The transport equation for $\tilde{\epsilon}$ is

$$\alpha_1\rho_1\frac{D_1\tilde{\epsilon}}{Dt}=\frac{\partial}{\partial x_m}\left(D_{\epsilon_1}\frac{\partial\tilde{\epsilon}_1}{\partial x_m}\right)-\alpha_1\rho_1\frac{\tilde{\epsilon}_1}{k_1}\left(f_1C_{\epsilon_1}M_{1ij}\frac{\partial U_{1i}}{\partial x_j}+f_2C_{\epsilon_2}\tilde{\epsilon}_1\right)+\prod_{11}+E,\tag{153}$$

where f_1 and f_2 are damping functions and E accounts for consistency at the wall. This term must satisfy

$$\alpha_1\rho_1\nu_1\frac{\partial^2\tilde{\epsilon}_1}{\partial y^2}+\alpha_1\rho_1f_2C_{\epsilon_2}\frac{\tilde{\epsilon}_1^2}{k_1}+\prod_{11}+E=0.\tag{154}$$

If the influence of particles can be neglected, E can be

modeled as for single-phase flows. When the dissipation rate equation (Eq. (151)) is solved for $\tilde{\epsilon}_1$, the transport equation for k_1 reads

$$\alpha_1\rho_1\frac{D_1k_1}{Dt}=\frac{\partial}{\partial x_m}\left(D_{k_1}\frac{\partial k_1}{\partial x_m}\right)-\alpha_1\rho_1M_{1im}\frac{\partial U_{1i}}{\partial x_m}+\alpha_1\rho_1\prod_1-\alpha_1\rho_1\tilde{\epsilon}_1-\alpha_1\rho_1\epsilon_w, \quad (155)$$

where the turbulent viscosity is defined by $\nu_1^t=C_\mu f_\mu k_1^2/\epsilon_1$ (see Eq. (146)) and f_μ is a damping function. The low Reynolds number model is then defined by a modified ϵ_1 equation, three damping functions, f_μ, f_1 and f_2, the value of the dissipation rate at the wall, ϵ_w, and an additional term, E, for consistency at the wall. The boundary conditions are $k_1=\tilde{\epsilon}_1=0$ for $y=0$.

The second possible implementation is to solve the dissipation rate equation for ϵ_1 ($\epsilon_w=0$ and $E=0$) and find a suitable boundary condition at the wall. The low Reynolds number k–ϵ model is then defined by the three damping functions, f_μ, f_1 and f_2, and the boundary conditions $k_1=0$ and $\epsilon_1=\nu_1\partial k_1^2/\partial y^2$ or $\partial\epsilon_1/\partial y=0$.[94] Reviews of these models can be found in Patel *et al.*[93] and Wilcox.[59]

In the two-phase flow approach, the formulation of a low Reynolds number k–ϵ model is quite intricate. Damping functions and boundary conditions must account for the presence of particles. There has been almost no work done in this field; most researchers use the single-phase results. In general, more research is needed in this field.

4.6. *Concluding Remarks*

The formulation of a model which describes the velocity fluctuations in the gas phase is a difficult task. When using a k_1–ϵ_1 model, the main difficulties are: (1) to find values of the constants σ_{k_1}, σ_{ϵ_1}, C_μ, C_{ϵ_1}, C_{ϵ_2} and $C_{\epsilon 3}$, which account for the presence of particles; (2) to find an accurate form of the interaction terms, Π_1 and Π_{11}, if wake effects are important; and (3) to find a proper treatment of the wall layer when particles are present. More research is needed in this field.

5. DISCRETE PHASE FLUCTUATIONS

The models presented here are a direct application of the kinetic theory of granular flow (Section 2) and of the models of fluid–particle interactions (Section 3). Three models are presented, the models of Koch[23] (algebraic models), a two-equation model and a second-order closure model. The two-equation model, called the k_2–k_{12} model, is based on two transport equations, one for the turbulent kinetic energy of the discrete phase, k_2, and one for the fluid–particle velocity covariance, k_{12}. The second-order closure model, similar to an RSM in single-phase flow, is based on the transport equation for the second-order velocity moment, M_{2ij} (Eq. (30)).

5.1. *Algebraic Models*

Koch[23] gave asymptotic steady state solutions of the energy equations for $Re \ll 1$ and $St \gg 1$ (Section 3). For very massive particles, $St \gg \alpha_2^{-3/2}$, in a homogeneous suspension at steady state, the granular temperature is given by $T_2=St^{-2/3}\mathbf{U}_r^2/(36\pi)^{1/3}$, where the Stokes number has been redefined as $St=2|\mathbf{U}_r|\tau_{12}^x/d_p$. For moderately massive particles, $\alpha_2^{-3/4} \ll St \ll \alpha_2^{-3/2}$, in a homogeneous suspension at steady state, the stress tensor is defined by (Section 3): $M_{2\|}=0.802\mathbf{U}_r^2St^{-2/3}$ and $M_{2\perp}=0.034\mathbf{U}_r^2St^{-2/3}$.

Algebraic models can also be derived from the two-equation model (see Section 5.2). These models are based on the assumption of local equilibrium: the only terms remaining are production, dissipation and interaction terms. Examples of such models are given, for example, by Boemer *et al.*[95]

5.2. *Two-equation Model*

The transport equation for turbulent kinetic energy of the discrete phase, $k_2=<u_{2i}'u_{2i}'>_2/2$ related to the granular temperature by $k_2=\frac{3}{2}T_2$, can be written using Eq. (30) with $i=j$. This equation reads

$$\alpha_2\rho_2\frac{D_2k_2}{Dt}=-\frac{1}{2}\frac{\partial}{\partial x_i}E_{ijj}-\Sigma_{2ij}\frac{\partial U_{2i}}{\partial x_j}-\frac{\alpha_2\rho_2}{\tau_{12}^x}(2k_2-k_{12})+\frac{1}{2}\chi_{ij}. \quad (156)$$

From the previous results, Eq. (156) becomes

$$\alpha_2\rho_2\frac{D_2k_2}{Dt}=\frac{\partial}{\partial x_i}\left(D_{k_2}\frac{\partial k_2}{\partial x_i}\right)-\Sigma_{2ij}\frac{\partial U_{2i}}{\partial x_j}-\frac{\alpha_2\rho_2}{\tau_{12}^x}(2k_2-k_{12})+\alpha_2\rho_2\frac{e^2-1}{3\tau_2^c}k_2, \quad (157)$$

where $D_{k_2}=\alpha_2\rho_2(K_2^t+K_2^c)$, K_2^t and K_2^c are defined by Eqs (79) and (80), respectively. The effective stress tensor is given by $\Sigma_{2ij}=\theta_{ij}+\alpha_2\rho_2M_{2ij}$. The collisional stress tensor, θ_{ij}, is given by Eq. (64) and the second-order moment, M_{2ij}, by Eq. (68). The fluid–particle velocity covariance, k_{12}, is given by Eq. (119),

$$\alpha_2\rho_2\frac{D_2}{Dt}k_{12}=\frac{\partial}{\partial x_j}\left(D_{k_{12}}\frac{\partial k_{12}}{\partial x_j}\right)-\alpha_2\rho_2<u_{1i}''u_{2j}'>_2\frac{\partial U_{2i}}{\partial x_j}-\alpha_2\rho_2<u_{1j}''u_{2i}'>_2\frac{\partial U_{1i}}{\partial x_j}+\prod_{12}-\alpha_2\rho_2\epsilon_{12}, \quad (158)$$

where $D_{k_{12}}=\alpha_2\rho_2\nu_{12}^t/\sigma_{k_1}$. The turbulent fluid–particle viscosity is given by $\nu_{12}^t=k_{12}\tau_{12}^t/3$ and the destruction term by $\epsilon_{12}=k_{12}/\tau_{12}^t$. The fluid–particle velocity correlation tensor, $<u''_{1j}u_{2i}'>_2$, is defined by Eq. (121) and the phase interaction term, Π_{12}, is given by Eq. (120).

5.3. *Second-order Closure Model*

The second-order moment closure is based on the transport equations for the second-order moment of the particle velocity fluctuations, $M_{2ij} = <u_{2i}'u_{2j}'>_2$ (Eq. (30)), which reads

$$\alpha_2\rho_2\frac{D_2}{Dt}M_{2ij} = -\frac{\partial}{\partial x_m}E_{ijm} - \Sigma_{2im}\frac{\partial U_{2j}}{\partial x_m} - \Sigma_{2jm}\frac{\partial U_{2i}}{\partial x_m} - \frac{2\alpha_2\rho_2}{\tau_{12}^x}(M_{2ij} - M_{12ij}) + \chi_{ij}. \quad (159)$$

In this equation, the terms have been defined before: the third-order tensor, $E_{ijm} = \theta_{ijm} + \alpha_2\rho_2 M_{2ijm}$, where θ_{ijm} is defined by Eq. (65); the source term, χ_{ij}, is given by Eq. (61), and the fluid–particle velocity correlation tensor, M_{12ij}. To close the system, closure equations for the third-order velocity moment, $M_{2ijm} = <u_{2i}'u_{2j}'u_{2m}'>_2$, and M_{12ij} must be derived.

A closure equation for the third-order velocity moment can be derived from Eq. (32), neglecting the mean transport and mean gradient effects.[27] This gives

$$\frac{\partial}{\partial x_m}\alpha_2\rho_2 M_{2ijm} = -\frac{\partial}{\partial x_m}\left(\alpha_2\rho_2 K_{2mn}^t\frac{\partial}{\partial x_m}M_{2ij}\right), \quad (160)$$

where the diffusivity tensor is

$$K_{2mn}^t = \left(\frac{G^x}{\tau_{12}^x}\frac{\tau_{12}^t}{G^t}M_{12ij} + M_{2mn}\right)\Big/\left(\frac{G^x}{\tau_{12}^x} + \frac{D}{\tau_2^c}\right), \quad (161)$$

and where $D = (1+e)(49-33e)/100$. The constants G^x and G^t are 9/5 and $3C_\mu/2C_s'$, respectively, where $C_s' = 0.25$. Various models for a transport equation for the fluid–particle velocity correlation tensor are found in Eqs (119) and (121) or Eq. (136).

5.4. *Concluding Remarks*

The second-order velocity moment can be modeled in three ways: (1) algebraic models, (2) two-equation models and (3) second-order closure models. Whenever possible, algebraic models should be used for the sake of simplicity. However, time and spatial derivative terms are not always negligible: if the quasi-isotropy assumption (Boussinesq approximation) holds, two-equation models are a good alternative to algebraic models. When the flow is highly anisotropic, for example vertical gas–solid flows, second-order closure models should be used.

6. BOUNDARY CONDITIONS

An accurate description of the boundary conditions is necessary. An example of the importance of the wall boundary conditions in the discrete phase can be found in the computations of Louge *et al.*[54] For computations of dilute gas–solid flows in a vertical riser, Louge *et al.* noticed that, at least in their narrow rig, the overall pressure drop was very sensitive to changes in the value of the coefficient of dynamic friction. In the following section, boundary conditions at a solid wall are given for the continuous and the discrete phases. Inlet and outlet boundary conditions are not treated here, as these are case dependent, but, nevertheless, their importance should not be underestimated. In fluidization, it has been shown[96] that the pressure drop over the air distributor gives different types of flow patterns in the lower region of the riser, which in turn probably influences the upper regions. Consequently, in some applications, the inlet boundary conditions should definitely account for the coupling between the plenum or the pipe system and the combustion chamber. To our knowledge, such an attempt has not been made and this question is still open.

6.1. *Continuous Phase Boundary Conditions*

When local agglomeration of particles occurs in the near wall region, the flow field is disturbed. This is why, as mentioned by Rizk and Elgobashi[87] and He and Simonin,[18] the use of the law of the wall might be questionable. However, according to Louge *et al.*,[54] in very dilute suspensions, the law of the wall should not be greatly affected by the presence of particles. This might not be the case in fluidization, but the approach is presented as it can be used in other gas–solid flows. The first node of the computational domain is placed in the log-layer at $30 < y^+ < 100$, and the tangential velocity component is given by the law of the wall, $U_{1x}^+ = \ln(Ey)^+/\kappa$, where the dimensionless quantities are defined by $U_{1x}^+ = U_{1x}/u^*$ and $y^+ = yu^*/\nu_1$. Kármán's constants are $\kappa = 0.41$ and $E = 9.0$. The friction velocity is defined in terms of the stress tensor at the wall, τ_w, as $\tau_w = -\rho_1 u^{*2}$. In the log-layer, the solution to the momentum equation and the k_1–ϵ_1 equations is $U_{1x}^+ = \ln(Ey^+)/\kappa$, $k_1 = u^{*2}/\sqrt{C_\mu}$ and $\epsilon_1 = u^{*3}/\kappa y$. Solving the law of the wall for u^* gives the boundary conditions for k_1 and ϵ_1 and the value of the turbulent viscosity, $\nu_1^t = \nu_1 y^+\kappa/\ln(Ey^+)$. Boundary conditions for the velocity components are $\mathbf{U}_1 = \mathbf{0}$. If the low Reynolds number k–ϵ model is used, the boundary layer is solved in its integrality. The first node is placed, for example, at $y^+ = 1$. The boundary conditions for the mean velocity and the turbulent kinetic energy are $\mathbf{U}_1 = \mathbf{0}$ and $k_1 = 0$, respectively. The boundary condition for dissipation depends on the model which is used (Section 4). It can be $\tilde{\epsilon}_1 = 0$ or $\nu_1\partial k_1^2/\partial y$ or $\partial\epsilon_1/\partial y = 0$.

6.2. *Discrete Phase Boundary Conditions*

Boundary conditions have to be specified at the wall for the mean velocity, $\mathbf{U}_2$, the turbulent kinetic energy, k_2, the fluid–particle velocity covariance, k_{12}, and the mean particle volume concentration, α_2. For α_2 and k_{12}, it is customary to use $\partial\alpha_2/\partial n = 0$ and $\partial k_{12}/\partial n = 0$ or $k_{12} = 0$, where n is the direction normal to the wall. For the velocity field and the granular temperature, a zero momentum and turbulent kinetic energy flux at the wall, i.e. $\partial U_2/\partial n = 0$ (free slip) and $\partial k_2/\partial n = 0$ are often formulated.

In rapid granular flows, it has been observed experimentally that the roughness of the boundaries is a critical parameter concerning the magnitude, for example, of shear stresses (cf. Savage and Sayed[97] and Hanes and Inman[98]). The problem of the formulation of boundary conditions in rapid granular flows was first (in a formal way) addressed by Jenkins and Richman[99] and Richman[100] for frictionless spheres. Friction was accounted for by Johnsson and Jackson,[101] following the work of Hui *et al.*,[102] and by Jenkins[103] using different arguments. However, in the model of Johnsson and Jackson, colliding particles (distinction is made between colliding and sliding particles) are characterized by a specularity coefficient whose physical meaning is not obvious. As a matter of fact, attention is now focussed on the work of Jenkins, which is based on a more rigorous approach (probability density function approach together with wall–particle collision properties), and in the following it is assumed that the results of Jenkins are valid for gas–solid flows.

Jenkins derived a theory, using a simple velocity distribution function (it is assumed that the three components of the second-order moment of the fluctuating velocity are equal to the granular temperature at the wall), to calculate the rate at which momentum and energy are supplied to the flow per unit area of the wall. From these two quantities, boundary conditions can be derived for U_{2x} and k_2. According to Jenkins, the shear stress, S, and the energy flux, Q, at the wall can be related to the normal shear stress, N, wall–particle collisional properties (normal and tangential restitution coefficient, e_w, β_w and coefficient of friction μ_w) and the ratio $r = U_{2x}|_w/\sqrt{2k_2}$ (here x is the direction parallel to the wall and the normal direction will be denoted y). The latter parameter, r, represents the ratio of the slip velocity and the square root of the turbulent kinetic energy for the discrete phase. The analytical results of Jenkins are valid for two asymptotic cases: a case where the contact point slides (small friction/all sliding limit) and a case where the contact point sticks (large friction/no sliding limit; in this case it is necessary to assume $r \gg 1$). These results were extended by the computer simulations of Louge,[104] who gave an empirical fit. Louge noticed that, while the shear stress was well predicted by Jenkins, the energy flux was over-predicted in both limits.

In the following, the correlations of Louge are presented. For wall–particle collisional properties verifying $0.1 \le \mu_w \le 0.4$, $0.5 \le e_w \le 1$ and $0 \le \beta_0 \le 0.6$, the ratio of the shear stress S and the normal stress N is, according to Louge,

$$\frac{S}{N} = \mu_w(1 - \exp(-ar/\mu_w)), \tag{162}$$

where the exponent a is defined by

$$a = a_1 \exp(-a_2(1-e_w))(1-\exp(-a_3\mu))(1+\beta_0)^{a'}, \tag{163}$$

with $a' = a_4(1 - \exp(-a_5\mu))$. For the constants a_1–a_5, Louge gives $a_1 = 0.3537$, $a_2 = 1.042$, $a_3 = 4.453$, $a_4 = 2.068$ and $a_5 = 0.8468$. The ratio S/N is plotted in Fig. 5(a) for $e = 0.9$ and various friction coefficients. For the energy flux at the wall, Q, Louge identifies two asymptotic limits. When $r \to 0$,

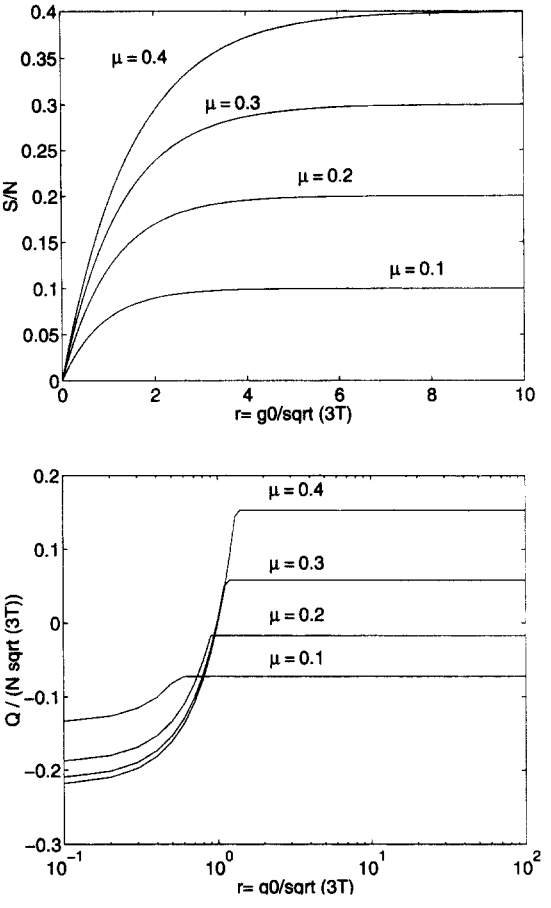

Fig. 5. S/N (a) and $Q/N\sqrt{3T_2}$ (b) as a function of r, with $e = 0.9$ and $\mu = 0.1$, 0.2, 0.3 and 0.4 (particle rotation is neglected, so that $\beta_0 = 0$).

$$\frac{Q}{N\sqrt{3T_2}} = B_1 r^2 + B_2 r - B_3, \tag{164}$$

where

$$B_1 = b_1/(1+e_w),$$
$$B_2 = b_2(1-e_w)(1-\exp(-b_3\mu_w)),$$
$$B_3 = B_4(1-\exp(-B_5\mu_w)),$$
$$B_4 = b_4(1-e_w)^2 + b_5(1-e_w) + b_6,$$
$$B_5 = b_7(1-e_w) + b_8.$$

The constants b_1–b_8 are given as $b_1 = 0.02$, $b_2 = 0.3$, $b_3 = 3.4$, $b_4 = 1.8$, $b_5 = 1.1$, $b_6 = 0.1$, $b_7 = 4.6$, and $b_8 = 8.6$. When $r \to \infty$,

$$\frac{Q}{N\sqrt{3T_2}} = d_1(1+e_w)\mu_w^2 + d_2(1-e)\mu_w - d_3(1-e_w), \tag{166}$$

where $d_1 = 0.522$, $d_2 = 2.57$ and $d_3 = 1.08$. The ratio $Q/N\sqrt{3T_2}$ is plotted in Fig. 5(b) for $e = 0.9$ and different friction coefficients (the transition value of r

between the two regions is given by the positive root of $B_1 r^2 + B_2 r - (B_3 + d_1(1+e_w)\mu_w^2 + d_2(1-e)\mu_w - d_3(1-e_w)) = 0$.

The boundary conditions can then be derived from $M_i \Sigma_{2ij} n_j$ and $q_i n_i = Q$ (cf. Jenkins[103]). Here, n_i is the unit vector normal to the wall and pointing into the flow. M_i, whose normal and tangential components are N and S, respectively, is the rate of momentum supplied to the flow per unit area of the wall, and q_i is the energy flux in the flow. The boundary conditions read

$$N = \Sigma_{2yy},\ S = \alpha_2 \rho_2 \nu_2 \frac{\partial U_{2x}}{\partial y},\ Q = \alpha_2 \rho_2 K_2 \frac{\partial k_2}{\partial y}. \quad (167)$$

Finally, in a recent paper, Jenkins and Louge[105] have improved the analytical results of Jenkins[103] for the energy flux in both limits, and the new expressions agree well with the computer simulations of Louge.

7. DISCUSSION

7.1. *Usefulness of the Models*

We start with some final remarks on the kinetic theory of granular flow presented in Section 2 and on the closure models presented in Section 5, where closure models for the collisional stress tensor, the diffusivity of the granular temperature, and a transport equation for the second-order velocity moments are given. These results are almost free from empirical constants: only the restitution coefficient, e, and the radial distribution function, g_0, have to be given. According to Lun and Savage,[37] the restitution coefficient depends, at least, on the material of the particles and on the relative velocity between two colliding particles. In our analysis the restitution coefficient is constant: its value has been measured for different cases.[43] Sensitivity analyses on the restitution coefficient have been carried out in dilute suspensions by Bolio *et al.*,[88] and only a minor sensitivity in the predictions was observed. In dense suspensions, Balzer *et al.*[29] found a great sensitivity of this parameter: numerical results showed that, for relatively small values of e (approximately 0.9), the non-stationary motion of the bed (bubbling motion) was changed (more bubbles were observed). Low values of the restitution coefficient decrease the granular temperature, which in turn decreases viscosity and diffusivity, and in this way larger gradients are observed. However, the limitations of the kinetic theory of granular flow do not only result from the empirical factors, but mostly from the assumptions made to derive this theory: flows with small spatial gradients, nearly elastic particles, low level of anisotropy, binary collisions and a simplified model of particle–particle collision. A more general formulation than the one of Grad[25] might be needed: this could be achieved by a more advanced particle velocity probability density function, but mathematical difficulties are encountered.[31] More research is needed to derive a general model of the particle–particle interactions. It should be emphasized that the model presented in this work includes the influence of the gas phase on the granular flow, an influence which is not taken into account in other formulations and therefore reduces the quantitative ability of models used by, for example, Ding and Gidaspow[14] and Bolio *et al.*[88] to predict accurate results in the dilute case, $\tau_2^c \gg \tau_{12}^x$. To illustrate this effect, a sensitivity analysis on the influence of an interstitial gas on granular flows was done by Boëlle *et al.*[31] This does not mean that particle–particle collision is not an important mechanism in dilute flows. For example, Louge *et al.*[54] found, in their computations for comparisons with the measurements of Tsuji *et al.*,[72] positive particle velocities through the whole cross-section of the duct, even close to the wall, where the gas velocity is near zero, and where the particles are consequently expected to fall. According to Louge *et al.*, observation of particle velocities higher than gas velocities in the near wall region is due to the shear stress in the particle phase. Particles located further away from the wall have a positive velocity and they transfer momentum through collisions with particles near the wall. In addition, in the kinetic theory proposed in the present work, only binary collisions were considered. It has been shown experimentally,[106] by means of a high speed video system and a reflective type of particle image scope, that triple or quadruple collisions occur. In dense suspensions, the probability of multiple collisions is expected to be relatively high, but in dilute suspensions a binary collision model seems to be appropriate. Other analyses are necessary to determine if collisions involving more than two particles are encountered as frequently as the binary collisions. Finally, as far as the turbulent motion is concerned (Section 5), it seems that the local equilibrium hypothesis (Boussinesq approximation) is satisfied in the case of dense fluidization, whereas in a dilute suspension this assumption is more uncertain. In this case, separate equations for the turbulent stresses have to be solved.[4] Anisotropy has been observed experimentally by Azario *et al.*,[107] who have reported a high level of anisotropy (about a factor of two) in dilute suspensions.

In Section 3, closure models are given for the drift velocity and the fluid–particle velocity correlation tensor. Practical closure models are limited to the case of homogeneous isotropic turbulence or homogeneous simple shear flows, because in these cases the description of turbulence is analytically simple. In the coarse particle case, $\eta_r \ll 1$ or $\tau_{12}^t \ll \tau_{12}^x$, particle motion is only slightly affected by the fluid fluctuations and the modeling of diffusion caused by the drift velocity is not critical. On the contrary, in the scalar case, $\eta_r \gg 1$ or $\tau_{12}^t \gg \tau_{12}^x$, particle motion is governed by the fluid turbulence, and the influence of the drift velocity is critical. Some models omit the drift velocity, whereas other models, for example, those of Louge *et al.*[54] and Bolio *et al.*,[88] use the simplified formulation of Koch.[23] For accurate modeling of this term, the general formulation of Simonin,[27] using the fluid–particle joint probability density function and the Langevin equation,

should be used. In addition, one of the key issues of the Eulerian/Eulerian formulation is to derive an accurate model for the fluid–particle velocity correlation tensor, as this term is very important for two-way coupling. This term appears in the interfacial terms of the transport equations for the fluctuating motion and can give production or destruction of the velocity fluctuations in both phases. More research is needed in this field for an accurate formulation of the transport equation of the fluid–particle velocity correlation tensor, $<u_{1i}''u_{2i}'>_2$. Indeed, the formulations of Simonin are given for very dilute flows, where the influence of particle–particle collisions can be neglected. As the suspension becomes denser, the effect of collisions should influence the fluid–particle velocity correlation tensor.

In Section 4, closure models are given for gas velocity fluctuations in the case of dilute flows with a low anisotropy level (k_1–ϵ_1 model). The limitations of this model are numerous, and the formulation as it stands is not satisfactory for the following reasons. (1) The values of the constants are not known for application to two-phase flow, and some studies in dilute flows have shown that they are different from the single-phase flow case,[91] depending on the loading and on the particles and the gas phase turbulence properties. (2) The interaction term represents momentum exchange between the phases; particles are accelerated by the gas phase and can give back some of their momentum to the gas phase in regions where the turbulent kinetic energy of the gas phase is small. However, this term does not represent the interaction at the particle level, such as wakes, which are supposed to be in local equilibrium. The present two-equation model is written for scales of turbulence which are large compared to the particle size, otherwise the model becomes very crude. (3) When particles agglomerate in the near wall region, the flow field is disturbed. Kaftori *et al.*[108] studied the wall region in a horizontal water–particle flow, with $\rho_2 = 1.05\ \mathrm{kg\ m^{-3}}$, $d_p = 100$, 275 and 900 μm, and $X_{12} = 10^{-4}$ and 2×10^{-4}. The study showed that the particles do not modify the structure of turbulence, but modify some of its characteristics: the frequency of the coherent structures is modified by the particles in the wall region. This has also been observed in numerical simulations by Komori *et al.*[109] In addition, the particles in the wall region follow a pattern which is directly related to the coherent structures in the wall region. Indeed, it has been shown that the particle motion in an horizontal wall region can be affected by different types of wall–particle interactions: (1) wall–particle collisions tend to lift up particles from the wall region;[110] (2) the Saffman force also tends to lift up particles from the wall region; (3) coherent structures, characterized by ejection and in-sweep motions, can influence particle motion both ways;[108] (4) if the inertia of the particles is sufficiently high, particles can be trapped in the viscous layer.[111] These results are valid for dilute suspensions and they cannot be readily generalized to dense suspensions.

7.2. *Application to Fluidization*

In this section, the discussion is separated into two parts, which correspond to two levels of understanding. The first level, the most fundamental, is an analysis of microphenomena, whereas the second level is an analysis of macrophenomena. By microphenomena is meant the mechanisms which are characteristic of the behavior of a single particle: to carry out an analysis of these phenomena, particle dispersion in simple turbulent flows is discussed, as well as estimates of the characteristic time scales in the freeboard region of a CFBC. By macrophenomena is meant an analysis of the mechanisms which are characteristic of the behavior of a group of particles (mechanisms which can be visualized by experiments): to do this, the flow pattern in a CFBC is discussed.

7.2.1. *Gas–solid flows in the frame of fluidization*

In this section, an analysis of the microphenomena is made. In fluidization, and especially in a CFB, the motion of a particle is described by three parameters: the particle relaxation time (drag force), gravity and particle–particle collision time (collision mechanisms). The particle mass loadings observed in a CFB render difficult comparisons between available results, mostly concerned with very dilute suspensions, and the real situation of a CFB riser. However, these results are presented here because they give a basic understanding of particle motion in a turbulent flow field. Few experimental results are available in the literature, so that most researchers use LES and DNS to generate turbulence in the continuous phase and a Lagrangian description of the discrete phase in order to study the behavior of particles in a turbulent flow field. Unfortunately, most of these studies assume one-way coupling (the flows are dilute enough to neglect the influence of particles on turbulence and the influence of particle–particle collisions). These studies have been carried out in ideal cases: homogeneous isotropic turbulence (with and without gravity) and homogeneous turbulent shear flows (without crossing trajectory effects). For homogeneous isotropic turbulence, many researchers have focussed their attention on particle dispersion. In this case, the combined effect of particle inertia and fluid turbulence results in a low level of particle velocity fluctuations, below that of the gas.[16] For particles in homogeneous isotropic turbulence in a gravity field, particle dispersion in the streamwise direction (gravity direction in the treated case) is higher than particle dispersion in the transverse direction due to the continuity effect.[17] A detailed study of the three-dimensional fluctuating motion of particles in homogeneous isotropic turbulence has been carried out by Hajji *et al.*[112] (the study is presented for a vertical flow, streamwise direction, with a given mean velocity). The computations show that, for particles in homogeneous isotropic turbulence in a gravity field, particle velocity fluctuations in the streamwise direction (gravity

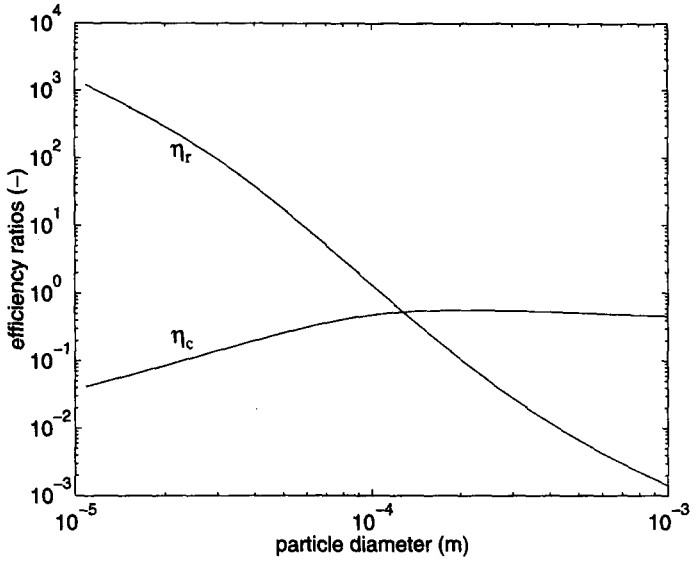

Fig. 6. Characteristic time scale ratios. From Peirano *et al.*[115]

direction) are higher than particle velocity fluctuations in the transverse direction, and that the particle velocity fluctuations are lower than the gas velocity fluctuations. Hajji *et al.* also made a sensitivity analysis on particle diameter, particle density, turbulent intensity of the fluid, Eulerian integral length scale and mean relative velocity. The study showed that when the particle diameter increases, the particle velocity fluctuations decrease. The difference between the streamwise and the spanwise fluctuations is of course smaller when particles have a small diameter (greater sensitivity to the fluid fluctuations), but converges towards a fixed value for larger diameters. The particle density influences the fluctuations in such a way that, the higher the density, the lower the particle velocity fluctuations (increased inertia). The rest of the study treated different particle densities and diameters. There was no effect of the turbulent intensity of the fluid: the ratio of the particle to fluid turbulent intensity was unchanged in both directions. On the contrary, the fluid Eulerian integral scale seems to be proportional to the particle velocity fluctuations in both directions. Finally, the higher the relative velocity, the higher the particle velocity fluctuations, with a stronger effect in the streamwise direction.

For homogeneous simple shear flows, in the absence of an imposed bodyforce (gravity), Simonin *et al.*[83] have observed that the degree of anisotropy between the particle and the gas velocity fluctuations increases with increasing particle relaxation time. More precisely, on the one hand, the particle velocity fluctuations in the streamwise direction increase with increasing particle relaxation time, and exceed the gas velocity fluctuations. On the other hand, particle velocity fluctuations in the transverse direction decrease with particle relaxation time. These results mean that inertia increases the degree of anisotropy. Such observations were also reported by Roger and Eaton,[113] Reeks[56] and Kulick *et al.*[114] This anisotropy can be measured in terms of the dimensionless anisotropy for the particle velocity fluctuations, $b_{2ij} = < u_{2i}'u_{2j}' > / < u_{2i}'u_{2i}' > - \delta_{ij}/3$.[83] The study of Simonin *et al.*[83] gives an answer on the influence of the first parameter (inertia) in a case where gravity (crossing trajectory effects) and collisions are not included. As far as collisions are concerned, they lead to a return to isotropy, a phenomenon that can be observed in numerical simulations of dense fluidized beds. In the general case, where all three mechanisms are considered, He and Simonin[85] presented a study concerning gas–particle vertical pneumatic conveying, including wall–particle bouncing. It was found that the streamwise particle velocity fluctuations are dominant due to the production by the mean gradient, whereas the transverse particle velocity fluctuations are controlled by particle–particle collisions, which act as a redistribution mechanism.

Two-way coupling (modulation of gas phase turbulence by particles) has not been included in the studies mentioned above. Some experimental and numerical results have been discussed in Section 4, and the conclusion seems to be that modulation of turbulence by particles follows a selective spectral redistribution rather than a uniform distribution. This is strengthened by the observations of Kulick *et al.*[114] in fully developed channel flow (the channel is vertical and gas is flowing downwards): turbulence modulation (destruction in this case) is stronger in the transverse direction than in the streamwise direction, with a particle mass loading varying from zero to one and particles smaller than the Kolmogorov scale, except in the near wall region. According to the authors, this phenomenon can be explained by the power spectra of single-phase flow, which show that energy in the transverse direction is contained at much higher wavenumbers than in the streamwise direction. Heavy particles are less responsive to the higher frequencies. In general, most studies are far

from the flow encountered in a CFB, but they give valuable information on the fundamental mechanisms involved in gas–solid suspensions. More research is needed for suspensions at higher mass loading before one knows to what extent the present results can be applied to fluidization.

Estimates of the time scales presented in Section 1 can be made, more precisely estimates of the characteristic time scale ratios, $\eta_r = \tau_{12}^t/\tau_{12}^x$ and $\eta_c = \tau_{12}^x/\tau_2^c$, in the core region of the transport zone of a CFBC. The ratios are evaluated from algebraic models for a simple shear flow[115] in the following case representative of the transport zone: hot conditions (850°C), $\alpha_2 = 0.005$, $\rho_2/\rho_1 = 2600$ and a fluidization velocity of 5 m sec^{-1}. The solution to the set of non-linear algebraic equations is plotted in Fig. 6. If we consider the range 80 μm to 1 mm, which is typical for a CFBC, the results show that in the transport zone, the ratio τ_{12}^x/τ_2^c is always smaller than one. This means that the particle mean free path is influenced by the presence of the gas, and therefore this effect should be accounted for in the expression of the discrete phase viscosity (Section 2 and Boëlle *et al.*[31]). In addition, the ratio τ_{12}^t/τ_{12}^x is larger than one for particles smaller than approximately 100 μm, and the motion of particles is governed by gas phase turbulence. In this case, the drift velocity is a key parameter for accurate modeling. For particle sizes above 100 μm the reverse is observed, and the motion of particles is governed by the mean flow.

7.2.2. *Gas–solid flows applied to CFB combustors*

In this section, an analysis of the macrophenomena is made. At Chalmers University of Technology, experimental studies in a 12-MW CFBC (1.7 m × 1.5 m × 12 m) and a two-dimensional cold rig model (0.7 m × 0.12 m × 8.5 m) have given an overall picture of the two-phase mean flow structure.[96,116,117] The riser is divided into three distinct, but interacting regions: the bottom bed, the splash zone and the transport zone. The bottom bed, typically 0.5 m in height with a particle concentration of 1000 kg m^{-3} (the particle density is typically 2600 kg m^{-3}), is a region which has the characteristics of a bubbling bed.[96,118] Above the bottom bed, the splash zone, typically 1.5 m in height with a particle concentration decreasing from 1000 to 20 kg m^{-3}, is a region with important concentration gradients and backmixing activity. Above the splash zone, the transport zone, typically with a particle concentration of 10 kg m^{-3}, is a region which exhibits a core/wall layer structure: particles are entrained upwards in the core region and fall down along the walls in a thin boundary layer.[119] In the transport zone, the volume concentration of the particle phase is not homogeneous; regions where the volume fraction is high compared to the mean volume concentration are characterized by particle agglomeration or clusters, which can be defined by various criteria.[120,121] A detailed description of the vertical distribution of solids in a CFBC can be found in Johnsson and Leckner.[122] The set of equations presented above to describe isothermal turbulent gas–solid flows must be able to predict the mean flow structure of a CFBC, and especially the bottom bed, the particle boundary layer and the inhomogeneities.

The bottom bed is a key parameter for combustion predictions, as it is the part of the combustor, where most of the fuel is contained. The bubbles formed in the bottom bed are believed to generate large scale turbulence,[123] which in turn should be coupled to the splash zone, where the breakdown of the gas phase turbulent scales takes place, or in other words, where particles are accelerated and decelerated. Comprehensive numerical simulations[4] display the main features of the flow field of a CFB combustion chamber. One of the principal items of discussion is the absence of a bottom bed in the calculations (sufficient measurements are lacking to verify if this is also the case in the boiler considered). There are some reasons for the lack of a bottom bed either in the calculations or in the real situation. (1) The total mass of particles in the combustion chamber is not sufficient to form a dense bottom bed (it has been observed experimentally that the bottom bed region can disappear when the total mass of solids in the combustion chamber is insufficient). (2) The granularity of the suspension in the boiler's bed differs from that of the single particle size of the calculations. (3) The boundary conditions: the set of equations is sensitive to boundary conditions. Proper boundary conditions at the wall, but also at the solid recirculation inlet, will give an accurate value of the recirculation rate, and this may affect the calculated bottom bed.

The particle boundary layer is a key factor for accurate prediction of heat transfer in the combustion chamber of a CFBC: particles in the boundary layer exchange heat with the wall as they descend, but they also influence the mean beam length of radiation. The mechanisms responsible for the formation of the particle boundary layer are believed to be (1) the gas phase boundary layer and (2) the particle transport between the core region and the wall region.[117,124] In addition, the boundary layer is not a stationary, homogeneous flow pattern, but fluctuations of the volume fraction of solids can be observed,[120] as well as backmixing of gas.[125] These phenomena seem to be predicted by preliminary numerical simulations,[60] but validation is a task for further calculations.

Inhomogeneities in the particle phase represent the non-stationary, non-homogeneous behavior of the flow pattern in a CFBC. There are three possible mechanisms which may cause inhomogeneities: the first mechanism is a local modification of the collision stress tensor.[40] A deeper insight into stability of rapid granular flows can be found, for example, in Babic[126] and McNamara.[127] In fluidization, particle collision is also identified as a reason for formation of inhomogeneities.[128] The second effect is the preference for certain particles for low vorticity and high strain rate regions.[51] The third effect can be large scale turbulence.[123] The preferential concentration of particles by turbulence is presented by Eaton and Fressler[129] in an extensive review article dealing with small particles at low mass loading (less

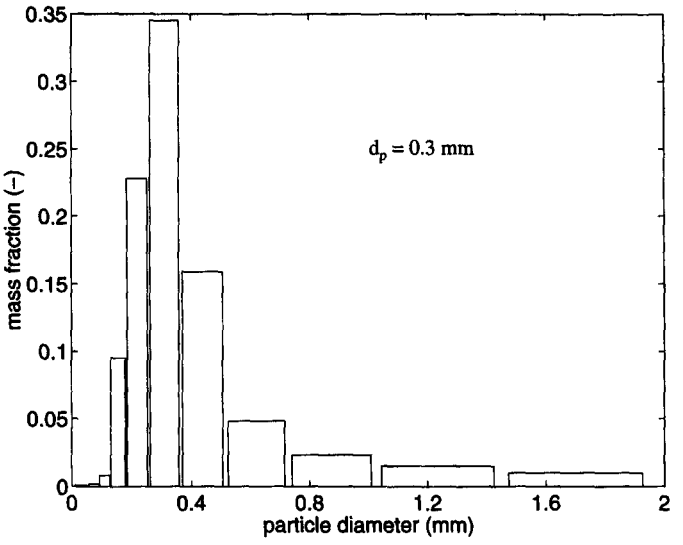

Fig. 7. Particle size distribution for bed material in the 12-MW boiler at Chalmers.

than unity). In such a case, two main mechanisms for preferential concentration are identified: centrifuging of particles away from vortex cores and accumulation of particles in convergence zones. These phenomena appear when the particle relaxation time is of the same order of magnitude as the relevant time scale of gas phase fluctuations. When considering high mass loading and coarse particles, other mechanisms may occur, for example coarse particles create disturbances (wakes) which may result in the formation of inhomogeneities.[130]

Finally, some comments on numerical simulations of CFBCs should be made. The research group at the Illinois Institute of Technology and the Argone National Laboratory initiated two-dimensional numerical simulations of CFBCs. The first simulations were performed using constant gas and particle phase viscosities.[131] Comparisons with measurements showed that the mean flow parameters (profiles of α_2, U_{2y} and U_{1y}, where y is the vertical direction) were predicted fairly well. Later, the simulations were improved by introducing the kinetic theory of dry granular flow and large eddy simulation.[132] No validation of the results was made but, as explained in Section 2, the theory of dry granular flow cannot be accurate in dilute suspensions and, in addition, large eddy simulation in a two-dimensional model is questionable as large scale eddies are always three-dimensional. Additional simulations of the same type were performed by the research group at RWTH,[133] with an algebraic model for the granular temperature. Different models for the drag coefficient and the radial distribution function were tested. Comparison with vertical and radial profiles of particle volume fraction, α_2, showed reasonable agreement. Similar computations were also made by the research group at the Telemark Technological R&D Centre and the Telemark Institute of Technology,[134] but with a significant improvement: the authors presented efforts to simulate, after the work of Syamlal,[135] two-dimensional multi-phase (three particle sizes, four phases) fluidization, based on the theoretical results of Jenkins and Mancini.[136] The model given by Mathiesen *et al.*[134] for effective stress tensor in each phase is, at present, that of a dry granular flow. The simulations were compared to the measurements of Tadrist and Azario.[137] The results seem to predict segregation effects and the particle velocity fluctuations quite well. The most advanced simulations were done by the group at Electricité de France (EDF):[4] three-dimensional simulations of an industrial CFBC unit with the complete set of equations presented in this work, Eqs (1), (2), (93), (149), (151), (157) and (158). The validation of the time-averaged vertical pressure profile over a period of 30 sec showed that, generally, the model predicted the main features of the mean flow field fairly well. An attempt to make simplified simulations of large CFB units has been made by Kallio.[138] The results also gave reasonable agreement with the experimental observations. As a concluding remark, most simulations were performed for small CFB units (pilot plants), except for those of the EDF group. All simulations seem to give reasonable predictions of the main features of the mean flow field, but a more complete review is necessary for a closer look at these simulations, as other parameters are of great importance, for example the drag models, the validation procedure and so on. A more complete review of publications on simulation of the hydrodynamics of bubbling and circulating fluidized beds is given by Enwald *et al.*[8]

7.3. *Polydisperse Suspensions*

So far, to derive the results, particles have been treated as a population of identical, smooth, rigid, non-rotating spheres. The influence of these assumptions has been discussed previously, except the first one: that of identical spheres. The kinetic theory of granular flow (Section 2), as well as the closure models for the drift

velocity and the stress tensors in both phases (Sections 3–5), are derived assuming that the particles have the same diameter (monodisperse suspension). In most engineering applications and more precisely in a CFBC, we are dealing with "**polydisperse suspensions**", which means that the suspension consists of particles with different diameters and densities. In CFB applications, the particle size distribution function covers a wide range of diameters, for a CFBC mainly particles between 100 μm and 1 mm, with a particle density ranging from 2600 (silica sand) to 2000 kg m^{-3} (coal). The range of particle diameters is variable depending on the applications: it is mainly controlled, for small diameters, by the fractional efficiency of the cyclone, and for large diameters it is a result of the characteristics of the fuel particles (ash content and related properties) and of the limestone particles (fragmentation properties). Figure 7 displays an example of a typical particle size distribution function.

Is it possible to draw conclusions for monodisperse suspensions which are valid for polydisperse ones represented by a mean diameter? This question needs to be answered both theoretically and experimentally. Experimentally, it can be shown that the mean diameter is not sufficient for the calculation of the recirculation rate in a CFBC; particle recirculation takes place for fluidization velocities lower than the free fall velocity of the mean particle diameter, mainly a contribution of the small particles whose free fall velocity is lower than that of the gas. On the contrary, it has been shown experimentally[139,140] that coarse particles (particles whose terminal velocity is higher than the fluidization velocity) can be fluidized and exit the combustion chamber. Fine particles collide with coarse particles and transfer momentum, so that the coarse particles can be fluidized. For accurate prediction of the recirculation mass flow rate, the particle size distribution of the bed material should be taken into account.[141] Theoretical descriptions of suspensions with more than one particle size, employing the kinetic theory of granular flow reformulated by Jenkins and Mancini,[136] seem to be able to capture these phenomena.[134] Yarin and Hetsroni[142] made a study of the influence of the particle size distribution function on the turbulence of the carrier fluid, taking into account two-way coupling. They studied dilute bidisperse suspensions (no collision mechanism), assuming that particles have Reynolds numbers below 110 (no wake effects) and that particles stay in the fluid element as long as this fluid element persists as en entity (non-settling particles). This implies a particle whose relaxation time and eddy–particle interaction time are at least of the same order of magnitude (Fig. 6). With these assumptions, Yarin and Hetsroni showed that the turbulence intensities of a bidisperse suspension depend on the mass fraction of each particle size, as well as on the total loading, diameter ratio, fluid–particle density ratio, particle Reynolds numbers and ratio of the mixing length to each particle diameter. They also showed that the fluid turbulence in a bidisperse system can be higher or lower than in a monodisperse system, depending on the ratio of the particle diameters and their mass contents. More precisely, let us consider the case of equal loading for the monodisperse and polydisperse suspensions, equal loading for each particle size. The diameters of the coarse and fine particles are denoted as d_{p1} and d_{p2}, respectively. The diameter of the monodisperse suspension is noted as d_0. The modulation of the carrier fluid turbulence is defined by $M = (u_{1b}' - u_{1m}')/u_{1m}'$, where u_{1b}' and u_{1m}' represent the fluctuating velocities of the continuous phase in the bidisperse and monodisperse suspensions, respectively. Yarin and Hetsroni found that if $d_{p2} = d_0$, then M increases when d_{p1} increases. On the contrary, if $d_{p1} = d_0$, then M decreases when d_{p2} decreases. According to Yarin and Hetsroni, this can be explained by an increase of the energy required to accelerate the particles when the diameter of the fine particles is reduced, whereas less energy is required to accelerate the particles when the diameter of the coarse particles is larger. In a second study, Yarin and Hetsroni[143] modeled the vortex shedding phenomenon by assuming that the wake behind a particle is a stationary boundary layer. Assuming a self-similar form of the turbulent kinetic energy in the cross-section of the wake, the authors showed that, for a polydisperse suspension of coarse particles (index p), the turbulent kinetic energy generated by the particles per unit volume of two-phase mixture can be written as

$$\Delta k_1 = C \sum_{p=1}^{n} \mathbf{u}_{rp^2} \left(\frac{\rho_1}{\rho_2} X_{1p} C_{Dp}^{1.5} \right)^{8/9}, \qquad (168)$$

where C is a constant which must be determined. Speaking in terms of turbulent intensity, the authors refer to this equation as the 4/9-power law. This result shows that, for coarse particles, turbulence modulation is a function of the gas–particle density ratio, the mass of particles in the suspension and the aerodynamic properties. In conclusion, the previous remarks show the difficulties encountered in modelling CFB flows with a single particle diameter. More research is needed to understand polydisperse suspensions, including the effects of particle diameter and particle density, as the CFBC consists of several groups of particles (inert material, fuel and limestone) which have different densities and different particle size distribution functions.

8. CONCLUSION

In the present work, it has been shown that turbulent non-reacting gas–solid flows can be modeled by classical transport equations, continuity and momentum equations, which are closed for the interfacial momentum transfer, the stress tensor in the particle phase, the drift velocity, the fluid–particle velocity correlation tensor and the second-order velocity moments in both phases. The derivations of the closure models were only possible with simplifying assumptions. It is found that, for the discrete phase (stress tensor and second-order

velocity moment), the most limiting assumption is that of the particles being a population of identical, rigid, smooth spheres, with a low level of anisotropy and a small departure from the Maxwellian state. The collision model is based on binary collisions between particles in translational motion. In contrast, the bed material of a CFBC is a polydisperse suspension of rigid, non-spherical, rotating particles, where the anisotropy level can be high. For the continuous phase (second-order velocity moment), the difficulty lies in the extension of the classical single-phase flow models to two-phase flows. Some specific problems are the value of the constants included in the equations, the treatment of the wall region and the form of the coupling term. For the fluid–particle velocity moments (drift velocity and fluid–particle velocity correlation tensor), a general formulation (fluid–particle joint probability density function and Langevin equation) is possible, but two-way coupling is omitted. Algebraic models can be derived for homogeneous isotropic turbulence, asymptotic cases, but these ideal cases are far from real CFB flows. The models formulated in this work need to be solved by numerical methods and further validated against experiments to see to what extent they capture the essential physical mechanisms of turbulent non-reacting gas–particle flows applied to fluidization.

Acknowledgements—Olivier Simonin, Georges Balzer and Arnaud Boëlle at EDF, France, are acknowledged for fruitful discussions on two-phase flow modeling. The discussions on single-phase flow turbulence with Lars Davidson, Gunnar Johansson and Lennart Löfdhal at the Department of Thermo- and Fluid Dynamics, are also greatly appreciated. Finally, thanks are extended to Filip Johnsson at the Department of Energy Conversion at Chalmers University of Technology, Sweden, and to Gennadi Palchonok, Luikov Institute of Heat and Mass Transfer, Minsk, for their discussions on fluidization. This project has been financially supported by the Swedish National Energy Administration.

REFERENCES

1. Werther, J., *4th Int. Conf. on CFB*, ed. A. A. Avidan, AIChE, Somerset, PA, pp. 1–14 (1–5 August 1993).
2. Geldart, D., *Powder Technol.*, 1973, **7**, 285–292.
3. Therdthianwong, A. and Gidaspow, D., *4th Int. Conf. on CFB*, ed. A. A. Avidan, AIChE, Somerset, PA, pp. 351–358 (1–5 August 1993).
4. Balzer, G., Simonin, O., Boëlle, A. and Lavieville, J., in *Circulating Fluidized Bed Technology I*, eds M. Kwauk and J. Li, Science Press, Beijing, pp. 432–439 (1996).
5. Kawaguchi, T., Yamamoto, Y., Tanaka, T. and Tsuji, Y., *2nd Int. Conf. on Multiphase Flow*, Kyoto, FB2, pp. 17–22 (3–7 April 1995).
6. Hoomans, B. P. B., Kuipers, J. A. M., Briels, W. J. and Van Swaaij, W. P. M., *Chem. Engng Sci.*, 1996, **51 (1)**, 99–108.
7. Yonemura, T., Tanaka, T. and Tsuji, Y., *2nd Int. Conf. on Multiphase Flow*, Kyoto, PT4, pp. 25–30 (3–7 April 1995).
8. Enwald, H., Peirano, E. and Almstedt, A. E., *Int. J. Multiphase Flow*, 1996, **22 (Suppl.)**, 21–26.
9. Ishii, M., *Thermo-Fluid Dynamic Theory of Two-Phase Flow*. Eyrolles, Paris (1975).
10. Peirano, E., The Eulerian/Eulerian formulation applied to gas–particle flows. Report A96-218, Department of Energy Conversion, Chalmers University of Technology, Sweden (1996).
11. Simonin, O., *5th Workshop on Two-Phase Flow Predictions*, Erlangen, Germany, pp. 156–166 (1990).
12. Jenkins, J. T. and Richman, M. W., *Arch. Ratio. Mech. Anal.*, 1985, **87**, 355–377.
13. Jenkins, J. T. and Savage, S. B., *J. Fluid Mech.*, 1983, **130**, 187–202.
14. Ding, J. and Gidaspow, D., *AIChE J.*, 1990, **36 (4)**, 523–538.
15. Sinclair, J. L., in *Circulating Fluidized Beds*, eds J. R. Grace, A. A. Avidan and T. M. Knowlton, Blackie Academic, pp. 149–180 (1997).
16. Deutsch, E. and Simonin, O., *Turbulence Modification in Multiphase Flow, ASME Fed.*, 1991, **1**, 34–42.
17. Csanady, G. T., *J. Atmos. Sci.*, 1963, **105**, 329–334.
18. He, J. and Simonin, O., Modélisation numérique des écoulements gaz–solides en conduite verticale. Rapport HE-44/94/021A, Laboratoire National d'Hydraulique, EDF, Chatou, France (1994).
19. Elgobashi, S. E., *Appl. Scient. Res.*, 1991, **48**, 301–314.
20. Clift, R., Grace, J. R. and Weber, M. E., *Bubbles, Drops and Particles*, Academic Press, New York (1978).
21. Gore, R. A. and Crowe, C. T., *Int. J. Multiphase Flow*, 1989, **15 (2)**, 279–285.
22. Yuan, Z. and Michaelides, E. E., *Int. J. Multiphase Flow*, 1992, **18 (5)**, 779–785.
23. Koch, D. L., *Phys. Fluids A*, 1990, **2 (10)**, 1711–1723.
24. Chapman, S. and Cowling, T. G., *The Mathematical Theory of Non-uniform Gases*. Cambridge Mathematic Library, Cambridge (1970).
25. Grad, H., *Comm. Pure Appl. Math.*, 1949, **2 (4)**, 331–407.
26. Lun, C. K. K., Savage, S. B., Jeffrey, D. J. and Chepurniy, N., *J. Fluid Mech.*, 1984, **140**, 223–256.
27. Simonin, O., Summer school on "Numerical Modelling and Prediction of Dispersed Two-Phase Flows", IMVU, Meserburg, Germany (1995).
28. Bel Fdhila, R. and Simonin, O., *6th Workshop on Two-Phase Flow Predictions*, Erlangen, Germany, pp. 264–273 (1992).
29. Balzer, G., Boëlle, A. and Simonin, O., *Fluidization*, VIII, Engineering Foundation, Tours, pp. 1125–1134 (14–19 May 1995).
30. Boëlle, A., Balzer, G. and Simonin, O., Application d'une modélisation á deux fluides á la prédiction des lits fluidisés denses. Rapport HE-44/94/017A, Laboratoire National d'Hydraulique, EDF, Chatou, France (1994).
31. Boëlle, A., Balzer, G. and Simonin, O., *Gas–Solid Flows, ASME Fed.*, 1995, **228**, 9–18.
32. Smith, W. R. and Henderson, D., *Molec. Phys.*, 1970, **32 (5)**, 411–415.
33. Carnahan, N. F. and Starling, K. E., *J. Chem. Phys.*, 1969, **51**, 635–636.
34. Ma, D. and Ahmadi, G., *J. Chem. Phys.*, 1986, **84 (6)**, 3449–3450.
35. Ree, F. H. and Hoover, W. G., *J. Chem. Phys.*, 1964, **51**, 939.
36. Alder, B. J. and Wainwright, T. E., *J. Chem. Phys.*, 1960, **33 (5)**, 1439–1451.
37. Lun, C. K. K. and Savage, S. B., *Acta Mech.*, 1986, **63**, 15–44.
38. Ogawa, S., Unemura, A. and Oshima, N. Z., *Angew. Math. Phys.*, 1980, **31**, 483–493.
39. Richman, M. W., *J. Rheol.*, 1989, **33 (8)**, 1293–1306.
40. Hopkins, M. A. and Louge, M. Y., *Phys. Fluids A*, 1991, **3 (1)**, 47–57.
41. Lun, C. K. K. and Bent, A. A., *J. Fluid Mech.*, 1994, **258**, 335–353.
42. Walton, O., *Mech. Mater.*, 1991, **16**, 239–247.
43. Foerster, S.F., Louge, M. Y., Chang, H. and Allia, K., *Phys. Fluids*, 1994, **6 (3)**, 1108–1115.
44. Dave, Yu. and Rosato, X., *ASME Winter Annual Meeting,*

Symposium on Mechatronics, DSC Vol. 50, pp. 217–222 (1993).
45. Massah, H., Shaffer, F., Sinclair, J. and Shahnam, M., *Proc. 8th Int. Conf. on Fluidization*, Engineering Foundation, pp. 641–648 (1995).
46. Lun, C. K. K., *J. Fluid Mech.*, 1991, **233**, 539–559.
47. Jenkins, J. T. and Richman, M. W., *Phys. Fluids*, 1985, **28**, 3485–3494.
48. Hinze, J.O., *Turbulence*, 2nd edn, McGraw-Hill, New York (1975).
49. Tchen, C. M., Mean value and correlation problems connected with the motion of small particles suspended in a turbulent fluid, Ph.D. thesis, Delft University of Technology (1947).
50. Well, M. R. and Stock, D. E., *J. Fluid Mech.*, 1983, **136**, 31–62.
51. Squires, K. D. and Eaton, J. K., *Phys. Fluids A*, 1990, **2**, 1191–1203.
52. Maxey, M. R., *J. Fluid Mech.*, 1987, **174**, 441–465.
53. Derevich, I. V. and Zaichik, L. I., *Applied Mathematics and Physics* (English translation of *Prikladnaya Matematika i Mekhanika*) 1990, **54**(5), 631–637.
54. Louge, M., Mastorakos, E. and Jenkins, J., *J. Fluid Mech.*, 1991, **231**, 345–359.
55. Reeks, M. W., *Phys. Fluids A*, 1992, **4 (6)**, 1290–1303.
56. Reeks, M. W., *Phys. Fluids A*, 1993, **5 (3)**, 750–761.
57. Kraichnan, R., *Phys. Fluids*, 1965, **8 (4)**, 574–598.
58. Derevich, I. V., *Inzhenerno-Fizicheskii Zhurnal*, 1988, **55 (1)**, 26–33.
59. Wilcox, D. C., *Turbelence Modeling for CFB*, DCW Industries, La Canada, CA (1993).
60. Peirano, E., Unpublished work, Department of Energy Conversion, Chalmers University of Technology (1996).
61. Pope, S. B., *Phys. Fluids*, 1983, **26 (2)**, 404–408.
62. Pope, S. B., *Prog. Energy Combust. Sci.*, 1985, **11**, 119–192.
63. Haworth, D. C. and Pope, S. B., *Phys. Fluids*, 1986, **29 (2)**, 387–405.
64. Minier, J. P. and Pozorski, J., *Phys. Fluids*, 1997, **9 (6)**, 1748–1753.
65. Haworth, D. C. and Pope, S. B., *Phys. Fluids*, 1987, **30 (4)**, 1026–1044.
66. Simonin, O., Deutsch, E. and Minier, J. P., *Appl. Scient. Res.*, 1993, **51**, 275–283.
67. Minier, J. P., *J. Fluid Mech.*, 1998, in press.
68. Hetsroni, G., *Int. J. Multiphase Flow*, 1989, **15**, 735–746.
69. Elgobashi, S. E. and Truesdell, G. C., *Phys. Fluids A*, 1993, **5 (7)**, 1790–1801.
70. McComb, W. D., *The Physics of Fluid Turbulence*, Clarendon Press, Oxford (1990).
71. Domaradzki, J. A. and Rogallo, R. S., *Phys. Fluids A*, 1990, **2 (3)**, 413–426.
72. Tsuji, T., Morikawa, Y. and Shioni, H., *J. Fluid Mech.*, 1984, **139**, 417–434.
73. Hetsroni, G. and Sokolov, M., *Trans. ASME, J. Appl. Mech.*, 1971, **38**, 315–327.
74. Baw, P. S. and Peskin, R. L., *Trans. ASME D, J. Basic Engng*, 1971, **93**, 631.
75. Jones, W. P. and Launder, B. E., *Int. J. Heat Mass Transfer*, 1972, **15**, 301–314.
76. Speziale, C. G., *J. Fluid Mech.*, 1987, **178**, 459–475.
77. Launder, B. E., Reece, G. J. and Rodi, W., *J. Fluid Mech.*, 1975, **68**, 537–566.
78. Rodi, W., *Z. Angew. Math. Mech.*, 1976, **56**, 219.
79. Deardoff, J. W., *J. Fluid Mech.*, 1970, **41**, 453–480.
80. Rogallo, R. S. and Moin, P., *Ann. Rev. Fluid Mech.*, 1984, **16**, 99–137.
81. Launder, B. E. and Spalding, D. B., *Comput. Meth. Appl. Mech. Engng*, 1974, **3**, 269–289.
82. Martinuzzi, R. and Pollard, A., *AIAA J.*, 1989, **27**, 39.
83. Simonin, O., Deutsch, E. and Bovin, M., Large eddy simulation and second-moment closure model of particle fluctuating motion in two-phase turbulent shear flows. Rapport HE-44/94/035/A, Laboratoire National d'Hydraulique, EDF, Chatou, France (1995).
84. Elgobashi, S. E. and Abou-Arab, T. W., *Phys. Fluids*, 1983, **26 (4)**, 931–938.
85. He, J. and Simonin, O., *Gas–Solid Flows, ASME Fed.*, 1993, **166**, 253–263.
86. Yakomine, T. and Shimizu, A., *2nd. Int. Conf. on Multiphase Flow*, Kyoto, MO2, pp. 17–23 (3–7 April 1995).
87. Rizk, M. and Elgobashi, S., *Int. J. Multiphase Flow*, 1989, **15**, 119–133.
88. Bolio, E. J., Yasuna, J. A. and Sinclair, J. L., *AIChE J.*, 1995, **41 (6)**, 1375–1388.
89. Myong, H. K. and Kasagi, N., *JSME Int. J., Ser. II*, 1990, **33 (1)**, 63–72.
90. Hrenya, C., Bolio, E., Chakrabarti, D. and Sinclair, J., *Chem. Engng Sci.*, 1995, **50 (12)**, 1923–1941.
91. Squires, K. D. and Eaton, J. K., *ASME J. Fluids Engng*, 1994, **116**, 778–784.
92. Cao, J. and Ahmadi, G., *Int. J. Multiphase Flow*, 1995, **21 (6)**, 1203–1228.
93. Patel, V. C., Rodi, W. C. and Scheuerer, G., *AIAA J.*, 1985, **23 (9)**, 1308–1319.
94. Lam, C. K. G. and Bremhorst, K. A., *ASME J. Fluids Engng*, 1981, **103**, 456–460.
95. Boemer, A., Qi, H., Renz, U., Vasquez, S. and Boyan, F., *Proc. 13th Int. Conf. on Fluidized Bed Combustion*, ed. K. J. Henschel, ASME, pp. 775–787 (1995).
96. Svensson, A., Fluid dynamics of the bottom bed of circulating fluidized bed boilers, Ph.D. thesis, Department of Energy Conversion, Chalmers University of Technology, Sweden (1995).
97. Savage, S. B. and Sayed, M., *J. Fluid Mech.*, 1984, **142**, 391.
98. Hanes, D. M. and Inman, D. L., *J. Fluid Mech.*, 1985, **150**, 357.
99. Jenkins, J. T. and Richman, M. W., *J. Fluid Mech.*, 1986, **171**, 53–69.
100. Richman, M. W., *Acta Mech.*, 1988, **75**, 227.
101. Johnsson, P. C. and Jackson, R., *J. Fluid Mech.*, 1987, **176**, 67–93.
102. Hui, K., Haff, P. K., Ungar, J. E. and Jackson, R., *J. Fluid Mech.*, 1984, **145**, 223–233.
103. Jenkins, J. T., *J. Appl. Mech.*, 1992, **59**, 120–127.
104. Louge, M., *Phys. Fluids*, 1994, **6 (7)**, 2253–2269.
105. Jenkins, J. T. and Louge, M. Y., *Phys. Fluids*, 1997, **9 (10)**, 2835–2840.
106. Hatano, H., Matsuda, S., Takeuchi, H., Pyatenko, A. T. and Tsuchiya, K., *2nd Int. Conf. on Multiphase Flow*, Kyoto, P7, pp. 23–30 (3–7 April 1995).
107. Azario, E., Tadrist, L., Santini, R. and Pantaloni, J., *2nd Int. Conf. on Multiphase Flow*, Kyoto, P7, pp. 33–40 (3–7 April 1995).
108. Kaftori, D., Hetsroni, G. and Banerjee, S., *2nd Int. Conf. on Multiphase Flow*, Kyoto, PT1, pp. 11–15 (3–7 April 1995).
109. Komori, S., Kurose, R., Murakami, Y. and Hanazaki, H., *2nd Int. Conf. on Multiphase Flow*, Kyoto, PT3, pp. 31–34 (3–7 April 1995).
110. Sommerfield, M., *Int. J. Multiphase Flow*, 1992, **18 (6)**, 905–926.
111. Rashidi, M., Hetsroni, G. and Banergee, S., *Int. J. Multiphase Flow*, 1990, **16**, 935–949.
112. Hajji, L., Pascal, Ph. and Oesterlé, B., *2nd Int. Conf. on Multiphase Flow*, Kyoto, PT4, pp. 19–24 (3–7 April 1995).
113. Roger, C. B. and Eaton, J. K., *Int. J. Multiphase Flow*, 1990, **16 (5)**, 819–834.
114. Kulick, J. D., Fessler, J. R. and Eaton, J. K., *J. Fluid Mech.*, 1994, **227**, 109–134.
115. Peirano, E., Palchonok, G., Johnsson, F. and Leckner, B. *Powder Technol.*, 1998, in press.
116. Johnsson, F., Fluid dynamics and heat transfer in fluidized

beds—with application to boilers, Ph.D. thesis, Department of Energy Conservation, Chalmers University of Technology, Sweden (1991).
117. Zhang, W., Johnsson, F. and Leckner, B., *Chem. Engng Sci.*, 1995, **50 (2)**, 201–210.
118. Werther, J. and Wein, J., *AIChE Symp. Ser., Fluid-Particle Technol.*, 1994, **301**, 31–44.
119. Johnsson, F., Zhang, W. and Leckner, B., *2nd Int. Conf. on Multiphase Flow*, Kyoto, FB1, pp. 25–32 (3–7 April 1995).
120. Johnsson, F., Zhang, W., Johnsson, H. and Leckner, B., in *Circulating Fluidized Bed Technology*, eds M. Kwauk and J. Li, Science Press, Beijing, pp. 652–657 (1996).
121. Soong, C. H., Tuzla, J. C. and Chen, J. C., *4th Int. Conf. on CFB*, ed. A. A. Avidan, AIChE, Somerset, PA, pp. 615–620 (1–5 August 1993).
122. Johnsson, F. and Leckner, B., *Proc. 13th Int. Conf. on FBC*, ed. K. J. Henschel, ASME, pp. 671–679 (1995).
123. Palchonok, G. I., Johnsson, F. and Leckner, B., in *Circulating Fluidized Bed Technology*, eds M. Kwauk and J. Li, Science Press, Beijing, pp. 440–445 (1996).
124. Horio, M., Taki, A., Hsieh, Y. S. and Muchi, I., *3rd Conf. on Fluidization*, Engineering Foundation, Henniker, pp. 509–518 (1980).
125. Sternéus, J. and Johnsson, F., *Proc. 14th FBC Conf.*, ed. F. Preto, ASME (1997).
126. Babic, M., *J. Fluid Mech.*, 1993, **254**, 127–150.
127. McNamara, A., *Phys. Fluids A*, 1993, **5**, 3056–3070.
128. Horio, M., *2nd Int. Conf. on Multiphase Flow*, Kyoto, FB1, pp. 1–12 (3–7 April 1995).
129. Eaton, J. K. and Fressler, J. R., *Int. J. Multiphase Flow*, 1994, **20**, 169–209.
130. Tori, E. M., Kamel, M. T. and Chan Man Fang, C. F., *Powder Technol.*, 1992, **73**, 219–238.
131. Tsuo, Y. P. and Gidaspow, D., *AIChE J.*, 1990, **36 (6)**, 885–896.
132. Gidaspow, D. and Therdthianwong, A., *AIChE J.*, 1993, **35 (5)**, 714–724.
133. Boemer, A., Qi, H. and Renz, U., Presented at the 28th IEA-FBC Meeting in Kitakyushu, International Energy Agency, Japan, (24–25 July 1994).
134. Mathiesen, V., Solberg, T., Manger, E. and Hjeretager, B. H., in *Circulating Fluidized Bed Technology*, eds M. Kwauk and J. Li, Science Press, Beijing, pp. 493–498 (1996).
135. Syamlal, M., Multiphase hydrodynamics of gas–solid flow, Ph.D. thesis, Department of Chemical Engineering, Illinois Institute of Technology (1985).
136. Jenkins, J. T. and Mancini, F., *J. Appl. Mech.*, 1987, **54**, 27–34.
137. Tadrist, L. and Azario, E., *4th Int. Conf. on CFB*, ed. A. A. Avidan, AIChE, Somerset, PA, pp. 582–587 (1–5 August 1993).
138. Kallio, S., *Fluidization*, VIII, Engineering Foundation, Tours, pp. 1109–1116 (14–19 May 1995).
139. Geldart, D. and Pope, D. J., *Powder Technol.*, 1983, **34**, 95–97.
140. Na, Y., Yan, G., Sun, X., Cui, P., He, J., Karlsson, M. and Leckner, B., in *Circulating Fluidized Bed Technology*, eds M. Kwauk and J. Li, Science Press, Beijing, pp. 194–199 (1996).
141. Wirth, K. E., *2nd Int. Conf. on Multiphase Flow*, Kyoto, FB1, pp. 19–24 (3–7 April 1995).
142. Yarin, L. P. and Hetsroni, G., *Int. J. Multiphase Flow*, 1994, **20 (1)**, 1–15.
143. Yarin, L. P. and Hetsroni, G., *Int. J. Multiphase Flow*, 1994, **20 (1)**, 27–44.